

NATIONAL INSTITUTE FOR FUSION SCIENCE

Atomic Data for Dielectronic Recombination into Mg-like Fe

I. Murakami, T. Kato, D. Kato, U.I. Safronova, T.E. Cowan and Yu. Ralchenko

(Received - Jan. 20, 2006)

NIFS-DATA-96

Mar. 2006

RESEARCH REPORT
NIFS-DATA Series

This report was prepared as a preprint of work performed as a collaboration research of the National Institute for Fusion Science (NIFS) of Japan. The views presented here are solely those of the authors. This document is intended for information only and may be published in a journal after some rearrangement of its contents in the future.

Inquiries about copyright should be addressed to the Research Information Office, National Institute for Fusion Science, Oroshi-cho, Toki-shi, Gifu-ken 509-5292 Japan.

E-mail: bunken@nifs.ac.jp

<Notice about photocopying>

In order to photocopy any work from this publication, you or your organization must obtain permission from the following organization which has been delegated for copyright for clearance by the copyright owner of this publication.

Except in the USA

Japan Academic Association for Copyright Clearance (JAACC)
6-41 Akasaka 9-chome, Minato-ku, Tokyo 107-0052 Japan
Phone: 81-3-3475-5618 FAX: 81-3-3475-5619 E-mail: jaacc@mtd.biglobe.ne.jp

In the USA

Copyright Clearance Center, Inc.
222 Rosewood Drive, Danvers, MA 01923 USA
Phone: 1-978-750-8400 FAX: 1-978-646-8600

Atomic data for dielectronic recombination into Mg-like Fe

I. Murakami, T. Kato, and D. Kato

National Institute for Fusion Science, Toki, Gifu 509-5292, Japan

U. I. Safronova and T. E. Cowan

Physics Department, University of Nevada, Reno, NV 89557, USA

Yu. Ralchenko

National Institute of Standards and Technology,

Gaithersburg, MD 20899-8422, USA

Abstract

Energy levels, radiative transition probabilities, and autoionization rates for $1s^2 2s^2 2p^6 3l' nl$ ($n=3-12$, $l \leq n-1$) and $1s^2 2s^2 2p^6 4l' nl$ ($n=4-7$, $l \leq n-1$) states in Mg-like iron (Fe^{14+}) are calculated by the Hartree-Fock-Relativistic method (Cowan code) and the relativistic many-body perturbation theory method (RMBPT code). Autoionizing levels above three thresholds $1s^2 2s^2 2p^6 3s$, $1s^2 2s^2 2p^6 3p$, and $1s^2 2s^2 2p^6 3d$ are considered. It is found that configuration mixing [$3sns + 3pnp + 3dnd$], [$3snp + 3pns + 3pnd + 3dnp$] play an important role for all atomic characteristics. Branching ratios relative to the first threshold and intensity factors for satellite lines are calculated, and dielectronic recombination (DR) rate coefficients are determined for the excited 444 odd-parity and 419 even-parity states. It is shown that the contribution of the highly-excited states is very important for calculation of DR rates. Contributions from the excited $1s^2 2s^2 2p^6 3l' nl$ states with $n \geq 12$ and $1s^2 2s^2 2p^6 4l' nl$ states with $n \geq 7$ to DR rate coefficients are estimated by extrapolation of all atomic characteristics. The total DR rate coefficient is derived as a function of electron temperature.

Key words: Mg-like iron, dielectronic recombination rate coefficients, energy levels, radiative transition probabilities, autoionization rates, excited states, dielectronic satellite lines

I. INTRODUCTION

Dielectronic satellites (DSs) are spectral lines that correspond to the same transitions as the resonance lines, but occur in the presence of additional electrons. For instance, satellites to resonance lines of Ne-like ions could be created by transitions from doubly-excited states of Na-like and other lower-charge ions. DSs often serve as an important tool for plasma diagnostics and as a testbed for atomic structure theories. As an example, the DS lines from Fe XVI (Na-like) and Fe XV (Mg-like) in vicinity of the strong $2p-3d$ transitions of Fe XVII (Ne-like) were recently recorded from plasmas created in three different laser facilities [1].

There are numerous theoretical and experimental studies devoted to DSs and dielectronic recombination (DR) of Na-like ions. For instance, the DR rate coefficients were calculated for Ar, Fe, and Mo target ions of the Na isoelectronic sequence [2] with both $\Delta n = 0$ and $\Delta n = 1$ transitions considered with full LS coupling. The DR rate coefficients of the Fe^{15+} ion were also studied in the isolated-resonance, distorted-wave approximation in Ref. [3]. The cross-section calculations included the dielectronic transitions associated with the $3s-3l$ and $3s-4l$ excitations. The energy-averaged cross sections associated with the $\Delta n = 1$ transition as a function of electron energy were also presented in Ref. [3]. Effect of the configuration interaction (CI) between resonances for the dielectronic recombination and resonant transfer excitation of Na-like ions was investigated in Ref. [4], and CI between the $1s^2 2s^2 2p^5 3s 3d 4p$ and $1s^2 2s^2 2p^5 3p^2 4p$ configurations were included to analyze the $1s^2 2s^2 2p^5 3s 3d 4p$ resonances. The absolute rates and cross sections for dielectronic recombination and ionization of Fe^{15+} ($1s^2 2s^2 2p^6 3s$) ion were measured at electron impact energies between 0 and 1030 eV using Heidelberg heavy ion storage ring TSR [5]. The doubly excited intermediate states ($1s^2 2s^2 2p^5 3s n l n' l'$) formed in the first step of the resonant-excitation-double-autoionization process decay by the emission of photons rather than electrons. The total process was considered as a dielectronic recombination process [5].

The effect of the low-temperature $\Delta n = 0$ dielectronic recombination on the relative populations of the Fe M -shell states was recently investigated in Ref. [6]. The ionization structure and temperature in astrophysical plasmas depend on ionization and recombination processes. It was pointed out in Ref. [6] that the low-temperature DR rates were not available for the M -shell ions of Fe. The DR rates of the M -shell Fe ions were estimated by the DR rates of the first four ionization states of the C, N, and O sequences and L -shell ions. The

iron unresolved transition arrays in active galactic nuclei were recently studied in Ref. [7] where simulations of photoionized plasmas failed to predict the ionization level of iron. The discrepancy was attributed to underestimation of the low-temperature DR rates for iron M -shell ions. Also, DR rate coefficients for Na-like ions of elements with $12 \leq Z \leq 30$ were calculated in the independent-process, isolated-resonance approximation [8]. Both $\Delta n = 0$ and $\Delta n > 0$ core excitation DR channels were taken into account in determination of the total DR rate coefficients.

In the present paper the state-selective DR rate coefficients to excited states of Mg-like iron as well as the total DR rate coefficients are calculated. The DR rate coefficients are calculated including $1s^2 2s^2 2p^6 3l'nl$ ($n=3-12$, $l \leq n-1$) and $1s^2 2s^2 2p^6 4l'nl$ ($n=4-7$, $l \leq n-1$) states. Contributions from the autoionizing $1s^2 2s^2 2p^6 3l'nl$ states with $n \geq 12$ and from the autoionizing $1s^2 2s^2 2p^6 4l'nl$ states with $n \geq 7$ are estimated by extrapolation of all atomic characteristics to derive the DR rate coefficients for the excited states and the total DR rate coefficients as a function of electron temperature. In the following description, we omit the core $1s^2 2s^2 2p^6$ from the configuration notation. The energy levels, transition probabilities, and autoionization rates required for calculation of the DR parameters are determined as well. The present paper continues our efforts on calculation of the low-temperature DR rates coefficients that were previously determined for C I [9], C II [10, 11], C III [12], O IV [13], O V [14], and Ne VII [15].

II. ENERGY LEVELS, TRANSITION PROBABILITIES, AND AUTOIONIZATION RATES

Determination of dielectronic recombination rate coefficients necessarily includes calculation of atomic parameters for intermediate and final states. Therefore, radiative and autoionization rates for the intermediate states $3l'nl$ ($n=3-12$, $l \leq n-1$) and $4l'nl$ ($n=4-7$, $l \leq n-1$) states for Mg-like iron (Fe^{14+}) were considered. The list of the $3lnl'$ configurations consists of 97 even-parity and 94 odd-parity configurations (see Table I). Table II lists 80 $4lnl'$ configurations as well as 95 $3lnl'$ configurations which are included to take into account the contributions of the $4lnl'$ configurations to DR rate coefficients of the excited $3lnl'$ states. The resulting list of levels, included in the set of configurations given in Table I, consists of 929 even-parity and 976 odd-parity states, while the configurations from Table II contain

905 even-parity and 979 odd-parity states.

The atomic energy levels, radiative transition probabilities and autoionization rates were calculated using the atomic structure code of Cowan [16, 17]. The scaling of electrostatic integrals in Cowan code allows to correct for correlation effects and obtain good agreement with experimental energies. We used one scaling factor (0.85) for all electrostatic integrals. The version of Cowan code used here [17] allowed us to remove transitions with small values of transition rates A_r below 10^5 s^{-1} . Even with this limitation the resulting list includes 172692 radiative transitions between the $3ln_1l_1$ and $3l'n_2l_2$ (with $n_1, n_2=3-12$; $l_1 \leq n_1 - 1$, $l_2 \leq n_2 - 1$; $l, l'=s, p, d$) states and 165806 transitions between the $3ln_1l_1$ and $4l'n_2l_2$ (with $n_1=3-12$, $l_1 \leq n_1 - 1$, $n_2=4-7$; $l_2 \leq n_2 - 1$; $l=s, p, d$; $l'=s, p, d, f$) states.

The relativistic many-body perturbation theory method (RMBPT code) was also used for calculating energy and radiative transition probabilities. This method was described in detail in Refs. [18, 19].

The results of calculations are given in Tables III - VII. In Tables III and IV, the theoretical (Cowan and RMBPT) energies for the $3l3l'$ and $3l4l'$ levels of Fe^{14+} ion are compared with the recommended NIST data [20] and other theoretical $3l3l'$ and $3l4l'$ excitation energies [21–23]. The SUPERSTRUCTURE code was used in Ref. [21], the configuration interaction with relativistic correction (CIV3 code) was employed in Refs. [22, 23], and the General Relativistic Atomic Structure Package (GRASP code) was used in Ref. [23]. Those data are given in columns “SPSTR”, “CIV”, and “GRASP” of Table III and IV, respectively.

As seen in Table III, the smallest differences between the theoretical calculations and NIST recommended data are for the present results obtained by the RMBPT code (about 0.1%). Slightly worse agreement of about 0.1% to 0.3% is noticed for the CIV3 results. The largest disagreement between theoretical calculations and NIST data is for the $3s3d^1 D_2$ level: 1000 cm^{-1} for the RMBPT and CIV3 codes, 10000 cm^{-1} for the COWAN and GRASP codes, and 15000 cm^{-1} for SUPERSTRUCTURE code. However, the smallest disagreement between theoretical calculations and NIST data is for the $3p^2 \ ^1D_2$ level: 6 cm^{-1} for the RMBPT code, 612 cm^{-1} for the GRASP code, 752 cm^{-1} for SUPERSTRUCTURE code.

The RMBPT and CIV3 [22, 23] results given in Table IV for the $3s4l'$ states agree with the NIST recommended data [20] better than the results obtained by the GRASP [23] and SUPERSTRUCTURE [21] codes. Unfortunately, there are only a few NIST energies for the $3p4f$ states and no data for the $3p4s$, $3p4p$, and $3p4d$ states. Note that there is large

disagreement of about 3000 cm^{-1} to 15000 cm^{-1} between the RMBPT and CIV3 results for the $3p4l'$ states. This difference could be explained by contribution of correlation correction for Mg-like Fe. The second-order contribution obtained by the RMBPT code for Fe^{14+} is about 10000 cm^{-1} to 30000 cm^{-1} for different states. Detailed discussion about contribution of correlation correction for the $3l3l'$ states in Mg-like ions were given in Refs. [19].

As seen in Table IV, the difference in the energy for the three $3p4f \ ^3G_J$ levels between the RMBPT and NIST data (350 cm^{-1} to 580 cm^{-1}) is smaller than that between the CIV3 and NIST data (3500 cm^{-1} to 15500 cm^{-1}) by a factor of 10 to 20. Note the difference between our RMBPT and COWAN data is about 2000 cm^{-1} to 3000 cm^{-1} for all $3l4l'$ states.

In Table V, we compare our results for energies of $4l4l'$ states obtained by the two codes, Cowan and RMBPT shown in the columns (a) and (b), respectively. Unfortunately, there is no recommended data for the $4l4l'$ states. One can see from Table V that disagreement between the results obtained by two codes is about 500 cm^{-1} to 3000 cm^{-1} for most of states except for the singlet states, $4s4p \ ^1P_1$, $4p^2 \ ^1S_0$, $4p4d \ ^1P_1$, $\ ^1F_3$, $4sp4f \ ^1D_2$, and $4d^2 \ ^1S_0$, $\ ^1G_4$. Different contribution of correlation corrections for singlet and triplet states was discussed in Ref. [18]. In Table V, the weighted sum of radiative transition rates ($\sum gA_r$ in s^{-1}), and the weighted autoionization rates (gA_a in s^{-1}) for the $4l4l'$ excited states of Mg-like Fe below the first 3s threshold ($I=3,686,000 \text{ cm}^{-1}$) and the second 3p threshold ($I=3,963,000 \text{ cm}^{-1}$) are also presented. Note that the $4l4l'$ excited states in Fe^{14+} are situated under the third 3d threshold ($I=4,361,000 \text{ cm}^{-1}$). The $4s4p \ ^3P_J$ levels are very near to the first threshold (about 1 eV) and the $4s^2 \ ^1S_0$ state is not autoionizing either.

In Table VI, the wavelengths λ (in Å) and transition rates A_r (in units of 10^8 s^{-1}) for the $3s3p - 3p^2$, $3s3p - 3s3d$, $3s3d - 3p3d$, and $3p^2 - 3p3d$ transitions are presented. Both LS -allowed (triplet-triplet and singlet-singlet) and intercombination (triplet-singlet) transitions are included here. Our results, obtained from the Cowan (columns 5 and 8) and RMBPT (columns 6 and 9) codes, can be compared with the NIST recommended data [20] shown in columns 7 and 10. The uncertainties in the recommended values were estimated to be less than 10% based on comparisons with experimental results from lifetime and emission measurements. Our theoretical results are seen to agree with each other and with the NIST data at the 10% to 30% level.

Additional comparison of our results with the recommended data [20] for the $3s^2 - 3s4p$, $3s3p - 3s4d$, $3s3p - 3s4s$, $3s3d - 3s4f$, $3p^2 - 3p4d$, and $3p3d - 3p4f$ transitions are given

in Table VII. The Cowan data for wavelengths are in good agreement with the NIST data [20]. The difference is only 0.1% to 0.3%. There is also in good agreement of 3% to 20% for transition rates for the $3s^2 - 3s4p$, $3s3d - 3s4f$, $3p^2 - 3s4f$, and $3p3d - 3p4f$ transitions; however, there is much larger disagreement for $3s3p\ ^1P_1 - 3s4d\ ^1D_2$ and $3p3d\ ^3F_3 - 3p4f\ ^3G_4$ transitions.

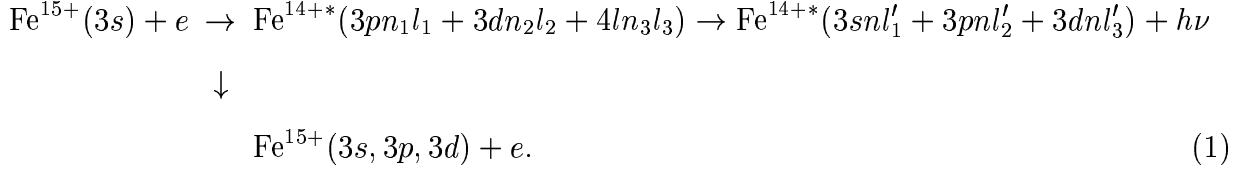
Wavelengths λ , autoionization rates A_a (in s^{-1}), sum of weighted radiative rates $\sum gA_r$ (in s^{-1}), and weighted radiative rates gA_r (in s^{-1}) for transitions between the $3ln_1l_1$ and $3l'n_2l_2$ (with $n_1, n_2=3-12$; $l_1 \leq n_1 - 1$, $l_2 \leq n_2 - 1$; $l, l'=s, p, d$) states are given in Tables VIII and IX. Note that one does not need all 172962 transitions to calculate the DR rate coefficients to excited states, but rather only the transitions from the excited states which are under the first threshold $1s^22p^22p^63s$ to the autoionizing states which are above the first threshold $1s^22p^22p^63s$. The $3dnl$ states become autoionizing states for $n \geq 7$, the $3pnl$ states become autoionizing states for $n \geq 10$, and the $3snl$ states do not autoionize for any n . Thus, we obtain 56875 transitions from the excited even-parity states to the $1s^22p^22p^63lnl'$ autoionizing odd-parity states (Table VIII) and 63108 transitions from the excited odd-parity states to the $1s^22p^22p^63lnl'$ autoionizing even-parity states (Table IX). In Tables VIII and IX, we choose for illustrations transitions with the large intensity factor Q_a that we will discuss in the next section.

Wavelengths, autoionization rates, sums of weighted radiative rates, and weighted radiative rates for transitions between the $3l'nl$ (with $n=3-12$; $l \leq n-1$ $l'=s, p, d$) non-autoionizing states and the $4l'nl$ ($n=4-7$, $l \leq n-1$) autoionizing states are given in Tables X and XI. Note that all $4l'nl$ states are autoionizing states except for the $4s^2\ ^1S_0$ state.

In the fifth column with heading A_a of Tables VIII–XI the autoionization rates relative to the first threshold, $1s^22s^22p^63s$, are given. Next column with heading $\sum A_a$ in Tables VIII–XI shows autoionization rates as sum of A_a calculated relative to the $1s^22s^22p^63l$ thresholds with $l = s, p, d$. A column with the heading E_S in Tables VIII–XI lists excitation energies E_S relative to the first threshold $1s^22s^22p^63s$ in eV. The E_S energy for the second and third thresholds equal to 36 eV and 84 eV, respectively. Of course, the $\sum A_a$ is equal to the A_a for $0 \leq E_S \leq 36$ eV.

III. DIELECTRONIC SATELLITE SPECTRA

The DR process to bound states of the Mg-like ion occurs as an electron capture by the Na-like ion to the autoionizing states of the Mg-like ion followed by the radiative decay to the singly excited bound states:



The ground state of Fe^{15+} , $3s$, is taken to be the initial state. The $3pn_1l_1$ ($n_1 \geq 10$), $3dn_2l_2$ ($n_2 \geq 7$), and $4ln_3l_3$ ($n_3 \geq 4$) levels are taken into account as autoionizing intermediate states.

During the DR process, the dielectronic satellite lines are emitted as electron transitions from doubly excited autoionization states to singly excited bound states. Radiative transitions from the $3pnl$ states to $3snl$ states and those from the $4pnl$ states to $3snl$ states give rise to satellite lines of the $3p - 3s$ and $4p - 3s$ lines of the Na-like iron. There also exist DR satellite transitions from autoionizing states $3dnl$ to $3dn'l$ and from $3pnl$ to $3pn'l$ with the change of the quantum principal number n . They appear at a shorter wavelength region.

The effective emission rate coefficient of the dielectronic satellite line is

$$C_S^{eff}(j, i) = 3.3 \times 10^{-24} \left(\frac{I_H}{kT_e} \right)^{3/2} \frac{Q_d(j, i)}{g_0} \exp\left(-\frac{E_S(i)}{kT_e}\right) \text{ photons cm}^{-3}\text{s}^{-1}, \quad (2)$$

$$Q_d(j, i) = \frac{g(i)A_a(i, i_0)A_r(j, i)}{\sum_{i'_0} A_a(i, i'_0) + \sum_k A_r(k, i)}, \quad (3)$$

where I_H is the ionization potential of hydrogen, j denotes the bound state, i is the autoionizing state, i_0 is the initial state, that is the ground state $3s$ of the Na-like ion, and i'_0 is the possible final state for autoionization such as, e.g., $3s$, $3p$ and $3d$. The statistical weight of the initial state i_0 is $g_0 = 2$, $g(i)$ is the statistical weight for a doubly excited state, $A_a(i, i_0)$ is the autoionization rate from i to i_0 , $A_r(j, i)$ is the radiative transition probability from i to j , $E_S(i)$ is the excitation energy of the autoionizing state i relative to the first threshold, $3s$, and T_e is the electron temperature. Maxwellian distribution is assumed for electron velocities. For some cases, $A_a \gg A_r$ and then Q_d is roughly estimated as $Q_d(j, i) \approx g(i)A_r(j, i)$.

As has already been mentioned above, autoionization rates $A_a(i, 3s)$, sum of autoionization rates $\sum A_a(i, i'_0) = A_a(i, 3s) + A_a(i, 3p) + A_a(i, 3d)$, and excitation energies E_S for even- and odd-parity states are presented in columns 5, 6, and 7 of Tables VIII–XI. Weighted radiative rates $g_i A_r(j, i)$, sum of weighted radiative rates $\sum_k g_i A_r(k, i)$, and wavelengths λ for dipole-allowed transitions are given in columns 8, 9, and 10 of Tables VIII–XI, respectively. The last two columns of Tables VIII–XI list relative intensity factors $Q_d(j, i)$ and effective emission rate coefficients $C_S^{eff}(j, i)$ defined by Eq. (2). The $C_S^{eff}(j, i)$ values are given for $T_e = 10$ eV. Note that the number of transitions listed in Tables VIII–XI is limited by including transitions with large values of relative intensity factors $Q_d(j, i)$. We include transitions with $Q_d(j, i) > 1.0 \times 10^{11} \text{ s}^{-1}$ in Tables VIII, IX and transitions with $Q_d(j, i) > 4.0 \times 10^{11} \text{ s}^{-1}$ in Table X, XI. That gives 104, 151, 94, and 99 out of total 56875, 63108, 54090, and 588829 transitions in Tables VIII, IX, X, and XI, respectively. The largest value of $Q_d(j, i)$ gives the largest value of effective emission rate coefficients $C_S^{eff}(j, i)$ when the ratio of E_S and kT_e is not very large.

Figures 1 and 2 show examples of dielectronic satellite line spectra for $kT_e = 10$ eV for two wavelength ranges. In these figures, we include data for 3322 even-odd parity transitions and 3901 odd-even parity transitions. Some of those transitions are presented in Tables VIII to XI. Wavelengths (given in the column 10 of Tables VIII to XI), effective emission rate coefficients $C_S^{eff}(j, i)$ (in units of $10^{-15} \text{ cm}^3/\text{s}$, in the column 12 of Tables VIII to XI) and Gaussian profiles with spectral resolution $R \equiv \lambda/\Delta\lambda = 500\text{--}700$ are used to synthesize these spectra. The limited set of transitions are included with $C_S^{eff}(j, i) > 10^{-15} \text{ cm}^3/\text{s}$. The synthetic spectrum of dielectronic satellite lines from Fe^{14+} ion at $T_e = 10$ eV is divided into eight parts: $\lambda = 25 - 100 \text{ \AA}$, $\lambda = 100 - 240 \text{ \AA}$, $\lambda = 240 - 400 \text{ \AA}$, and $\lambda = 400 - 520 \text{ \AA}$, (Fig. 1), $\lambda = 520 - 630 \text{ \AA}$, $\lambda = 660 - 780 \text{ \AA}$, $\lambda = 840 - 1040 \text{ \AA}$, and $\lambda = 1400 - 2000 \text{ \AA}$ (Fig. 2).

The strong lines shown in Fig. 1 are due to the Rydberg transitions $3p^2 - 3p10d$, $3d^2 - 3d7f$, $3p4f - 3p10g$, $3p5d - 3p10f$, $3p5f - 3p10g$, and $3p6f - 3p10g$ ($\lambda = 32, 40, 75, 127, 132, 224 \text{ \AA}$, respectively). The strong lines in the region of $50\text{--}65 \text{ \AA}$ are due to the $3p4s - 4s4d$, $3s4s - 4s4p$, $3p4p - 4s4p$, and $3s4d - 4s4p$ transitions. The last transition is the result of strong mixing of configurations $3s4d$ and $3p4p$. A large number of satellite lines of $3s - 3p$ transitions ($3s10l - 3p10l$ with $l = f, g, h, i, k$) are responsible for the spectra shown in Figs. 1 in the region of $\lambda = 330 - 335 \text{ \AA}$. The strong contributions of the $3d6h - 3d7i$

and $3d6g - 3d7h$ transitions to the region of $\lambda = 540 - 560 \text{ \AA}$ and the $3p8h - 3p10i$ and $3p8i - 3p10k$ transitions to the region of $\lambda = 715 - 720 \text{ \AA}$ are shown in Fig. 2. There are contributions of the transitions $3p8h - 3p11i$ and $3p8i - 3p11k$ to the region of $\lambda = 980 - 990 \text{ \AA}$ and the the $3p9i - 3p10k$ transitions to the region of $\lambda = 1710 \text{ \AA}$ of the spectrum of Fe^{14+} ion at $T_e = 10 \text{ eV}$.

IV. DIELECTRONIC RECOMBINATION RATE COEFFICIENTS FOR EXCITED STATES

The DR rate coefficients for excited states are obtained by summation of the effective emission rate coefficients (Eq. (2)) for DR processes through all possible intermediate doubly excited states:

$$\alpha_d(i_0, j) = 3.3 \times 10^{-24} \left(\frac{I_H}{kT_e} \right)^{3/2} \frac{1}{g_0} \sum_i Q_d(j, i) \exp \left(-\frac{E_s(i)}{kT_e} \right). \quad (4)$$

For the DR process described by Eq. (1), one has to calculate $\alpha_d(i_0, j)$ with $i_0 = 3s$ and all possible excited states j of Fe^{14+} with energies below the first threshold, $3s$ ($3,686,000 \text{ cm}^{-1}$). Among the $3snl$, ($n=3-12$), $3pnl$, ($n=3-9$), and $3dnl$, ($n=3-6$) states, 444 states of odd parity and 419 states of even parity have energies lower than $3,686,000 \text{ cm}^{-1}$.

The sum over i includes the autoionizing $3pnl$ states with $n \geq 10$, $3dnl$ states with $n \geq 7$, and $4lnl$ states with $n \geq 4$. In Figs. 3-5, we illustrate the contributions to $\alpha_d(3s, j)$ for some of j 's from sum over i with $n = 7-12$ for autoionizing $3lnl'$ states and from sum over i with $n = 4-7$ for autoionizing $4lnl'$ states. Those contributions are illustrated by curves "1" with designations "1=[$n=7-12$]" and curves "3" with designations "3=[$n=4-7$]", respectively. In Fig. 3, we show $\alpha_d(3s, j)$ with $j = 3s3p \ ^3P_1$, $3p3d \ ^3P_1$, $3s^2 \ ^1S_0$, $3s3d \ ^3D_2$, $3s4s \ ^1S_0$, and $3p4p \ ^3D_1$. We can see from these figures that the curves "3" are above the curves "1" for the $3s4s \ ^1S_0$, and $3p4p \ ^3D_1$ levels and under the curves "1" for $3s3p \ ^3P_1$, $3p3d \ ^3P_1$, $3s^2 \ ^1S_0$, and $3s3d \ ^3D_2$ levels. In Figs. 4, we illustrate the contributions to $\alpha_d(3s, j)$ of the odd-parity states with $j = 3s4p \ ^1P_1$, $3p4s \ ^3P_1$, $3s4f \ ^3F_3$, $3p4d \ ^3P_2$, $3d4p \ ^3F_2$, and $3d4f \ ^1D_2$. For all these states the contributions of the $3lnl'$ autoionizing states are more important for low temperature (1 eV to 5 eV) than the contributions of $4lnl'$ autoionizing states while their relative contributions are opposite for higher temperatures. The same behavior of the curves describing the $3lnl'$ and $4lnl'$ states for $\alpha_d(3s, j)$ of even-parity states is seen from the plots

shown in Fig. 5 except for two cases with $j = 3d4d \ ^3G_4$ and $j = 3d4s \ ^3D_1$. In the first case with $j = 3d4d \ ^3G_4$, the curve “1” is above the curve “3”, however, in the case with $j = 3d4s \ ^3D_1$, the curve “3” is above the curve “1”. We can see that the contribution of the $4lnl'$ in the sum over i in Eq. (4) is important for calculation of $\alpha_d(3s, j)$ for many values of j .

In order to estimate contributions from the high- n autoionizing states to the DR rate coefficients for excited states which are obtained by sum over i with $n > 12$ for autoionizing $3lnl'$ states and sum over i with $n > 7$ for autoionizing $4lnl'$ states, we use empirical scaling laws [9], which can be only implemented to include the one-electron $3s - np$, $3p - ns$, $3p - nd$, $3d - np$, and $3d - nf$ dipole transitions. Additional contributions from high- n states appear for the first low-lying configurations $3l3l'$ and $3l4l'$. For these configurations the $[3s3p - 3pnp]$, $[3s3d - 3dnp]$, $[3p3d - 3pnp, 3pnf, 3dns, 3dnd]$, $[3p^2 - 3pns, 3pnd]$, and $[3d^2 - 3dnp, 3dnf]$ transitions with $n > 12$ are to be included as well. Transitions with $n > 7$ are considered for the $3l4l'$ configurations: $[3s4s - 4snp]$, $[3s4p - 4pnp]$, $[3s4f - 4fnp]$, $[3p4s - 4sns, 4snd]$, $[3p4p - 4pns, 4pnd]$, $[3p4d - 4dns, 4dnd]$, $[3p4f - 4fnns, 4fnd]$, $[3d4s - 4snp, 4snf]$, $[3d4p - 4pnp, 4pnf]$, $[3d4d - 4dnp, 4dnf]$, and $[3d4f - 4fnp, 4fnf]$.

To estimate $Q_d(j, i)$ in Eq.(2) for autoionization states i with high principal quantum number n for the $3lnl'$ states and for the $3s - np$, $3p - ns, nd$, and $3d - np, nf$ dipole transitions, we used our calculated data for $n = 11$ and the $1/n^3$ scaling law for A_a and A_r . For example, the formulas for the $3s3p - 3pnp$ case are:

$$A_a(3pnl \ ^{1,3}L_J) = \left(\frac{11}{n}\right)^3 A_a(3p11l \ ^{1,3}L_J), \quad (5)$$

$$\begin{aligned} & A_r(3s3p \ ^{1,3}P_{J'} - 3pnl \ ^{1,3}L_J) \\ &= \left(\frac{11}{n}\right)^3 A_r(3s3p \ ^{1,3}P_{J'} - 3p11l \ ^{1,3}L_J) \\ &\quad \times \left(\frac{E(3s3p \ ^{1,3}P_{J'} - 3pnl \ ^{1,3}L_J)}{E(3s3p \ ^{1,3}P_{J'} - 3p11l \ ^{1,3}L_J)}\right)^3. \end{aligned} \quad (6)$$

In order to obtain the energies of the $3pnl \ ^{1,3}L_J$ states as a function of nl , the following asymptotic formula was proposed in Ref. [24].

$$E(3pnl) - E(3p) = -\frac{1}{2n^2} \left(Z - 11 + \frac{b(l)}{n}\right)^2, \quad (7)$$

where $b(s) = 2.873$, $b(p) = 1.761$, $b(d) = 0.721$, $b(f) = 0.137$, and $b(g) = 0.010$ [24]. The energy differences in Eq. (7) can be found using the following formula:

$$\begin{aligned} & E \left(3s3p \ ^1,3P_{J'} - 3pnl \ ^1,3L_J \right) \\ &= E \left(3s3p \ ^1,3P_{J'} - 3p11l \ ^1,3L_J \right) - \frac{225}{2} \left(\frac{1}{n^2} - \frac{1}{11^2} \right) \times 219474 \text{ cm}^{-1}. \end{aligned} \quad (8)$$

A similar formula was used for the excitation energies $E_S(i)$ in Eq. (4) when $i=3pnl \ ^1,3L_J$:

$$E_S(3pnl \ ^1,3L_J) = E_S(3p11l \ ^1,3L_J) - \frac{225}{2} \left(\frac{1}{n^2} - \frac{1}{11^2} \right) \times 219474 \text{ cm}^{-1}. \quad (9)$$

Using these scaling formulas for $A_a(3pnl \ ^1,3L_J)$ and $A_r(3s3p \ ^1,3P_{J'} - 3pnl \ ^1,3L_J)$, we calculated $Q_d(3s3p \ ^1,3P_{J'} - 3pnl \ ^1,3L)$ as a function of n and then, using Eq. (9) for E_S , we calculate the sums over n for $\alpha_d(3s, 3s3p \ ^1,3P_J)$ vs. n and T_e .

To estimate $Q_d(j, i)$ in Eq.(2) for autoionizing states i with high principal quantum number n for the $3l4l'$ states, such as the $3s4s - 4snp$ dipole transitions, we used the calculated data for $n = 7$ and the $1/n^3$ scaling law for A_a and A_r as shown above in Eqs. (5) - (9).

The results of the calculations are illustrated in Figs. 3-5. In order to check the scaling, the explicitly calculated data for $n = 12$ and the scaled data for $n = 12$ obtained from the calculated data for $n = 11$ were compared. It was found that the difference is about 10 % except for some cases when mixing of configurations is very important. In Figs. 3-5, the contribution of scaled data from $n = 12$ up to $n = 1000$ (curve "2") for the $3lnl'$ autoionizing states and from $n = 8$ up to $n = 1000$ (curve "4") for the $4lnl'$ autoionizing states are presented. The dependence of the present results on the upper limit of n was also tested. We found that there is a small difference for low temperature (4% for $T_e = 10$ eV) with $n = 40$ being the upper limit, and the difference is increased for high temperatures reaching 7% for $T_e = 30$ eV.

The high- n state contributions are very important for high temperature. One can see from Figs. 3-5 that for $T_e > 10$ eV the curves "2" describing contributions of the high $3lnl'$ states $n=13-1000$ are above the curves "1" describing contributions of the low $3lnl'$ states $n=7-12$ (see plots for the $3s3p \ ^3P_1$, $3s^2 \ ^1S_0$, $3p4p \ ^3D_1$, $3s4f \ ^3F_3$, $3p4s \ ^3P_1$, $3p4d \ ^3P_2$, $3p4f \ ^3G_3$, and $3p4f \ ^3G_5$). The contribution of the high- n $4lnl'$ states becomes important for very high $T_e > 100$ eV. The curves "4" describing contributions of the high $4lnl'$ states with $n=8-1000$ are mostly below the curves "3" showing contributions of the low $4lnl'$ states with $n=4-7$; however, the curves "4" are above curves "2" and "1" for $3s4s \ ^1S_0$, $3s4p \ ^1P_1$,

$3p4s\ ^3P_1$, $3s4f\ ^3F_3$, $3p4f\ ^3G_5$, and $3d4s\ ^3D_1$. Sum of the contributions presented by the curves “1”, “2”, “3”, and “4” gives the DR rate coefficients for excited states.

The results of our calculations of $\alpha_d(3s, j)$ are shown in Figs. 6–8 (even-parity j 's) and Figs.9–11 (odd-parity j 's). The electron temperature for these plots varies from $T_e=0.1$ eV to $T_e=1600$ eV. As can be seen from Figs. 6–11, the DR rate coefficients can be divided into three different groups. There are curves without any maximum as, e.g., $\alpha_d(3s, j)$ for $j = 3p^2\ ^1D_2\ ^1S_0$, 3P_0 , 3P_1 (Fig. 6) and $3s3d\ ^1D_2$ (Fig. 6). As the second group, there are curves with two maxima (at about 0.6 - 0.8 eV and 19.0 eV), e.g., $\alpha_d(3s, j)$ for $j = 3d4s\ ^3D_J$ (Fig. 7) and $3p4s\ ^3P_0$, 3P_1 (Fig. 10). Most of the DR rate coefficients exhibit only one maximum around 0.8 eV to 2.3 eV or 19.0 eV. The limited set of tabulated data of $\alpha_d(3s, j)$ for 38 points of electron temperature $0.1\text{ eV} < T_e < 1600\text{ eV}$ are presented in Table XII (70 states out of 419 states of even parity) and Table XIII (70 states out of 444 states of odd parity).

V. TOTAL DIELECTRONIC RECOMBINATION RATE COEFFICIENTS

The total DR rate coefficients are obtained by summation of the rate coefficients of DR processes through all possible intermediate singly and doubly excited states:

$$\alpha_d(i_0) = 3.3 \times 10^{-24} \left(\frac{I_H}{kT_e} \right)^{3/2} \frac{1}{g_0} \sum_i \sum_j Q_d(j, i) \exp \left(-\frac{E_s(i)}{kT_e} \right). \quad (10)$$

We have already discussed the contribution from doubly excited states with high- n levels to the DR rate coefficients (sum over i in Eq. (4)). For the total DR rate coefficients one has to consider also the contribution from singly excited states with high n , i.e., the $3snl$ states. For these states, the most important transitions are $3snl - 3pnl$ [9, 11, 12, 14, 15].

To estimate $Q_d(j, i)$ in Eq. (3) for $j = 3snl$ and $i = 3pnl$ for $n > 12$, we used the calculated data for $n = 11$ and the $1/n^3$ scaling law for A_a (Eq. (5)) and E_s (Eq. (9)). The values of A_r for the $3snl - 3pnl$ transitions are almost independent of n since this is a single-electron $3s - 3p$ transition. One has to take into account the change of the energy difference following Eq. (7):

$$A_r \left(3snl^{1,3}L'_{J'} - 3pnl\ ^{1,3}L_J \right) = A_r \left(3s11l^{1,3}L'_{J'} - 3p11l\ ^{1,3}L_J \right) \times \left(\frac{E(3snl^{1,3}L'_{J'} - 2pnl\ ^{1,3}L_J)}{E(3s11l^{1,3}L'_{J'} - 2p11l\ ^{1,3}L_J)} \right)^3. \quad (11)$$

Using asymptotic formula given by Eq. (8), we obtain in first approximation:

$$E \left(3snl^{1,3}L'_{J'} - 3pnl^{1,3}L_J \right) = E \left(3s11l^{1,3}L'_{J'} - 3p11l^{1,3}L_J \right) \quad (12)$$

and finally [11]:

$$A_r \left(3snl^{1,3}L'_{J'} - 3pnl^{1,3}L_J \right) = A_r \left(3s11l^{1,3}L'_{J'} - 3p11l^{1,3}L_J \right). \quad (13)$$

Again, the calculated data for $n = 11$ and the $1/n^3$ scaling law for A_a were used for estimates of $Q_d(j, i)$ in Eq.(3) for autoionization states i with high n . For the $3snl - 3pnl$ transitions, the scaling begins from $n = 12$. Using scaling formulas for $A_r(3snl^{1,3}L'_{J'} - 3pnl^{1,3}L_J)$ (Eq.(13)) and $A_a(3pnl^{1,3}L_J)$ (Eq.(5)), we calculated $Q_d(3snl^{1,3}L'_{J'} - 3pnl^{1,3}L_J)$ and then, using Eq. (9) for E_S , we calculated $C_S^{\text{eff}}(3snl^{1,3}L'_{J'} - 3pnl^{1,3}L_J)$. The sum over LSJ and for $C_S^{\text{eff}}(3snl^{1,3}L'_{J'} - 3pnl^{1,3}L_J)$ gives data for $C_S^{\text{eff}}(3snl - 3pnl)$ as a function of nl and T_e .

Results of calculations for $C_S^{\text{eff}}(3snl - 3pnl)$ are illustrated in Fig. 12 for the $3sns - 3pns$, $3snp - 3pnp$, $3snf - 3snf$, and $3snh - 3snh$ transitions. In Fig. 12, we demonstrate the contribution of scaled data for for $n = 13$ to $n = 40$ (curves “2”), and for $n = 13$ to $n = 1000$ (curves “3”). As one can see from these plots, the difference between the results calculated with $n \leq 40$ and $n \leq 1000$ increases with increasing temperature (20-30% for $T_e = 5$ eV, 50-70% for $T_e = 19$ eV). It is worth noting that the convergence for the $3snl - 3pnl$ transitions is slower than for the $3l_13l_2 - 3lnl'$ and $3l_14l_2 - 4lnl'$ transitions considered in the previous section. The results of the summed calculated-data for $C_S^{\text{eff}}(3lnl - 3pnl)$ from $n = 10-12$ are also presented in Figs. 12 (curve “1”). As can be seen from Figs. 12, the curve “1” describing those data is above the curves “2” and “3” describing the scaled data only for low electron temperature T_e . For $T_e > 10$ eV, the curve “1” is under the curves “2” ($n = 13-40$) and the curves “3” describing contribution from the scaled data for $n = 13$ to $n = 1000$. We already mentioned previously that the importance of the contributions from highly excited states for the DR rate coefficients was emphasized by Hahn [25] and confirmed by the results of Refs. [9, 11, 12, 14, 15].

The final result of our $3snl - 3pnl$ scaling is shown by Fig. 13. In this figure, $\sum_{n=13}^{n=1000} C_S^{\text{eff}}(3snl - 3pnl)$ is presented as a function of l and T_e . As seen in Fig. 13, the value of $\sum_{n=13}^{n=1000} C_S^{\text{eff}}(3snl - 3pnl)$ increases with increasing l up to $l = 6$ (“ ni ” curve), while for $l = 7$ (“ nk ” curve) it becomes smaller.

The total DR rate coefficients (α_d^{tot} in cm^3/s) are calculated as a sum of five terms: α_d^{3a} , α_d^{3b} , α_d^{33} , α_d^{4a} , and α_d^{4b} :

$$\alpha_d^{3a} = \sum_{n=10}^{n=12} C_S^{eff} (3l_1 n_2 l_2 - 3l' n l), \quad \alpha_d^{3b} = \sum_{n=13}^{n=1000} C_S^{eff} (3l_1 n_2 l_2 - 3l' n l),$$

$$\alpha_d^{4a} = \sum_{n=4}^{n=7} C_S^{eff} (3l_1 n_2 l_2 - 4l' n l), \quad \alpha_d^{4b} = \sum_{n=8}^{n=1000} C_S^{eff} (3l_1 n_2 l_2 - 4l' n l),$$

$$\alpha_d^{33} = \sum_{n=13}^{n=1000} C_S^{eff} (3s n l - 3p n l).$$

The contributions of α_d^{3a} and α_d^{3b} are the sums from the $3l_1 n_2 l_2 - 3l' n l$ transitions with $n=10-12$ and $n=13-1000$, respectively. The parameter α_d^{33} is the contribution from the $3s n l - 3p n l$ transitions with $n=13-1000$. The contributions of α_d^{4a} and α_d^{4b} are the sum from the $3l_1 n_1 l_1 - 4l' n l$ transitions with $n=4-7$ and $n=8-1000$, respectively. The $3l_1 n_1 l_1$ excited states include the $3s n_1 l_1$ states with $n_1 = 3 - 12$ and $l = 0 - 7$, $3p n_1 l_1$ states with $n_1 = 3 - 9$ and $l = 0 - 7$, and $3d n_1 l_1$ states with $n_1 = 3 - 6$ and $0 \leq l \leq n - 1$.

The results of our calculations of α_d^{3a} , α_d^{3b} , α_d^{33} , α_d^{4a} , and α_d^{4b} are shown in Fig.14. The electron temperature for these plots varies from $T_e=0.1$ eV to $T_e=1600$ eV. It is clearly seen from this figure that the contribution from the low excited states is responsible for the total DR rate coefficient at low T_e , and contribution from the high- n excited states becomes more important with increasing temperature. The curves describing the contribution of the $3l_1 n_2 l_2 - 3l' n l$, $3s n l - 3p n l$, and $3l_1 n_1 l_1 - 4l' n l$ transitions have maxima near 19 eV, 24 eV, and 155 eV, respectively.

The tabulated data α_d^{3a} , α_d^{3b} , α_d^{33} , α_d^{4a} , α_d^{4b} , and α_d^{tot} ($\alpha_d^{tot} = \alpha_d^{3a} + \alpha_d^{3b} + \alpha_d^{33} + \alpha_d^{4a} + \alpha_d^{4b}$) are given in Table XIV as a function of electron temperature in the interval of $T_e=0.1$ eV to $T_e=1624$ eV on a logarithmic grid $T_e = 0.1 \times 1.3^{N-1}$ with $N = 1-38$.

Sum of the scaled data ($\alpha_d^{3b} + \alpha_d^{33} + \alpha_d^{4b}$) and sum of the calculated results ($\alpha_d^{3a} + \alpha_d^{4a}$) (Tables XIV) are shown in Fig. 15. The contribution from the low excited states is responsible for the total DR rate coefficient at low T_e , and contribution from the high- n excited states becomes more important with increasing temperature. The curve describing the contribution of these states has a maximum near 19 eV. The resulting curve for the total DR rate coefficient $\alpha_d(2s^2 2p)$ has two maxima for T_e near 1.4 eV and 14.6 eV. Our results are compared with the results by Gu [8] in Fig. 15. As seen in this figure, the values of $\alpha_d(3s)$ from Ref. [8] agree well with our data for $100 \text{ eV} > T_e > 10 \text{ eV}$. The disagreement for

high T_e could be explained by the inner-shell excitation of a $2l$ electron with the maximum in the region of T_e equal to 200 eV [8]. We could not comment the disagreement for small T_e since the results for low T_e are given in Ref. [8] starting from $T_e = 1$ eV only.

VI. CONCLUSION

In the present paper, we calculate a set of atomic data related to dielectronic recombination of astrophysically important Na-like ion of Fe into Mg-like Fe^{14+} .

Energy levels, wavelengths, weighted radiative transition probabilities, and autoionization rates are calculated for Mg-like iron ion using two theoretical methods; the Hartree-Fock-Relativistic method (Cowan code) and the relativistic many-body perturbation theory (RMBPT) method for limited number of states. Calculated atomic data are used to obtain the dielectronic satellite lines as well as the DR rate coefficients.

We take into account doubly excited states $3pnl$ ($n \geq 10, l \leq 7$), $3dnl$ ($n \geq 7, l \leq n-1$), and $4l'nl$ ($n \geq 4, l \leq n-1$) as intermediate resonance states with n up to 1000 to calculate the DR rate coefficients.

Most of state selective DR rate coefficients show double peaks as a function of electron temperature. The transitions through intermediate states $3lnl$ and $4lnl$ make a peak in the DR rate coefficients at T_e at about 0.6 - 0.8 eV and 19.0 eV.

Configuration mixing for $[3sns + 3pnp + 3dnd]$ and $[3snp + 3pns + 3pnd + 3dnp]$ states plays an important role for the DR rate coefficients of $3snl$ levels with $n \leq 7$ at low temperature.

We calculated the state-selective DR rate coefficients from the ground state of Na-like Fe ion to the bound states of Mg-like Fe ion in this paper. The total DR rate coefficient is in good agreement with the previous results by Gu [8] for middle temperatures.

The state selective rate coefficients can be used in a collisional-radiative model for examining the population kinetics and plasma diagnostics for recombining plasma. We plan to calculate spectral line intensities of Mg-like Fe ions in a collisional-radiative model with the DR rate coefficients obtained in this paper to compare with measurements of laboratory plasmas elsewhere.

Acknowledgments

The work of U. I. S. and T. E. C. was supported in part DOE-NNSA/NV Cooperative Agreement DE-FC08-01NV14050. U. I. S. would like to thank the members of the Atomic and Molecular Data Research Center, the National Institute for Fusion Science for their hospitality and the financial support. U. I. S. would like to thank Dr. A. Kramida for supervising the usage of his version of COWAN code. U. I. S. would like to thank Dr. M. F. Gu for sending tabulated data used in Fig. 15 of present paper.

-
- [1] M. J. May, P. Beiersdorfer, J. Dunn, N. Jordan, S. B. Hansen, A. L. Osterheld, A. Ya. Faenov, T. A. Pikuz, I. Yu. Skobelev, F. Flora, et al., *ApJ, Suppl.* **158**, 230 (2005).
 - [2] K. J. LaGattuta and Y. Hahn, *Phys. Rev. A* **30**, 316 (1984).
 - [3] D. C. Griffin and Pindzola, *Phys. Rev. A* **35**, 2821 (1987).
 - [4] T. W. Gorczyca and N. R. Badnell, *Phys. Rev. A* **54**, 4113 (1990).
 - [5] J. Linkemann, J. Kenntner, A. Müller, A. Wolf, D. Habs, D. Schwalm, W. Spies, O. Uwira, A. Frank, A. Liedtke, et al., *Nucl. Instr. and Methods Phys. Res. B* **98**, 154 (1995).
 - [6] S. B. Kraemer, G. L. Ferland, and J. R. Gabel, *ApJ* **604**, 556 (2004).
 - [7] H. Netzer, *ApJ* **604**, 551 (2004).
 - [8] M. F. Gu, *ApJ, Suppl.* **153**, 389 (2004).
 - [9] U. I. Safronova and T. Kato, *J. Phys. B* **31**, 2501 (1998).
 - [10] U. I. Safronova and T. Kato, *Phys. Scr.* **53**, 461 (1996).
 - [11] T. Kato, U. I. Safronova, and M. Ohira, *Phys. Scr.* **55**, 185 (1997).
 - [12] U. I. Safronova, T. Kato, and M. Ohira, *J. Quant. Spectr. Radiat. Transfer* **58**, 193 (1997).
 - [13] I. Murakami, U. I. Safronova, A. A. Vasilyev, and T. Kato, *At. Data Nucl. Data Tables* **90**, 1 (2005).
 - [14] I. Murakami, U. I. Safronova, and T. Kato, *Can. J. Phys.* **80**, 1525 (2002).
 - [15] I. Murakami, U. I. Safronova, and T. Kato, *J. Phys. B* **32**, 5351 (1999).
 - [16] R. D. Cowan, *The Theory of Atomic Structure and Spectra* (University of California Press, Berkeley, 1981).

- [17] URL <http://das101.isan.troitsk.ru/cowan.htm>.
- [18] M. S. Safronova, W. R. Johnson, and U. I. Safronova, *Phys. Rev. A* **53**, 4036 (1996).
- [19] U. I. Safronova, W. R. Johnson, and H. G. Berry, *Phys. Rev. A* **61**, 52503 (2000).
- [20] Yu. Ralchenko, F.-C. Jou, D.E. Kelleher, A.E. Kramida, A. Musgrove, J. Reader, W.L. Wiese, and K. Olsen (2005). NIST Atomic Spectra Database (version 3.0.2), [Online]. Available: <http://physics.nist.gov/asd3> [2006, January 4]. National Institute of Standards and Technology, Gaithersburg, MD.
- [21] A. K. Bhatia, H. E. Mason, and C. Blancard, *At. Data Nucl. Data Tables* **66**, 83 (1997).
- [22] N. C. Deb and A. Z. Msezane, *J. Phys. B* **31**, L281 (1998).
- [23] N. C. Deb, K. M. Aggarwal, and A. Z. Msezane, *ApJ, Suppl.* **121**, 265 (1999).
- [24] U. I. Safronova, I. Y. Tolstikhina, R. Bruch, T. Tanaka, F. Hao, and D. Schneider, *Phys. Scr.* **47**, 364 (1993).
- [25] Y. Hahn, *Advance in Atomic and Molecular Physics* **21**, 123 (1985).

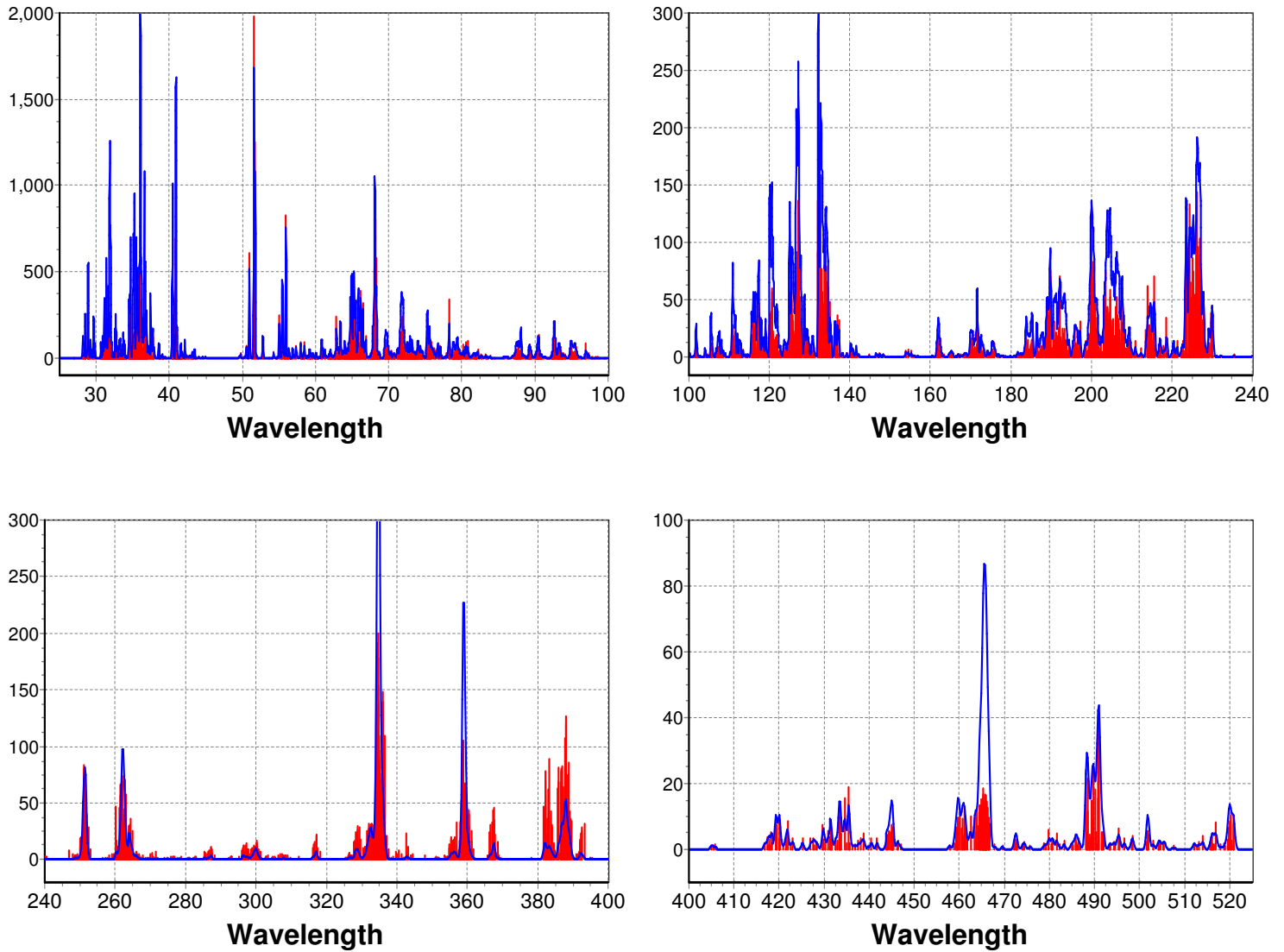


FIG. 1: Synthetic spectra of dielectronic satellite lines from Fe^{14+} ion at $T_e = 10 \text{ eV}$ for $\lambda = 25 - 520 \text{ \AA}$. Resolution power, $R = \lambda/\Delta\lambda = 500$ is assumed to produce a Gaussian profile. The scale in the ordinate is in units of $10^{-15} \text{ cm}^3/\text{s}$.

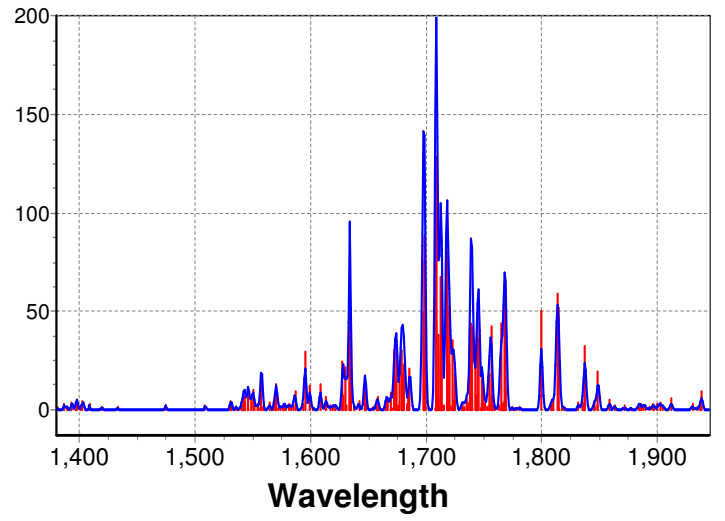
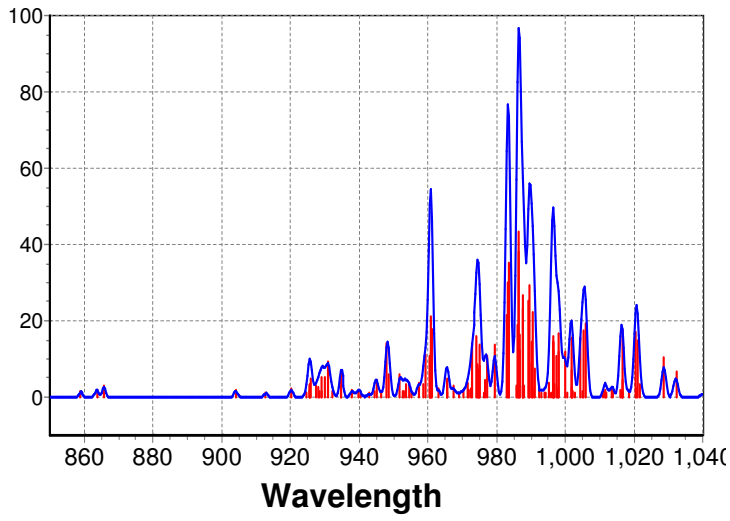
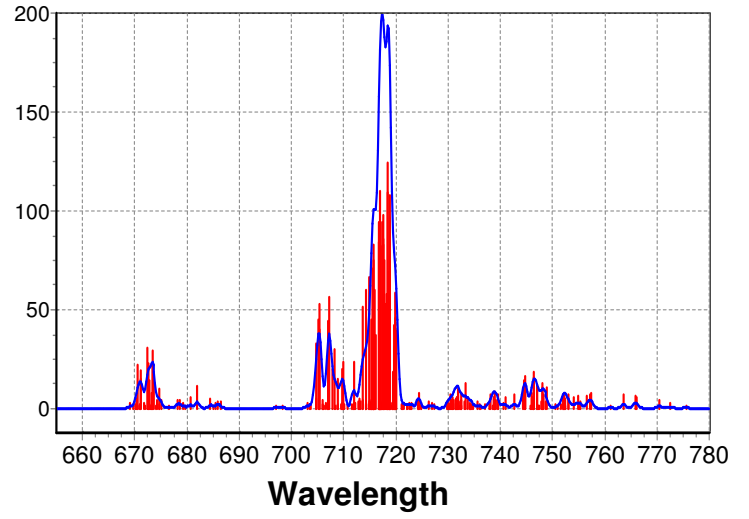
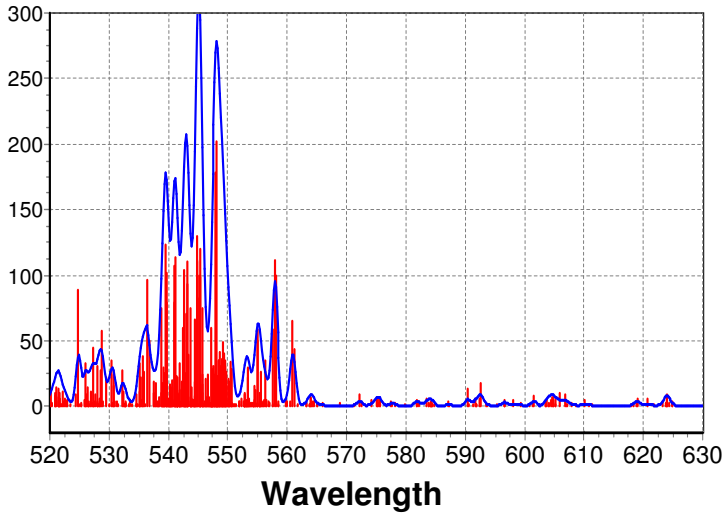


FIG. 2: Synthetic spectra of dielectronic satellite lines from Fe^{14+} ion at $T_e = 10$ eV for $\lambda = 520 - 2000$ Å. Resolution power, $R = \lambda/\Delta\lambda = 700$ is assumed to produce a Gaussian profile. The scale in the ordinate is in units of 10^{-15} cm³/s.

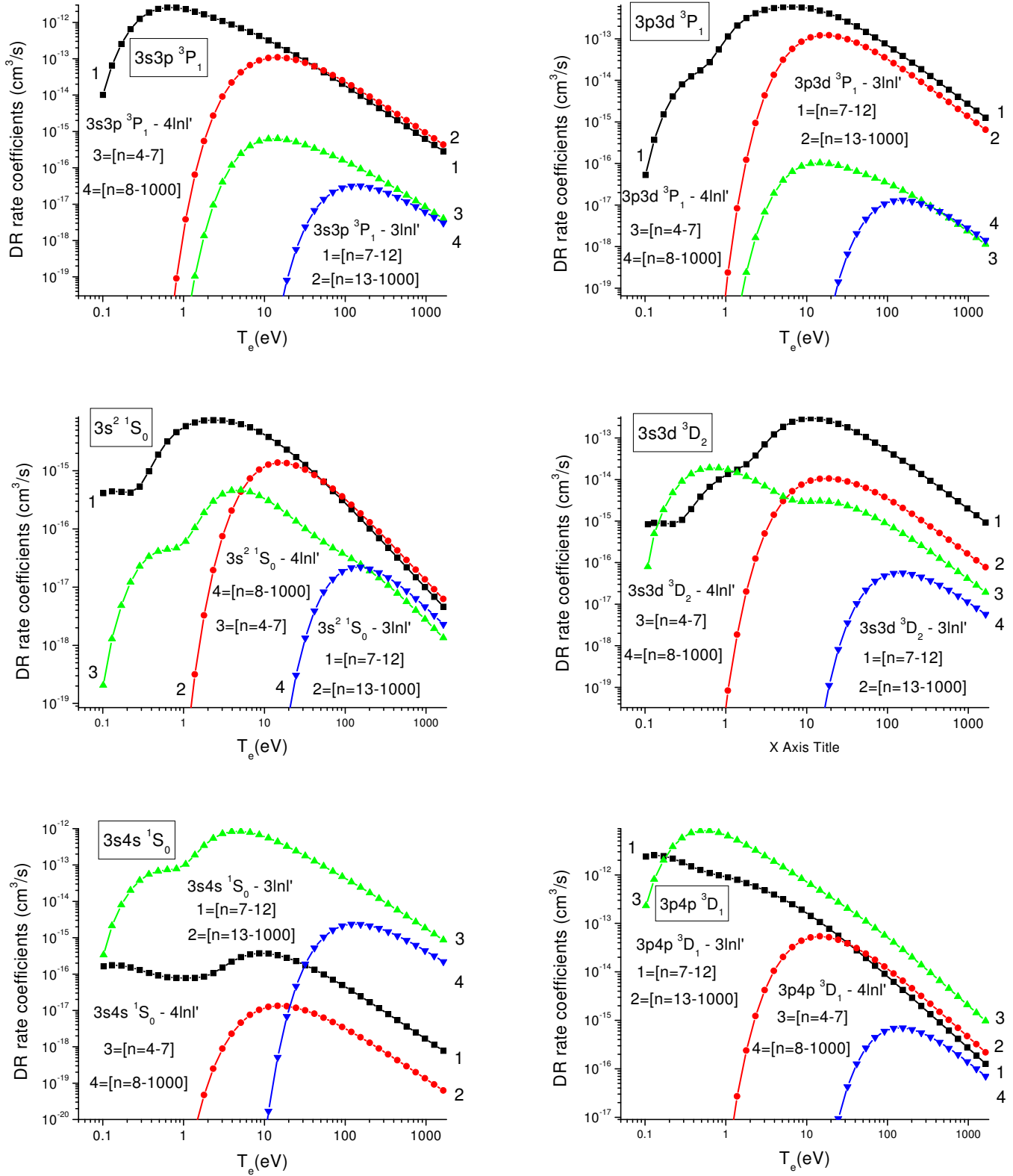


FIG. 3: Contribution of the $3lnl'$ and $4lnl'$ states to the Dielectronic Recombination rate coefficient $\alpha_d(\gamma|3s)$ for the $3l3l'$ and $3l4l'$ states as a function of T_e in Mg-like Fe.

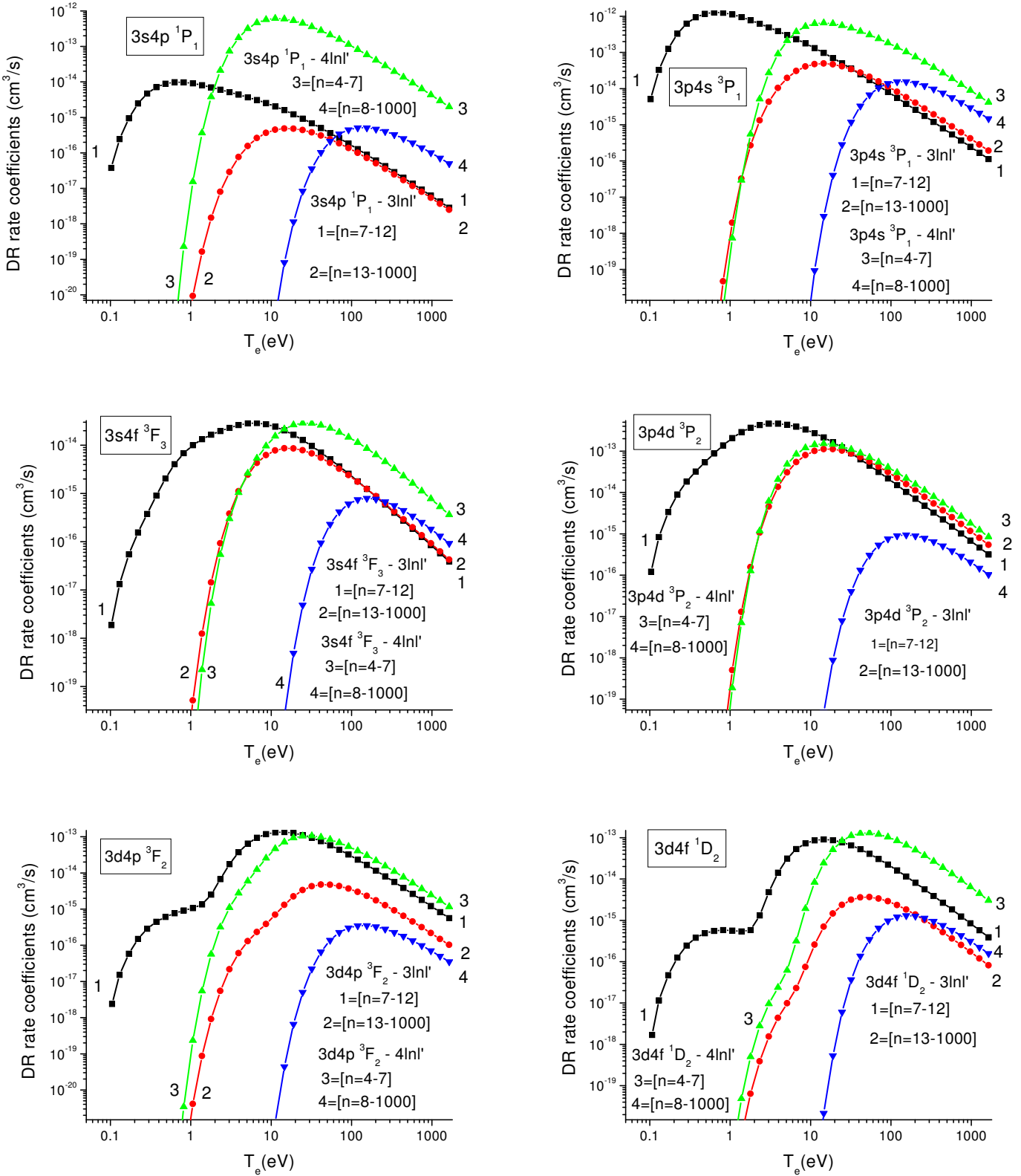


FIG. 4: Contribution of the $3lnl'$ and $4lnl'$ states to the Dielectronic Recombination rate coefficient $\alpha_d(\gamma|3s)$ for the $3l4l'$ odd-parity states as a function of T_e in Mg-like Fe.

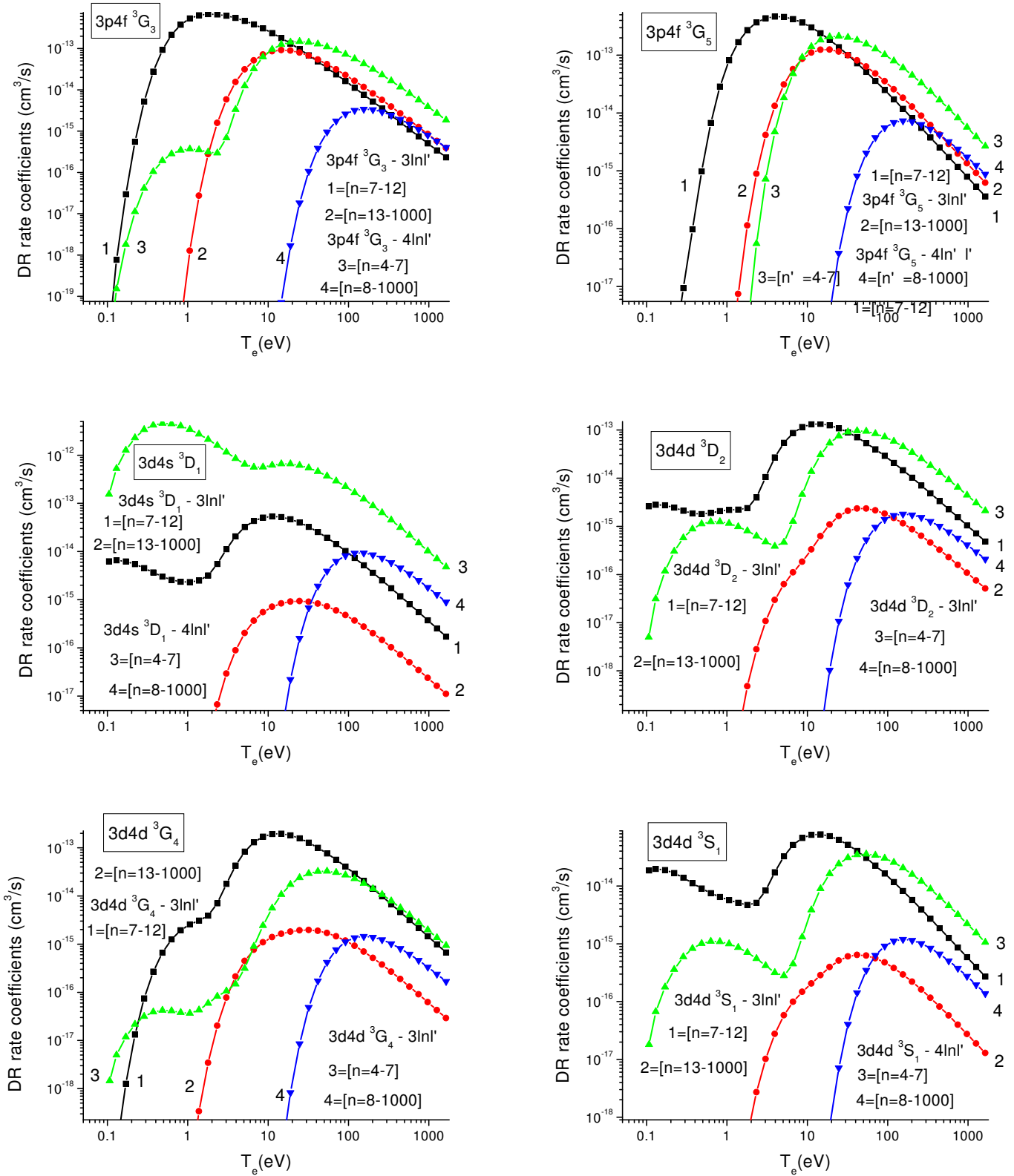


FIG. 5: Contribution of the $3lnl'$ and $4lnl'$ states to the Dielectronic Recombination rate coefficient $\alpha_d(\gamma|3s)$ for even-parity states as function of T_e in Mg-like Fe.

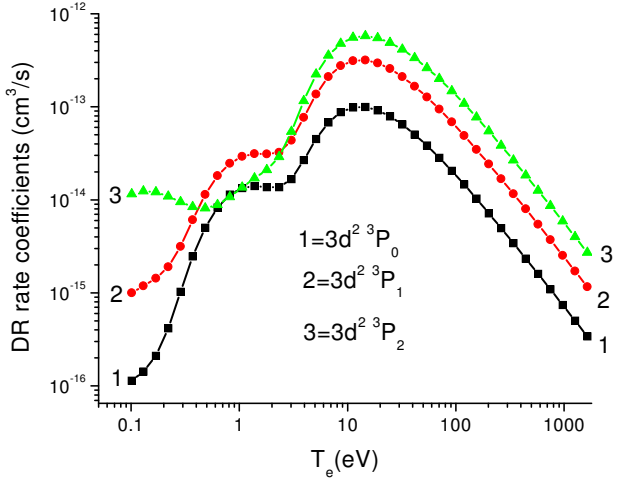
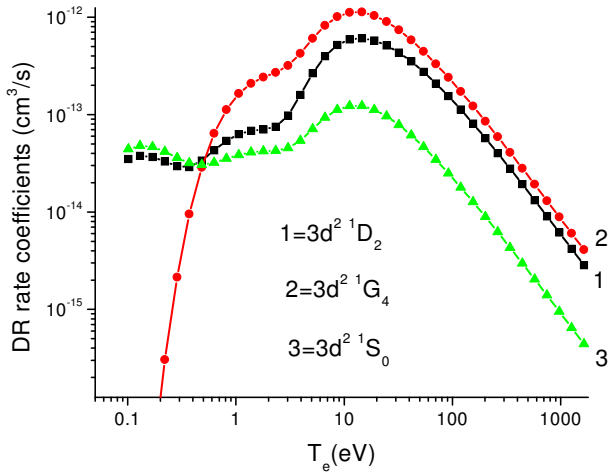
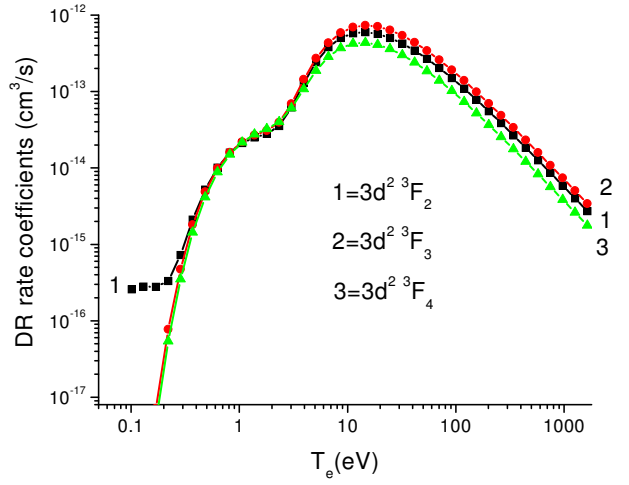
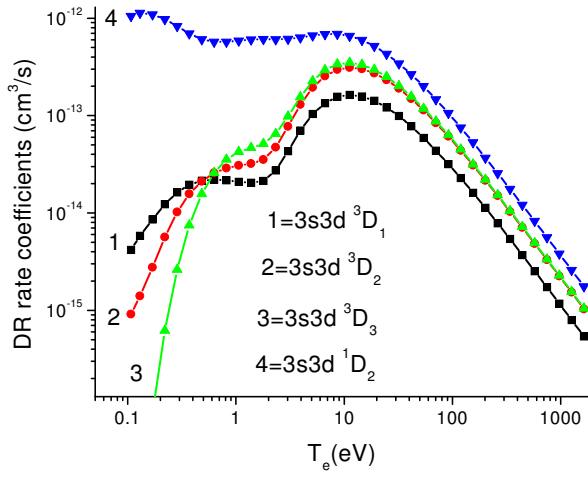
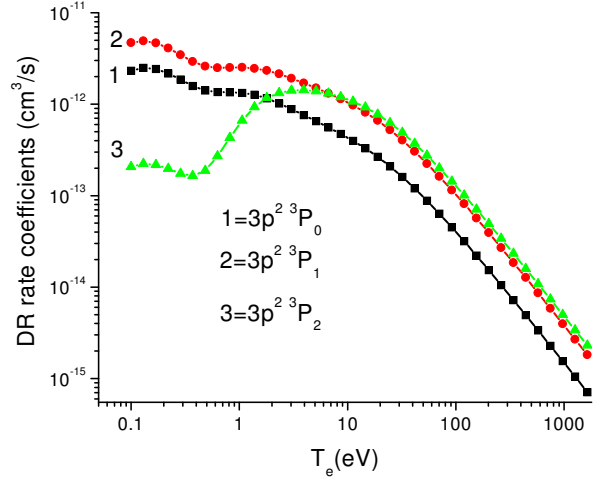
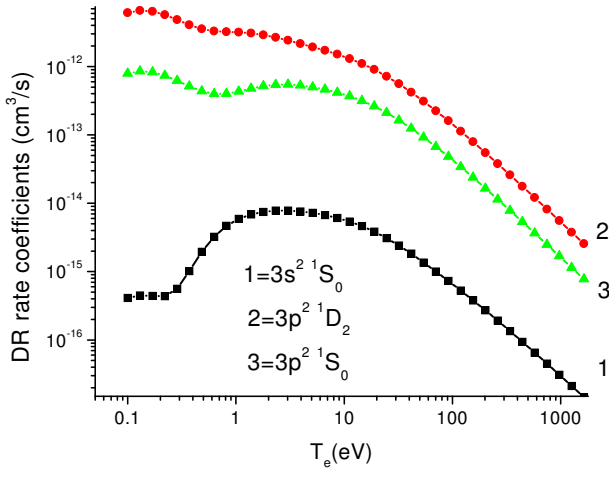


FIG. 6: Dielectronic Recombination rate coefficient $\alpha_d(\gamma|3s)$ for the $3l3l'$ even-parity states as a function of T_e in Mg-like Fe.

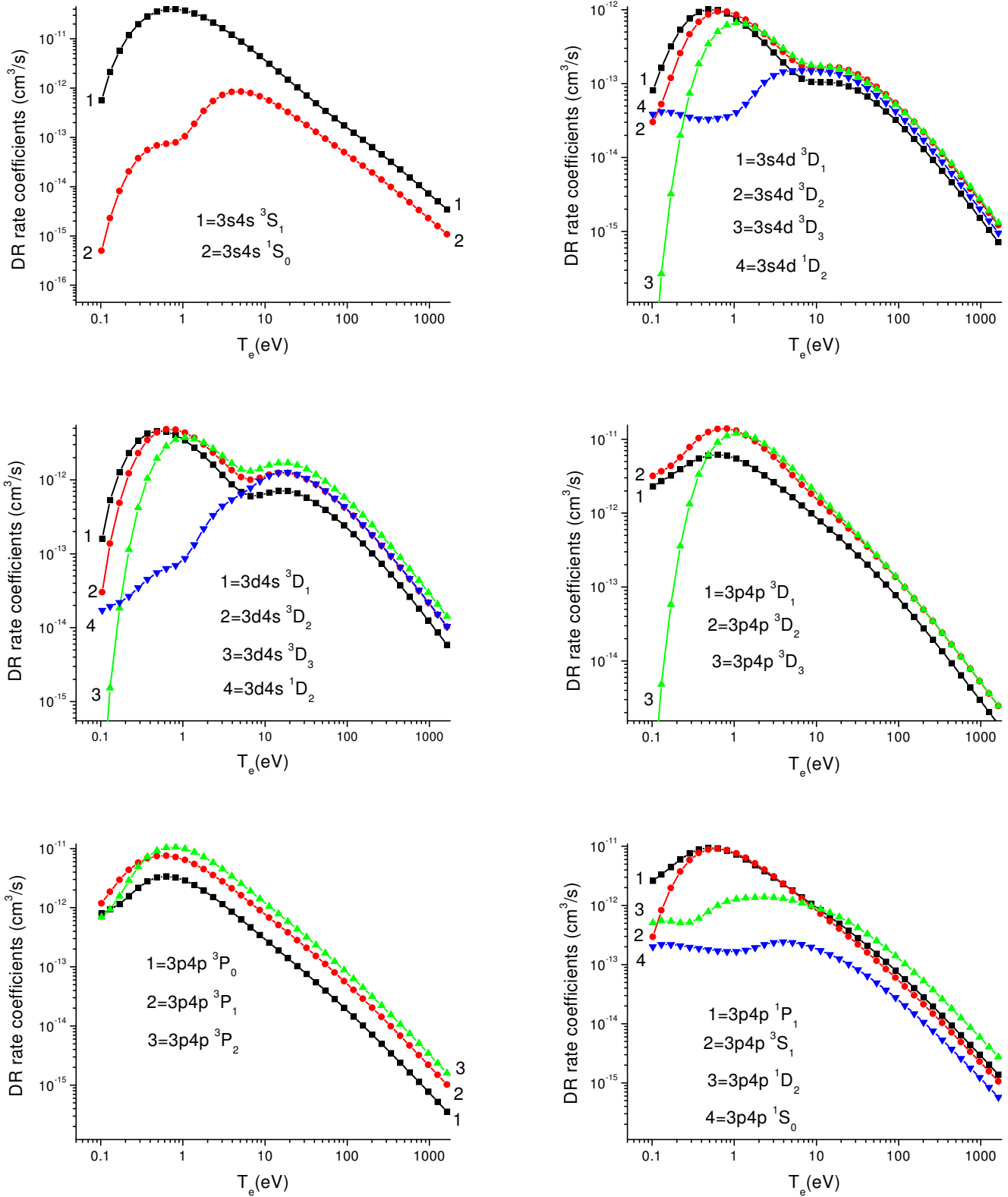


FIG. 7: Dielectronic Recombination rate coefficient $\alpha_d(\gamma|3s)$ for the $3l4l'$ even-parity states as a function of T_e in Mg-like Fe.

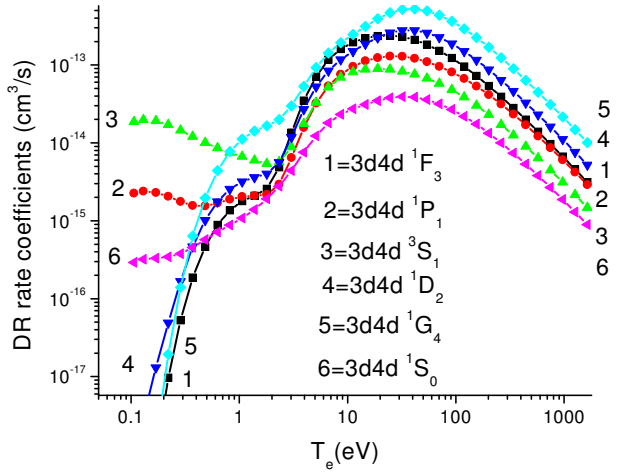
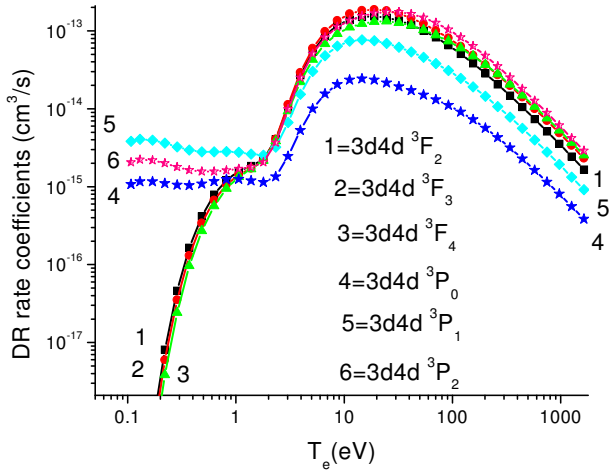
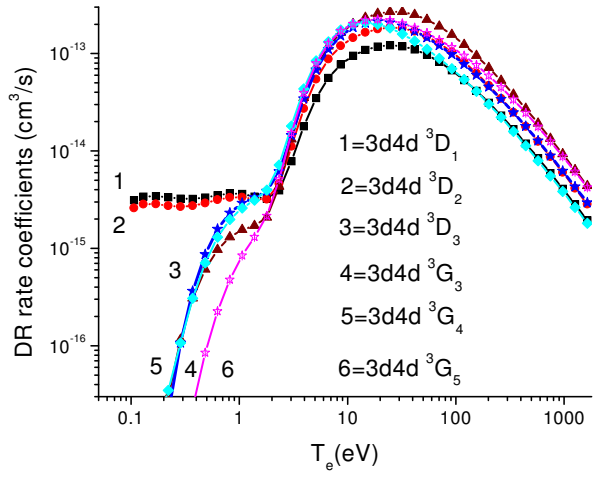
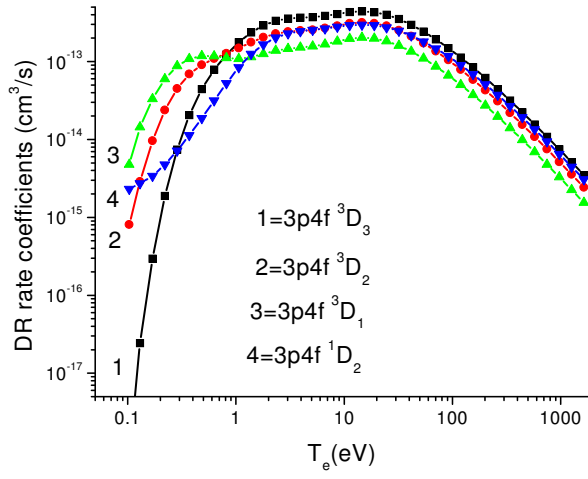
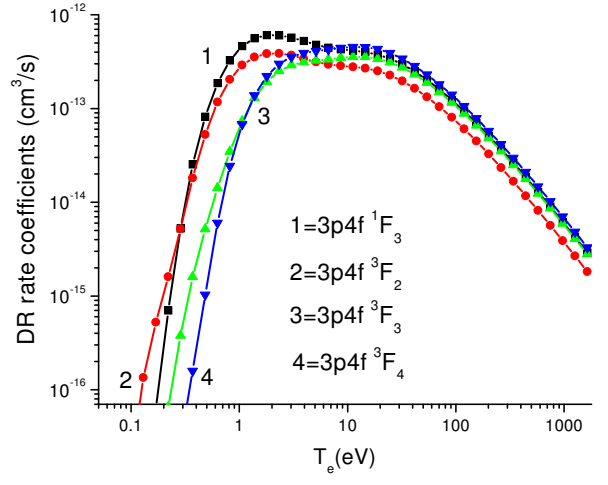
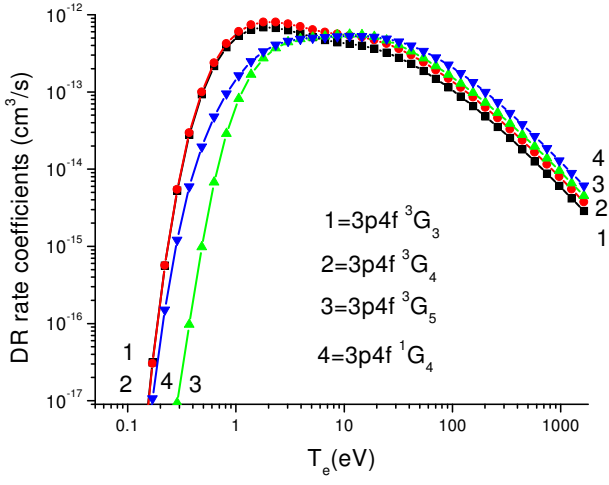


FIG. 8: Dielectronic Recombination rate coefficient $\alpha_d(\gamma|3s)$ for the $3l4l'$ even-parity states as a function of T_e in Mg-like Fe.

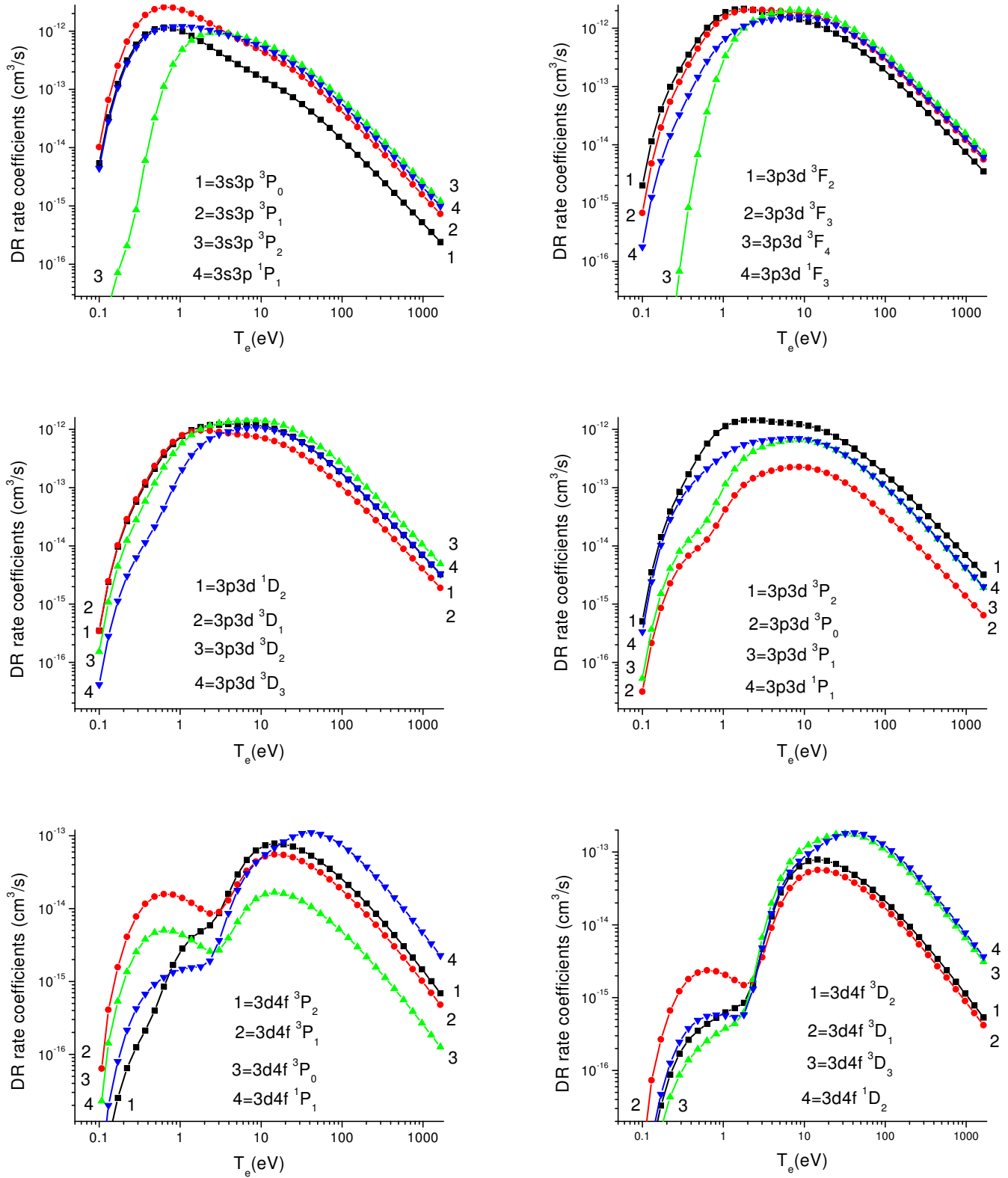


FIG. 9: Dielectronic Recombination rate coefficient $\alpha_d(\gamma|3s)$ for the $3l3l'$ and $3l4l'$ odd-parity states as a function of T_e in Mg-like Fe.

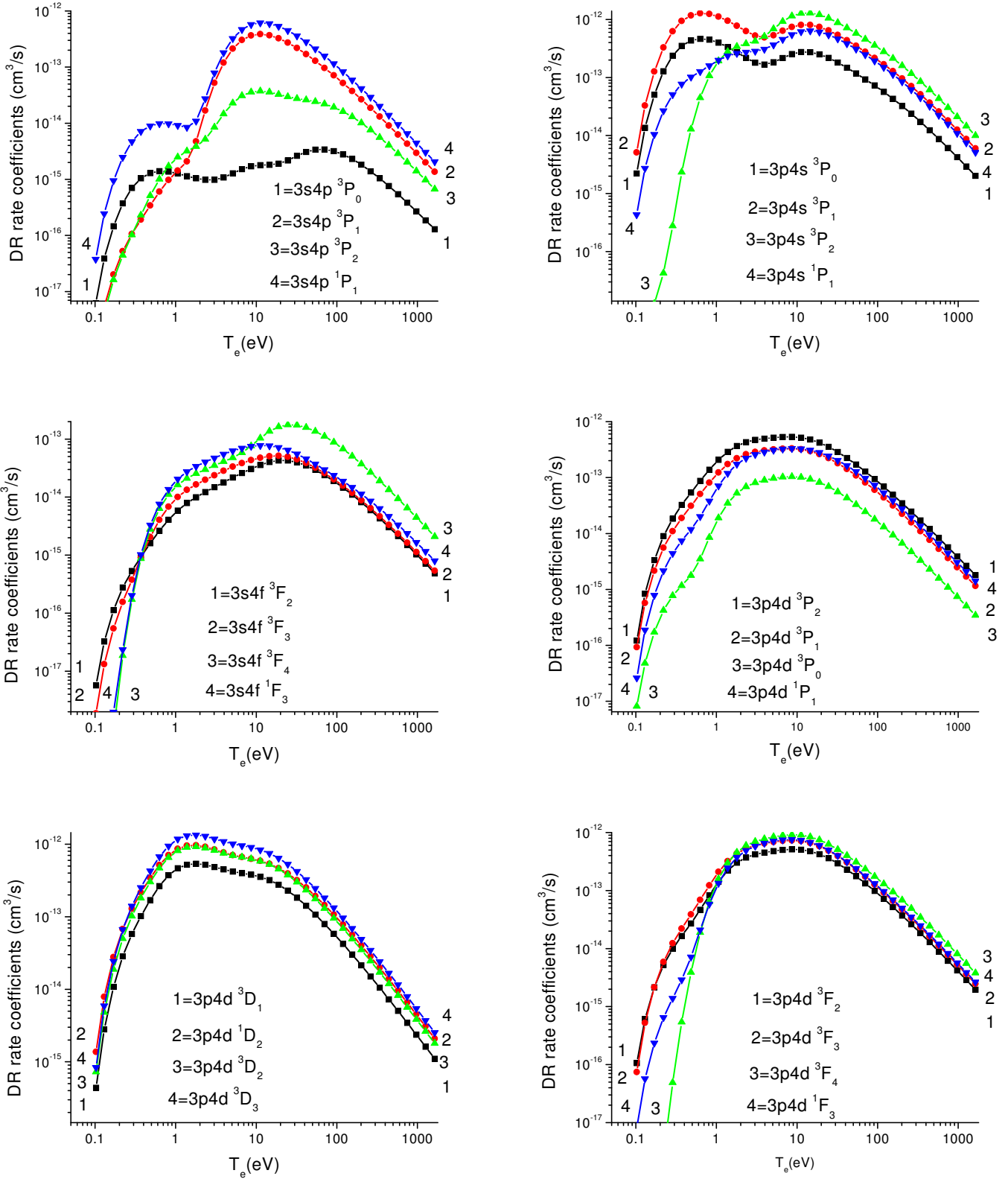


FIG. 10: Dielectronic Recombination rate coefficient $\alpha_d(\gamma|3s)$ for the $3l4l'$ odd-parity states as a function of T_e in Mg-like Fe.

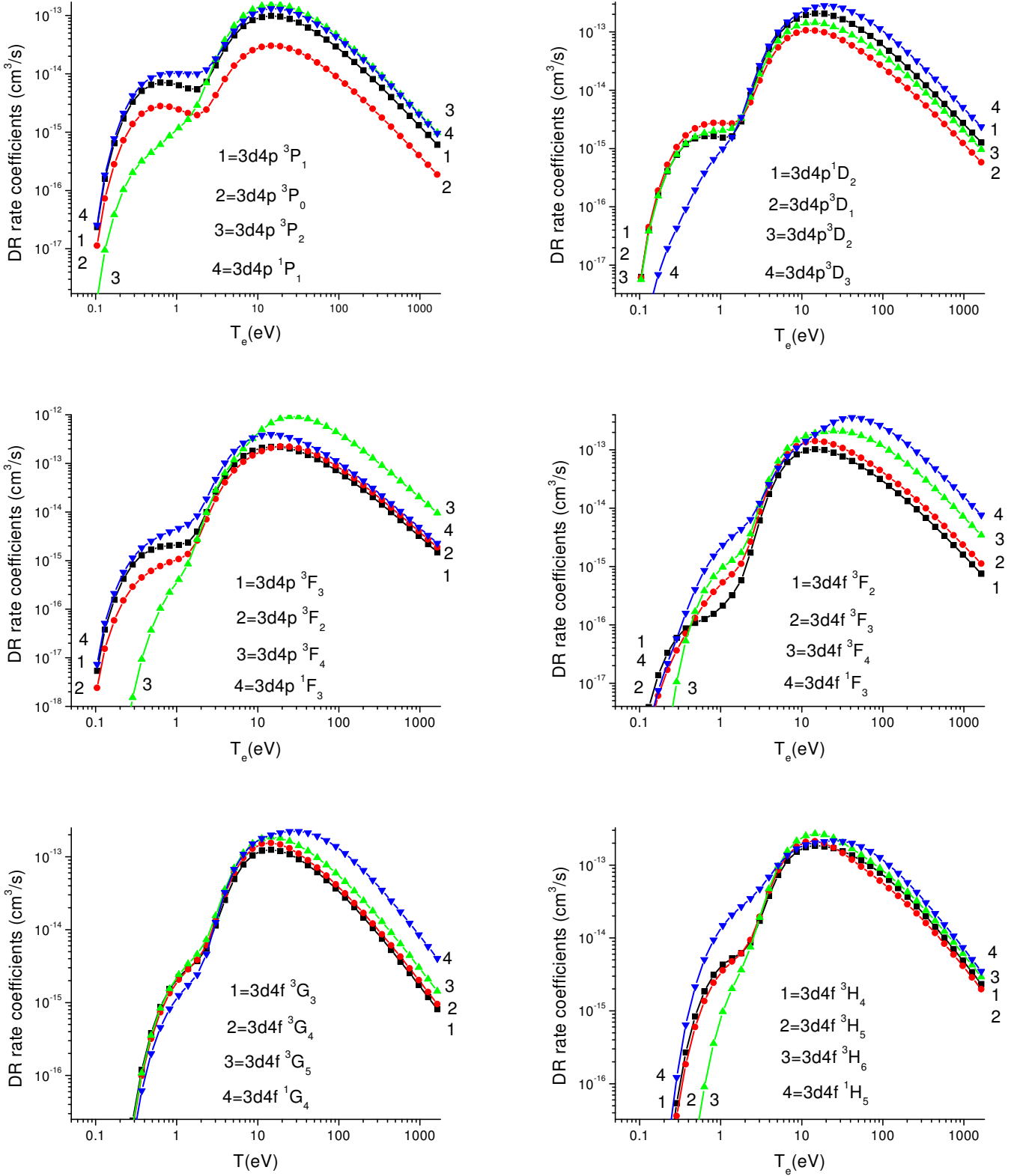


FIG. 11: Dielectronic Recombination rate coefficient $\alpha_d(\gamma|3s)$ for the $3l4l'$ odd-parity states as a function of T_e in Mg-like Fe.

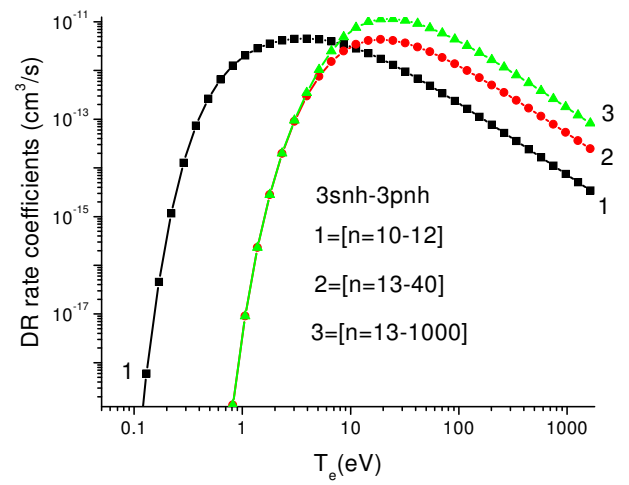
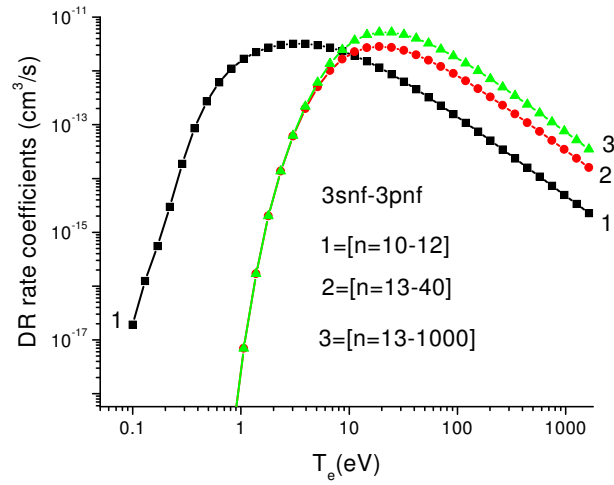
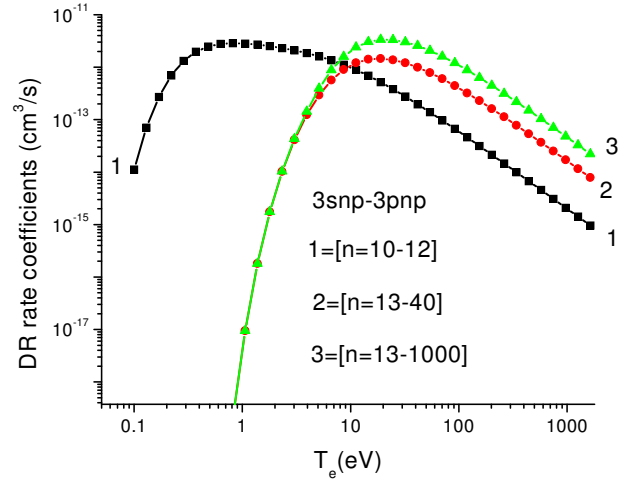
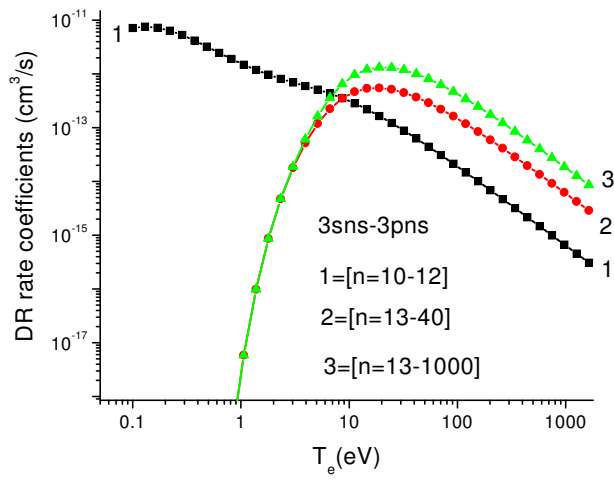


FIG. 12: The $3snl - 3pnl$ contribution of high states to the total DR rate coefficient $\alpha_d(3s, j)$ in sum over i and j in Eq. (10).

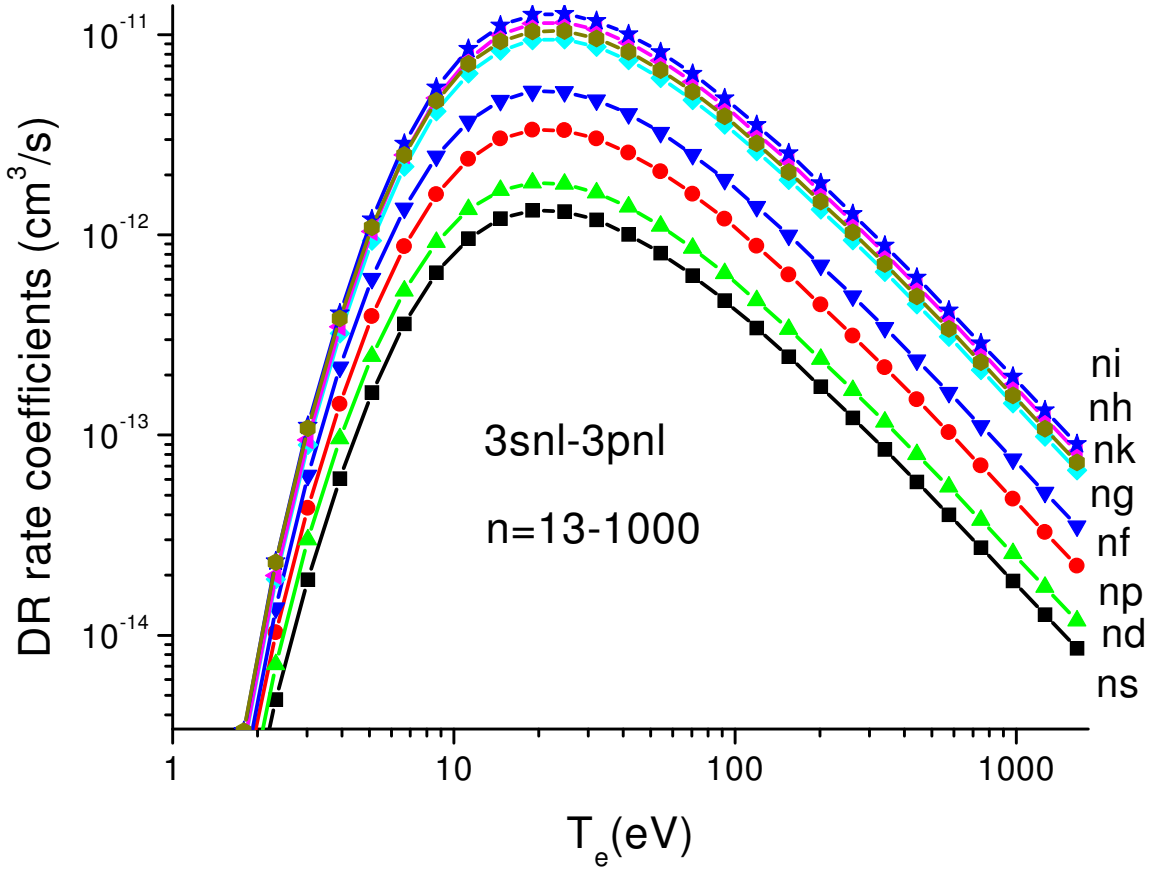


FIG. 13: The $3snl - 3pnl$ contribution of high states to the total DR rate coefficient $\alpha_d(3s, j)$ as a function of l and T_e in Mg-like iron.

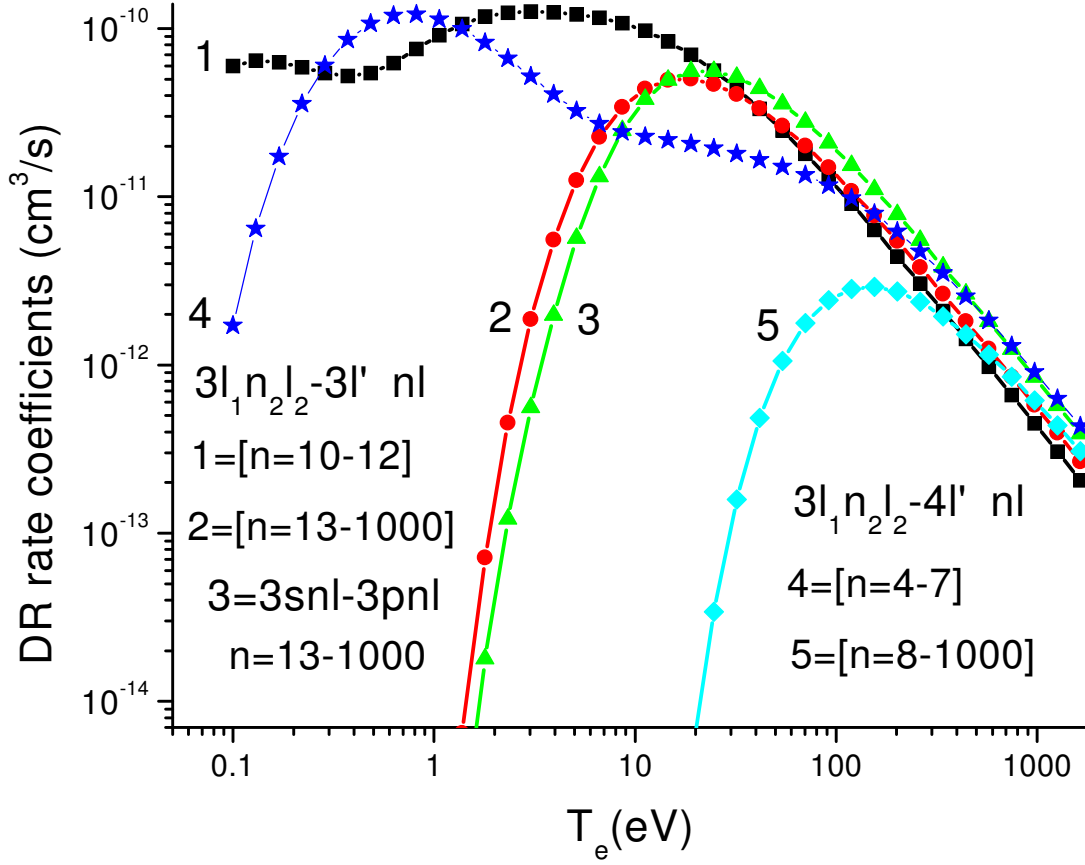


FIG. 14: Contribution of the $3l_1 n_1 l_1 - 3l' n l$, $3snl - 3pnl$, and $3l_1 n_1 l_1 - 4l' n l$ transitions to the total DR rate coefficient $\alpha_d(3s, j)$ as a function of n and T_e in Mg-like iron. $3l_1 n_1 l_1$ excited states include $3sn_1 l_1$ ($n_1 = 3 - 12$), $3pn_1 l_1$ ($n_1 = 3 - 9$), and $3dn_1 l_1$ ($n_1 = 3 - 6$) configurations.

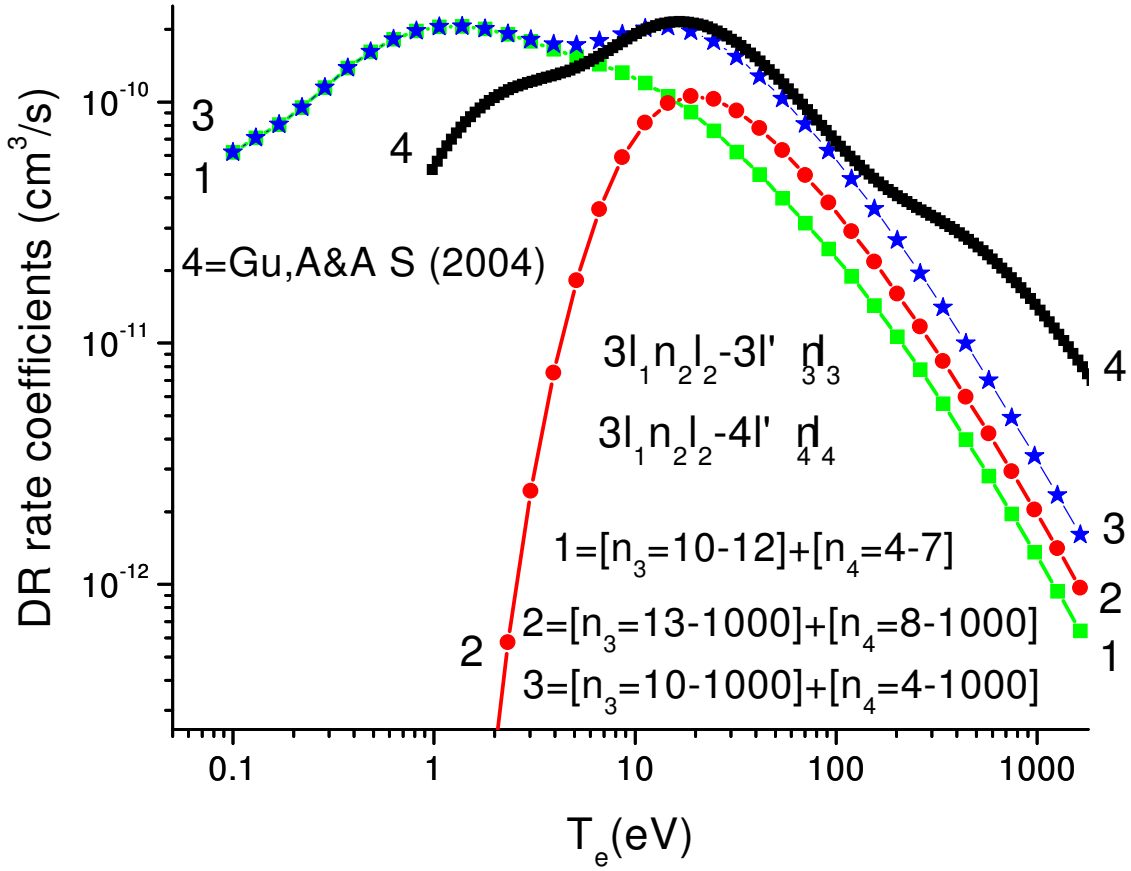


FIG. 15: Total DR rate coefficient (α_d^{total}) as a function of T_e in Mg-like iron. Results by Gu from Ref. [15] are also shown for comparison.

Table I: Labeling of the $3lnl'$ configurations in Mg-like ions for even-parity and odd-parity complexes.

even-parity states						odd-parity states					
N	Conf.	N	Conf.	N	Conf.	N	Conf.	N	Conf.	N	Conf.
1	$3s^2$	33	$3p7h$	65	$3s10i$	1	$3s3p$	33	$3d7f$	65	$3p10g$
2	$3p^2$	34	$3d7s$	66	$3p10p$	2	$3p3d$	34	$3d7h$	66	$3p10i$
3	$3d^2$	35	$3d7d$	67	$3p10f$	3	$3s4p$	35	$3s8p$	67	$3d10p$
4	$3s3d$	36	$3d7g$	68	$3p10h$	4	$3s4f$	36	$3s8f$	68	$3d10f$
5	$3s4s$	37	$3d7i$	69	$3p10k$	5	$3p4s$	37	$3s8h$	69	$3d10h$
6	$3s4d$	38	$3s8s$	70	$3d10s$	6	$3p4d$	38	$3s8k$	70	$3d10k$
7	$3p4p$	39	$3s8d$	71	$3d10d$	7	$3d4p$	39	$3p8s$	71	$3s11p$
8	$3p4f$	40	$3s8g$	72	$3d10g$	8	$3d4f$	40	$3p8d$	72	$3s11f$
9	$3d4s$	41	$3s8i$	73	$3d10i$	9	$3s5p$	41	$3p8g$	73	$3s11h$
10	$3d4d$	42	$3p8p$	74	$3s11s$	10	$3s5f$	42	$3p8i$	74	$3s11k$
11	$3s5s$	43	$3p8f$	75	$3s11d$	11	$3p5s$	43	$3d8p$	75	$3p11s$
12	$3s5d$	44	$3p8h$	76	$3s11g$	12	$3p5d$	44	$3d8f$	76	$3p11d$
13	$3s5g$	45	$3p8k$	77	$3s11i$	13	$3p5g$	45	$3d8h$	77	$3p11g$
14	$3p5p$	46	$3d8s$	78	$3p11p$	14	$3d5p$	46	$3d8k$	78	$3p11i$
15	$3p5f$	47	$3d8d$	79	$3p11f$	15	$3d5f$	47	$3s9p$	79	$3d11p$
16	$3d5s$	48	$3d8g$	80	$3p11h$	16	$3s6p$	48	$3s9f$	80	$3d11f$
17	$3d5d$	49	$3d8i$	81	$3p11k$	17	$3s6f$	49	$3s9h$	81	$3d11h$
18	$3s6s$	50	$3s9s$	82	$3d11s$	18	$3s6h$	50	$3s9k$	82	$3d11k$
19	$3s6d$	51	$3s9d$	83	$3d11d$	19	$3p6s$	51	$3p9s$	83	$3s12p$
20	$3s6g$	52	$3s9g$	84	$3d11g$	20	$3p6d$	52	$3p9d$	84	$3s12f$
21	$3p6p$	53	$3s9i$	85	$3d11i$	21	$3p6g$	53	$3p9g$	85	$3s12h$
22	$3p6f$	54	$3p9p$	86	$3s12s$	22	$3d6p$	54	$3p9i$	86	$3s12k$
23	$3p6h$	55	$3p9f$	87	$3s12d$	23	$3d6f$	55	$3d9p$	87	$3p12s$
24	$3d6s$	56	$3p9h$	88	$3s12g$	24	$3d6h$	56	$3d9f$	88	$3p12d$
25	$3d6d$	57	$3p9k$	89	$3s12i$	25	$3s7p$	57	$3d9h$	89	$3p12g$
26	$3d6g$	58	$3d9s$	90	$3p12p$	26	$3s7f$	58	$3d9k$	90	$3p12i$
27	$3s7s$	59	$3d9d$	91	$3p12f$	27	$3s7h$	59	$3s10p$	91	$3d12p$
28	$3s7d$	60	$3d9g$	92	$3p12h$	28	$3p7s$	60	$3s10f$	92	$3d12f$
29	$3s7g$	61	$3d9i$	93	$3p12k$	29	$3p7d$	61	$3s10h$	93	$3d12h$
30	$3s7i$	62	$3s10s$	94	$3d12s$	30	$3p7g$	62	$3s10k$	94	$3d12k$
31	$3p7p$	63	$3s10d$	95	$3d12d$	31	$3p7i$	63	$3p10s$		
32	$3p7f$	64	$3s10g$	96	$3d12g$	32	$3d7p$	64	$3p10d$		
				97	$3d12i$						

Table II: Labeling of the $3lnl'$ and $4lnl'$ configurations in Mg-like ions for even-parity and odd-parity complexes.

even-parity states						odd-parity states					
N	Conf.	N	Conf.	N	Conf.	N	Conf.	N	Conf.	N	Conf.
1	$3s^2$	31	$3p7p$	61	$4d5s$	1	$3s3p$	31	$3p7i$	61	$4s6p$
2	$3p^2$	32	$3p7f$	62	$4d5d$	2	$3p3d$	32	$3d7p$	62	$4s6f$
3	$3d^2$	33	$3p7h$	63	$4d5g$	3	$3s4p$	33	$3d7f$	63	$4s6h$
4	$3s3d$	34	$3d7s$	64	$4f5p$	4	$3s4f$	34	$3d7h$	64	$4p6s$
5	$3s4s$	35	$3d7d$	65	$4f5f$	5	$3p4s$	35	$3s8p$	65	$4p6d$
6	$3s4d$	36	$3d7g$	66	$4s6s$	6	$3p4d$	36	$3s8f$	66	$4p6g$
7	$3p4p$	37	$3d7i$	67	$4s6d$	7	$3d4p$	37	$3s8h$	67	$4d6p$
8	$3p4f$	38	$3s8s$	68	$4s6g$	8	$3d4f$	38	$3s8k$	68	$4d6f$
9	$3d4s$	39	$3s8d$	69	$4p6p$	9	$3s5p$	39	$3p8s$	69	$4d6h$
10	$3d4d$	40	$3s8g$	70	$4p6f$	10	$3s5f$	40	$3p8d$	70	$4f6s$
11	$3s5s$	41	$3s8i$	71	$4p6h$	11	$3p5s$	41	$3p8g$	71	$4f6d$
12	$3s5d$	42	$3p8p$	72	$4d6s$	12	$3p5d$	42	$3p8i$	72	$4f6g$
13	$3s5g$	43	$3p8f$	73	$4d6d$	13	$3p5g$	43	$3d8p$	73	$4s7p$
14	$3p5p$	44	$3p8h$	74	$4d6g$	14	$3d5p$	44	$3d8f$	74	$4s7f$
15	$3p5f$	45	$3p8k$	75	$4f6p$	15	$3d5f$	45	$3d8h$	75	$4s7h$
16	$3d5s$	46	$3d8s$	76	$4f6f$	16	$3s6p$	46	$3d8k$	76	$4p7s$
17	$3d5d$	47	$3d8d$	77	$4f6h$	17	$3s6f$	47	$4s4p$	77	$4p7d$
18	$3s6s$	48	$3d8g$	78	$4s7s$	18	$3s6h$	48	$4s4f$	78	$4p7g$
19	$3s6d$	49	$3d8i$	79	$4s7d$	19	$3p6s$	49	$4p4d$	79	$4p7i$
20	$3s6g$	50	$4s^2$	80	$4s7g$	20	$3p6d$	50	$4d4f$	80	$4d7p$
21	$3p6p$	51	$4p^2$	81	$4s7i$	21	$3p6g$	51	$4s5p$	81	$4d7f$
22	$3p6f$	52	$4d^2$	82	$4p7p$	22	$3d6p$	52	$4s5f$	82	$4d7h$
23	$3p6h$	53	$4f^2$	83	$4p7f$	23	$3d6f$	53	$4p5s$	83	$4f7s$
24	$3d6s$	54	$4s4d$	84	$4p7h$	24	$3d6h$	54	$4p5d$	84	$4f7d$
25	$3d6d$	55	$4p4f$	85	$4d7s$	25	$3s7p$	55	$4p5g$	85	$4f7g$
26	$3d6g$	56	$4s5s$	86	$4d7d$	26	$3s7f$	56	$4d5p$		
27	$3s7s$	57	$4s5d$	87	$4d7g$	27	$3s7h$	57	$4d5f$		
28	$3s7d$	58	$4s5g$	88	$4f7p$	28	$3p7s$	58	$4f5s$		
29	$3s7g$	59	$4p5p$	89	$4f7f$	29	$3p7d$	59	$4f5d$		
30	$3s7i$	60	$4p5f$	90	$4f7h$	30	$3p7g$	60	$4f5g$		

Table III: Energies (10^3 cm^{-1}) for the $3l3l'$ excited states of Mg-like Fe. Comparison of theoretical results (Cowan and RMBPT codes) with recommended NIST data (Ref. 20) and theoretical results obtained CV3 code (Ref. 23), by GRASP code (Ref. 23), and by SUPERSTRUCTURE code (Ref. 21).

Level		E (10^3 cm^{-1})					
Conf.	<i>LSJ</i>	COWAN	RMBPT	CV3	GRASP	SPSTR	NIST
$3s^2$	1S_0	0.000	0.000	0.000	0.000	0.000	0.000
$3s3p$	3P_0	233.897	233.839	234.692	232.915	231.809	233.910
$3s3p$	3P_1	239.497	239.682	240.391	238.767	237.563	239.662
$3s3p$	3P_2	253.079	253.853	254.589	252.805	251.167	253.820
$3s3p$	1P_1	342.730	351.804	351.307	357.088	355.538	351.914
$3p^2$	3P_0	555.683	554.498	555.447	556.986	558.887	554.500
$3p^2$	1D_2	562.242	559.596	561.741	560.202	560.342	559.590
$3p^2$	3P_1	565.490	564.565	565.415	566.818	567.956	564.570
$3p^2$	3P_2	582.386	581.776	582.983	583.568	584.013	581.690
$3p^2$	1S_0	651.744	659.446	662.902	666.323	683.314	660.970
$3s3d$	3D_1	678.018	678.264	679.542	681.603	681.728	678.830
$3s3d$	3D_2	679.245	679.293	680.466	682.597	682.981	679.785
$3s3d$	3D_3	681.142	680.882	682.092	684.151	683.314	681.410
$3s3d$	1D_2	752.851	761.190	761.165	772.607	777.871	762.163
$3p3d$	3F_2	931.628	927.837	930.170	930.067	931.063	928.420
$3p3d$	3F_3	941.180	937.708	938.996	939.836	940.584	938.180
$3p3d$	1D_2	951.011	948.210	950.354	951.188	951.191	
$3p3d$	3F_4	952.319	949.235	963.516	950.964	951.506	949.660
$3p3d$	3D_1	980.765	982.361	1002.185	989.028	988.376	
$3p3d$	3P_2	981.825	982.991	1002.803	989.255	989.064	
$3p3d$	3P_0	992.795	995.356	1012.532	1001.634	1000.387	
$3p3d$	3D_3	993.070	994.424	1012.532	1000.856	1000.226	
$3p3d$	3P_1	993.477	995.730	1012.950	1002.055	1000.947	
$3p3d$	3D_2	994.291	996.133	1013.605	1002.471	1001.587	
$3p3d$	1F_3	1054.794	1060.890	1086.606	1076.619	1074.642	
$3p3d$	1P_1	1063.955	1073.127	1099.034	1092.230	1090.434	
$3d^2$	3F_2	1372.121	1369.722	1375.542	1374.651		
$3d^2$	3F_3	1374.110	1371.391	1377.517	1376.255		
$3d^2$	3F_4	1376.546	1373.420	1379.970	1378.228		
$3d^2$	1D_2	1401.468	1402.249	1410.508	1410.058		
$3d^2$	3P_0	1403.478	1404.851	1412.168	1411.596		
$3d^2$	3P_1	1404.250	1405.342	1412.955	1412.204		
$3d^2$	3P_2	1406.346	1405.495	1415.118	1413.877		
$3d^2$	1G_4	1406.550	1406.003	1416.819	1415.263		
$3d^2$	1S_0	1477.854	1485.186	1499.809	1501.378		

Table IV: Energies (10^3 cm^{-1}) for the $3l3l'$ excited states of Mg-like Fe. Comparison of theoretical results (Cowan and RMBPT codes) with recommended NIST data (Ref. 20) and theoretical results obtained CV3 code (Ref. 23), by GRASP code (Ref. 23), and by SUPERSTRUCTURE code (Ref. 21).

Level		E (10^3 cm^{-1})					
Conf.	<i>LSJ</i>	COWAN	RMBPT	CV3	GRASP	SPSTR	NIST
<i>3s4s</i>	3S_1	1761.322	1764.503	1764.376	1761.477	1764.348	1763.700
<i>3s4p</i>	3P_0	1879.836	1882.700	1882.823	1879.934	1883.780	
<i>3s4p</i>	3P_1	1880.457	1883.148	1883.409	1880.544	1884.205	
<i>3s4p</i>	3P_2	1887.106	1890.294	1889.756	1887.417	1890.502	
<i>3s4p</i>	1P_1	1888.048	1890.725	1890.775	1888.243	1891.923	1889.970
<i>3s4d</i>	3D_1	2030.134	2032.654	2032.073	2030.386	2033.983	2031.310
<i>3s4d</i>	3D_2	2030.817	2033.440	2032.768	2095.191	2034.767	2032.020
<i>3s4d</i>	3D_3	2032.010	2034.691	2033.913	2032.355	2035.999	2033.180
<i>3s4d</i>	1D_2	2033.416	2036.452	2036.031	2034.579	2038.294	2035.280
<i>3p4s</i>	3P_0	2050.611	2053.437	2070.328	2053.959	2058.295	
<i>3p4s</i>	3P_1	2053.898	2057.012	2073.552	2057.935	2062.110	
<i>3p4s</i>	3P_2	2070.298	2073.932	2087.091	2074.429	2077.189	
<i>3p4s</i>	1P_1	2081.902	2086.823	2100.822	2090.848	2093.652	
<i>3s4f</i>	3F_2	2104.407	2108.884	2109.238	2107.314	2111.952	2108.520
<i>3s4f</i>	3F_3	2104.618	2109.088	2109.320	2107.522	2112.194	2108.620
<i>3s4f</i>	3F_4	2104.904	2109.377	2109.577	2107.817	2112.517	2108.880
<i>3s4f</i>	1F_3	2118.274	2122.775	2123.925	2125.923	2130.264	2123.150
<i>3p4p</i>	1P_1	2152.977	2154.800	2169.909	2154.946	2158.458	
<i>3p4p</i>	3D_1	2166.364	2168.972	2182.741	2169.524	2172.604	
<i>3p4p</i>	3D_2	2167.636	2170.742	2184.670	2172.068	2175.167	
<i>3p4p</i>	3P_0	2172.307	2174.896	2190.014	2176.203	2180.952	
<i>3p4p</i>	3P_1	2180.517	2183.314	2196.335	2183.972	2187.530	
<i>3p4p</i>	3D_3	2186.180	2182.527	2197.114	2187.298	2189.144	
<i>3p4p</i>	3P_2	2187.637	2190.865	2203.229	2192.091	2195.373	
<i>3p4p</i>	3S_1	2193.826	2189.274	2206.010	2196.076	2198.235	
<i>3p4p</i>	1D_2	2209.076	2203.808	2221.704	2217.190	2219.850	
<i>3p4p</i>	1S_0	2235.894	2228.474	2253.519	2250.344	2251.138	
<i>3p4d</i>	3D_1	2311.844	2313.665	2328.948	2315.747	2320.143	
<i>3p4d</i>	1D_2	2311.913	2313.923	2329.499	2313.443	2317.818	
<i>3p4d</i>	3D_2	2312.599	2314.381	2330.063	2315.710	2320.269	
<i>3p4d</i>	3D_3	2314.096	2315.951	2331.729	2318.302	2322.908	
<i>3p4d</i>	3F_2	2328.616	2331.195	2344.198	2331.591	2334.744	
<i>3p4d</i>	3D_3	2330.037	2332.552	2345.692	2334.165	2337.414	
<i>3p4d</i>	3F_4	2336.193	2339.378	2352.380	2339.957	2342.990	
<i>3p4d</i>	1F_3	2336.779	2339.646	2352.924	2348.578	2352.178	
<i>3p4d</i>	3P_2	2343.507	2339.370	2357.915	2344.996	2348.198	
<i>3p4d</i>	3P_1	2344.547	2340.152	2359.091	2347.369	2350.425	
<i>3p4d</i>	3P_0	2348.569	2343.764	2362.381	2350.253	2353.043	
<i>3p4d</i>	1P_1	2352.001	2347.444	2367.021	2360.805	2364.114	
<i>3p4f</i>	3G_3	2377.958	2380.511	2383.688	2380.143	2385.765	2380.160
<i>3p4f</i>	3F_3	2384.268	2387.197	2390.900	2387.634	2391.567	
<i>3p4f</i>	3G_4	2384.270	2387.222	2402.178	2400.028	2392.747	2386.700
<i>3p4f</i>	3F_2	2387.568	2390.842	2402.863	2403.728	2394.647	
<i>3p4f</i>	3F_3	2397.423	2400.731	2406.897	2389.846	2404.062	
<i>3p4f</i>	3G_5	2399.277	2402.678	2412.816	2386.343	2407.911	2402.100
<i>3p4f</i>	3F_4	2403.411	2399.920	2414.037	2402.962	2406.804	
<i>3p4f</i>	3D_3	2414.478	2409.564	2428.959	2415.051	2419.483	
<i>3p4f</i>	3D_2	2417.440	2412.243	2432.108	2418.380	2422.642	
<i>3p4f</i>	3D_1	2420.670	2415.182	2434.821	2421.808	2425.877	
<i>3p4f</i>	1G_4	2430.069	2424.453	2450.592	2437.746	2438.333	
<i>3p4f</i>	1D_2	2436.148	2430.083	2454.677	2440.913	2444.313	

Table V: Energies (10^3 cm^{-1}), sum of weighted radiative transition rates ($\sum gA_r$ in s^{-1}), and weighted autoionization rates (gA_a in s^{-1}) for the $4l4l'$ excited states of Mg-like Fe calculated by Cowan (a) and RMBPT (b) codes.

Level		E (10^3 cm^{-1})		$\sum gA_r$ (s^{-1})	gA_a (s^{-1})	
Conf.	<i>LSJ</i>	<i>a</i>	<i>b</i>	<i>a</i>	3 <i>s</i> <i>a</i>	3 <i>p</i> <i>a</i>
$4s^2$	1S_0	3604.647	3606.320	6.137[11]	0.000[00]	0.000[00]
$4s4p$	3P_0	3691.536	3693.018	5.412[11]	2.448[13]	0.000[00]
$4s4p$	3P_1	3693.798	3695.390	1.626[12]	7.435[13]	0.000[00]
$4s4p$	3P_2	3699.079	3700.893	2.719[12]	1.218[14]	0.000[00]
$4s4p$	1P_1	3743.639	3750.241	1.684[12]	2.678[14]	0.000[00]
$4p^2$	1D_2	3817.442	3816.662	2.724[12]	3.982[13]	0.000[00]
$4p^2$	3P_0	3821.944	3823.596	4.931[11]	1.413[12]	0.000[00]
$4p^2$	3P_1	3825.543	3827.290	1.478[12]	4.687[09]	0.000[00]
$4p^2$	3P_2	3831.132	3833.178	2.308[12]	3.243[12]	0.000[00]
$4s4d$	3D_1	3856.425	3856.618	2.072[12]	1.455[14]	0.000[00]
$4s4d$	3D_2	3856.934	3857.130	3.442[12]	2.446[14]	0.000[00]
$4s4d$	3D_3	3857.716	3857.921	4.770[12]	3.452[14]	0.000[00]
$4p^2$	1S_0	3866.581	3872.298	5.154[11]	6.985[13]	0.000[00]
$4s4d$	1D_2	3897.832	3900.939	3.228[12]	3.440[14]	0.000[00]
$4s4f$	3F_2	3925.285	3925.744	5.585[12]	1.057[14]	0.000[00]
$4s4f$	3F_3	3926.036	3926.764	7.927[12]	1.488[14]	0.000[00]
$4s4f$	3F_4	3926.929	3927.941	1.035[13]	1.907[14]	0.000[00]
$4s4f$	1F_3	3929.568	3928.364	7.825[12]	6.341[14]	0.000[00]
$4p4d$	3F_2	3957.848	3960.771	3.576[12]	3.311[11]	0.000[00]
$4p4d$	3F_3	3961.948	3965.365	5.046[12]	1.274[12]	0.000[00]
$4p4d$	1D_2	3962.810	3965.352	3.254[12]	8.092[11]	0.000[00]
$4p4d$	3F_4	3965.580	3968.998	5.093[12]	2.561[11]	3.313[14]
$4p4d$	3P_2	3978.185	3983.255	3.098[12]	1.613[13]	3.473[14]
$4p4d$	3P_1	3978.643	3983.923	1.893[12]	8.691[12]	2.084[14]
$4p4d$	3P_0	3981.568	3986.741	6.318[11]	4.392[12]	7.283[13]
$4p4d$	3D_1	3982.883	3988.277	1.921[12]	6.303[12]	2.021[14]
$4p4d$	3D_2	3983.983	3989.460	3.178[12]	5.131[12]	3.237[14]
$4p4d$	3D_3	3984.512	3990.076	4.416[12]	5.530[11]	4.369[14]
$4p4d$	1P_1	4017.032	4027.728	1.923[12]	1.599[14]	6.607[14]
$4p4d$	1F_3	4027.615	4038.452	5.161[12]	4.176[13]	9.625[14]
$4p4f$	1F_3	4036.062	4039.419	8.305[12]	3.918[12]	7.290[13]
$4p4f$	3F_2	4037.355	4039.301	5.881[12]	3.099[11]	2.249[14]
$4p4f$	3F_3	4037.399	4040.049	8.214[12]	2.355[12]	2.655[14]
$4p4f$	3F_4	4038.162	4040.177	1.052[13]	5.056[12]	4.056[14]
$4p4f$	3G_3	4043.642	4046.341	8.232[12]	1.448[13]	6.039[13]
$4p4f$	3G_4	4045.004	4047.667	1.052[13]	2.024[13]	1.530[14]
$4p4f$	3G_5	4047.663	4050.741	1.287[13]	3.206[13]	7.643[12]
$4p4f$	1G_4	4052.086	4053.369	9.885[12]	1.230[13]	1.808[15]
$4p4f$	3D_3	4057.097	4062.330	8.228[12]	7.581[12]	2.274[14]
$4p4f$	3D_2	4058.549	4063.926	5.880[12]	5.728[12]	1.825[14]
$4p4f$	3D_1	4060.069	4065.525	3.548[12]	3.268[12]	9.796[13]
$4p4f$	1D_2	4069.646	4075.458	5.563[12]	1.216[13]	8.372[14]
$4d^2$	3F_2	4120.056	4123.690	3.987[12]	1.831[11]	2.111[13]
$4d^2$	3F_3	4120.916	4124.488	5.541[12]	8.270[08]	2.895[13]
$4d^2$	3F_4	4121.980	4125.485	7.083[12]	2.659[09]	3.749[13]
$4d^2$	3P_0	4129.755	4134.433	7.890[11]	6.879[10]	1.016[13]
$4d^2$	3P_1	4130.100	4134.758	2.346[12]	8.396[06]	2.985[13]
$4d^2$	3P_2	4130.595	4135.264	3.877[12]	6.624[11]	5.218[13]
$4d^2$	1D_2	4138.642	4141.442	4.191[12]	7.359[13]	2.570[14]
$4d^2$	1G_4	4147.408	4153.773	7.814[12]	5.476[11]	8.040[14]

Level	E (10 ³ cm ⁻¹)	$\sum gA_r$ (s ⁻¹)		A _a (s ⁻¹)		
				3s	3p	
Conf.	LSJ	a	b	a	a	
4d ²	¹ S ₀	4158.605	4166.260	8.264[11]	3.496[13]	1.477[14]
4d4f	¹ G ₄	4174.384	4176.092	1.176[13]	1.146[11]	5.641[11]
4d4f	³ H ₄	4175.990	4177.484	1.162[13]	1.104[12]	7.601[10]
4d4f	³ H ₅	4176.623	4178.114	1.417[13]	1.488[12]	7.467[10]
4d4f	³ H ₆	4177.528	4178.990	1.665[13]	1.710[12]	4.623[10]
4d4f	³ F ₂	4180.440	4183.101	6.549[12]	3.764[12]	2.997[12]
4d4f	³ F ₃	4180.845	4183.483	9.144[12]	5.325[12]	4.247[12]
4d4f	³ F ₄	4181.365	4183.980	1.174[13]	6.840[12]	5.496[12]
4d4f	¹ D ₂	4188.383	4192.283	6.552[12]	3.005[10]	1.962[12]
4d4f	³ G ₃	4196.286	4201.292	9.453[12]	3.150[11]	9.790[12]
4d4f	³ G ₄	4196.867	4201.842	1.214[13]	2.916[09]	1.244[13]
4d4f	³ G ₅	4197.548	4202.485	1.478[13]	1.215[11]	1.529[13]
4d4f	³ D ₁	4203.466	4209.483	3.983[12]	2.750[10]	4.267[11]
4d4f	³ D ₂	4203.608	4209.630	6.619[12]	6.852[10]	9.028[11]
4d4f	³ D ₃	4203.849	4209.854	9.251[12]	1.081[12]	1.119[12]
4d4f	³ P ₂	4206.932	4213.204	6.523[12]	4.242[12]	2.447[13]
4d4f	³ P ₁	4207.169	4213.439	3.919[12]	2.572[12]	1.486[13]
4d4f	³ P ₀	4207.298	4213.576	1.310[12]	8.626[11]	4.996[12]
4d4f	¹ F ₃	4213.086	4217.573	9.218[12]	2.822[14]	9.691[13]
4d4f	¹ H ₅	4225.129	4230.715	1.492[13]	6.736[14]	5.193[14]
4d4f	¹ P ₁	4239.248	4247.244	3.864[12]	1.514[13]	3.069[13]
4f ²	³ H ₄	4255.961	4260.225	1.658[13]	3.784[11]	2.064[14]
4f ²	³ H ₅	4256.306	4260.561	2.022[13]	3.760[06]	2.519[14]
4f ²	³ H ₆	4256.712	4260.951	2.385[13]	2.245[10]	2.980[14]
4f ²	³ F ₂	4263.207	4268.543	9.326[12]	1.922[10]	1.938[12]
4f ²	³ F ₃	4263.425	4268.755	1.304[13]	6.897[05]	2.670[12]
4f ²	³ F ₄	4263.676	4268.996	1.675[13]	7.512[12]	1.161[13]
4f ²	¹ G ₄	4266.238	4270.541	1.643[13]	6.551[14]	7.191[14]
4f ²	¹ I ₆	4276.162	4279.647	2.284[13]	3.082[14]	3.668[15]
4f ²	¹ D ₂	4281.267	4287.322	9.184[12]	5.079[13]	5.519[13]
4f ²	³ P ₀	4284.657	4292.272	1.858[12]	2.595[09]	3.810[12]
4f ²	³ P ₁	4284.739	4292.394	5.568[12]	9.898[05]	1.137[13]
4f ²	³ P ₂	4284.917	4292.509	9.264[12]	3.582[11]	1.908[13]
4f ²	¹ S ₀	4330.778	4339.021	1.767[12]	2.028[13]	5.650[13]

Table VI: Wavelengths (λ in Å), and radiative rates (A_r in 10^8 s^{-1}) for $3l_13l_2 - 3l_33l_4$ transitions of Mg-like iron. Comparison of present results (Cowan and RMBPT codes) with recommended NIST data (Ref. 20).

Low level		Upper level		λ (Å)			$A_r(10^8 \text{ s}^{-1})$		
Conf.	LSJ	Conf.	LSJ	COWAN	RMBPT	NIST	COWAN	RMBPT	NIST
$3s3p$	3P_2	$3p^2$	3P_2	303.67	304.95	305.00	123	124	130
$3s3p$	3P_1	$3p^2$	3P_1	306.75	307.80	307.78	50.1	47.3	49.1
$3s3p$	3P_2	$3p^2$	3P_1	320.09	321.84	321.76	73.7	68.6	71
$3s3p$	3P_1	$3p^2$	3P_0	316.27	317.65	317.62	183	171	177
$3s3p$	3P_1	$3p^2$	3P_2	291.64	292.32	292.36	41.7	43.7	45
$3s3p$	3P_0	$3p^2$	3P_1	301.57	302.37	302.45	70.8	66.8	69
$3s3p$	3P_2	$3p^2$	1D_2	323.45	327.07	327.03	27.0	18.0	20
$3s3p$	3P_1	$3p^2$	1D_2	309.84	312.58	312.55	14.8	10.1	11
$3s3p$	1P_1	$3p^2$	1D_2	455.55	481.25	481.52	18.9	14.4	16
$3s3p$	1P_1	$3p^2$	1S_0	323.61	325.05	324	202	193	197
$3s3p$	3P_2	$3s3d$	3D_3	233.61	234.18	233.86	224	211	220
$3s3p$	3P_1	$3s3d$	3D_2	227.40	227.47	227.21	182	172	180
$3s3p$	3P_0	$3s3d$	3D_1	225.16	225.01	224.76	140	132	138
$3s3p$	3P_2	$3s3d$	3D_2	234.65	235.05	234.76	55.7	52.0	55
$3s3p$	3P_1	$3s3d$	3D_1	228.04	228.01	227.70	100	94.2	98
$3s3p$	3P_2	$3s3d$	3D_1	235.33	235.62	235.27	6.11	5.68	6.2
$3s3p$	1P_1	$3s3d$	1D_2	243.83	244.27	243.79	419	397	420
$3s3p$	3P_2	$3s3d$	1D_2	200.09	197.11	196.74	0.108	0.154	0.16
$3s3p$	3P_1	$3s3d$	1D_2	194.80	191.75	191.41	3.65	3.17	3.5
$3s3d$	3D_3	$3p3d$	3F_4	368.76	372.64	372.78	59.3	54.4	60
$3s3d$	3D_2	$3p3d$	3F_3	381.77	386.97	387.00	42.9	39.4	41
$3s3d$	3D_1	$3p3d$	3F_2	394.30	400.68	400.65	33.2	29.9	32
$3s3d$	3D_3	$3p3d$	3F_3	384.56	389.37	389.48	9.98	8.68	10
$3s3d$	3D_2	$3p3d$	3F_2	396.22	402.34	402.16	9.18	7.94	9.1
$3s3d$	3D_3	$3p3d$	3F_2	399.22	404.93	404.94	0.130	0.123	0.11
$3s3d$	1D_2	$3p3d$	1D_2	504.64	534.70	540	9.24	6.66	7.3
$3s3d$	1D_2	$3p3d$	1F_3	331.19	333.67	333	174	166	180
$3s3d$	1D_2	$3p3d$	1P_1	321.44	320.58	324	120	117	130
$3p^2$	1D_2	$3p3d$	1D_2	257.22	257.33	258	139	146	140
$3p^2$	1S_0	$3p3d$	1P_1	242.59	241.73	243	248	237	240
$3p^2$	1D_2	$3p3d$	1F_3	203.02	199.48		199	191	
$3p^2$	1D_2	$3p3d$	1P_1	199.32	194.73	196	2.75	4.48	3.8
$3p^2$	3P_2	$3p3d$	3D_3	243.50	242.34	243	225	239	230
$3p^2$	3P_2	$3p3d$	3D_1	251.02	249.64	251	3.20	2.61	2.8
$3p^2$	3P_2	$3p3d$	3D_2	242.77	241.34		174	179	
$3p^2$	3P_1	$3p3d$	3D_1	240.80	239.35	241	39.8	42.0	42
$3p^2$	3P_1	$3p3d$	3D_2	233.21	231.71		52.8	47.5	
$3p^2$	3P_0	$3p3d$	3D_1	235.25	232.13	235	256	200	250
$3p^2$	3P_2	$3p3d$	3P_1	243.25	243.50	243	64.2	67.8	64
$3p^2$	3P_2	$3p3d$	3P_2	250.35	249.24		13.4	10.6	
$3p^2$	3P_1	$3p3d$	3P_1	233.65	231.93	233	152	144	150
$3p^2$	3P_1	$3p3d$	3P_2	240.19	238.99		229	227	
$3p^2$	3P_1	$3p3d$	3P_0	234.02	232.13	233	204	200	200

Table VII: Wavelengths (λ in Å), and radiative rates (A_r in 10^8 s^{-1}) for $3l_13l_2 - 3l_34l_4$ transitions of Mg-like iron. Comparison of present results (Cowan code) with recommended NIST data (Ref. 20).

Low level		Upper level		λ (Å)		$A_r(10^8 \text{ s}^{-1})$	
Conf.	LSJ	Conf.	LSJ	COWAN	NIST	COWAN	NIST
$3s^2$	1S_0	$3s4p$	1P_1	52.96	52.91	2538	2940
$3s3p$	1P_1	$3s4d$	1D_2	59.15	59.40	2468	3400
$3s3p$	3P_2	$3s4d$	3D_3	56.21		4161	
$3s3p$	3P_1	$3s4d$	3D_2	55.82		3194	
$3s3p$	3P_2	$3s4s$	3S_1	66.30	66.24	1917	1600
$3s3p$	3P_1	$3s4s$	3S_1	65.71	65.61	1175	980
$3s3p$	3P_0	$3s4s$	3S_1	65.47	65.37	399	320
$3s3p$	1P_1	$3s4s$	1S_0	69.46	69.7	2274	1900
$3s3p$	1P_1	$3p4p$	1D_2	53.73		2010	
$3s3d$	3D_3	$3s4f$	3F_4	70.24	70.05	8743	8800
$3s3d$	3D_2	$3s4f$	3F_3	70.16	69.99	7793	7900
$3s3d$	3D_1	$3s4f$	3F_2	70.11	69.94	7378	7400
$3s3d$	1D_2	$3s4f$	1F_3	73.24	73.47	6369	6200
$3s3d$	1D_2	$3d4p$	1F_3	54.43		1954	
$3s3d$	3D_3	$3d4p$	3F_4	52.80		1476	
$3s3d$	1D_2	$3s4f$	1F_3	73.24		6369	
$3p^2$	1D_2	$3s4f$	1F_3	64.27	63.96	1643	1600
$3p^2$	3P_1	$3p4d$	3D_2	57.24		3688	
$3p^2$	3P_2	$3p4d$	3D_3	57.22		2971	
$3p^2$	1D_2	$3p4d$	3D_3	57.08		2589	
$3p^2$	3P_0	$3p4d$	3D_1	56.94		3543	
$3p^2$	3P_2	$3p4d$	3P_2	56.92		2542	
$3p^2$	1D_2	$3p4d$	1F_3	56.35		2681	
$3p3d$	3F_3	$3p4f$	3G_4	69.30	68.86	7083	9200
$3p3d$	3D_3	$3p4f$	3D_3	70.60	70.59	1923	1700
$3p3d$	3P_0	$3p4f$	3D_1	70.30	70.22	4317	4130
$3p3d$	1F_3	$3p4f$	1G_4	73.01	73.20	7226	8800
$3p3d$	1P_1	$3p4f$	1D_2	73.20		6578	7000

Table VIII: Autoionization rates (A_a in s^{-1}) and excitation energies (E_S in eV) for even-parity states. Wavelengths (λ in Å), weighted radiative rates (gA_r in s^{-1}), factor intensities (Q_d in s^{-1}) and effective emission rate coefficients (C_S^{eff} in cm^3/s) for transitions between the excited even-parity and the $3lnl'$ autoionization odd-parity states of Mg-like iron.

Low level Conf.	Upper level Conf.	A_a s^{-1}	ΣA_a s^{-1}	E_S eV	ΣgA_r s^{-1}	gA_r s^{-1}	λ Å	Q_d s^{-1}	C_S^{eff} cm^3/s		
$3p2$	1D_2	$3p10d$	3F_3	2.15[11]	2.15[11]	1.989	3.86[11]	1.55[11]	31.85	1.23[11]	2.64[-13]
$3p2$	1D_2	$3p10d$	1F_3	3.61[11]	3.61[11]	4.492	4.83[11]	1.20[11]	31.65	1.01[11]	1.68[-13]
$3p2$	1D_2	$3p11d$	3F_3	2.81[11]	2.81[11]	7.471	3.15[11]	1.20[11]	31.41	1.03[11]	1.28[-13]
$3p2$	3P_1	$3p10d$	3P_2	1.17[13]	1.17[13]	1.984	2.83[11]	1.21[11]	31.88	1.20[11]	2.58[-13]
$3p2$	3P_2	$3p10d$	3P_2	1.17[13]	1.17[13]	4.472	2.83[11]	1.12[11]	31.85	1.11[11]	1.86[-13]
$3s3d$	3D_2	$3d7p$	3F_3	1.13[12]	1.13[12]	15.215	7.07[11]	2.00[11]	31.95	1.83[11]	1.05[-13]
$3s3d$	3D_2	$3d8p$	3F_3	8.62[11]	8.62[11]	31.515	5.17[11]	1.21[11]	30.67	1.11[11]	1.24[-14]
$3s3d$	3D_3	$3d7p$	3D_3	2.48[11]	2.48[11]	15.404	7.15[11]	2.25[11]	31.96	1.59[11]	8.93[-14]
$3s3d$	3D_3	$3d7p$	3F_4	1.12[11]	1.12[11]	15.575	8.62[11]	2.92[11]	31.94	1.57[11]	8.67[-14]
$3s3d$	3D_3	$3d7p$	3P_2	3.51[12]	3.51[12]	15.657	4.92[11]	1.25[11]	31.94	1.22[11]	6.66[-14]
$3s3d$	1D_2	$3d7p$	1F_3	6.03[12]	6.03[12]	15.706	7.63[11]	2.38[11]	32.68	2.33[11]	1.27[-13]
$3s3d$	1D_2	$3d8p$	1F_3	2.60[12]	2.60[12]	31.938	5.42[11]	1.18[11]	31.34	1.14[11]	1.23[-14]
$3d2$	1G_4	$3d7f$	1H_5	3.41[12]	3.41[12]	20.535	3.30[12]	2.23[12]	40.90	2.05[12]	6.89[-13]
$3d2$	3F_2	$3d7f$	3F_2	2.85[12]	2.85[12]	19.484	8.00[11]	2.16[11]	40.47	2.05[11]	7.64[-14]
$3d2$	3F_2	$3d7f$	3F_3	3.15[12]	3.15[12]	19.551	1.16[12]	2.87[11]	40.46	2.73[11]	1.01[-13]
$3d2$	3F_2	$3d7f$	3G_3	8.59[12]	8.59[12]	19.743	1.70[12]	6.90[11]	40.43	6.71[11]	2.44[-13]
$3d2$	3F_2	$3d8f$	3F_2	2.26[12]	2.26[12]	34.343	5.43[11]	1.29[11]	38.60	1.23[11]	1.04[-14]
$3d2$	3F_3	$3d7f$	3H_4	4.59[11]	4.59[11]	19.483	9.89[11]	3.31[11]	40.50	2.67[11]	9.95[-14]
$3d2$	3F_3	$3d7f$	3F_3	3.15[12]	3.15[12]	19.551	1.16[12]	1.66[11]	40.49	1.58[11]	5.84[-14]
$3d2$	3F_3	$3d7f$	3G_3	8.59[12]	8.59[12]	19.743	1.70[12]	1.50[11]	40.47	1.46[11]	5.29[-14]
$3d2$	3F_3	$3d7f$	3G_4	4.37[11]	4.37[11]	20.006	2.12[12]	9.89[11]	40.43	6.43[11]	2.28[-13]
$3d2$	3F_3	$3d8f$	3G_4	9.29[11]	9.29[11]	34.349	1.04[12]	3.00[11]	38.63	2.67[11]	2.25[-14]
$3d2$	3F_4	$3d7f$	3F_4	2.28[12]	2.28[12]	19.809	1.29[12]	2.31[11]	40.50	2.18[11]	7.85[-14]
$3d2$	3F_4	$3d7f$	3G_4	4.37[11]	4.37[11]	20.006	2.12[12]	2.68[11]	40.47	1.74[11]	6.16[-14]
$3d2$	3F_4	$3d7f$	3G_5	4.70[10]	4.70[10]	20.072	2.75[12]	1.70[12]	40.46	2.69[11]	9.44[-14]
$3d2$	3F_4	$3d8f$	3G_4	9.29[11]	9.29[11]	34.811	1.04[12]	1.95[11]	38.61	1.74[11]	1.40[-14]
$3d2$	1D_2	$3d7f$	3G_3	8.59[12]	8.59[12]	19.743	1.70[12]	2.14[11]	40.92	2.08[11]	7.57[-14]
$3d2$	1D_2	$3d7f$	1D_2	1.52[12]	1.52[12]	19.762	9.24[11]	1.89[11]	40.92	1.68[11]	6.11[-14]
$3d2$	1D_2	$3d7f$	3D_3	5.88[12]	5.88[12]	20.061	1.46[12]	3.61[11]	40.88	3.48[11]	1.23[-13]
$3d2$	1D_2	$3d7f$	1F_3	2.86[13]	2.86[13]	20.247	1.59[12]	3.20[11]	40.85	3.18[11]	1.10[-13]
$3d2$	3P_0	$3d7f$	3D_1	1.06[12]	1.06[12]	19.897	6.37[11]	2.54[11]	40.93	2.12[11]	7.58[-14]
$3d2$	3P_1	$3d7f$	1D_2	1.52[12]	1.52[12]	19.762	9.24[11]	2.35[11]	40.96	2.09[11]	7.58[-14]
$3d2$	3P_1	$3d7f$	1D_2	1.52[12]	1.52[12]	20.005	9.24[11]	2.52[11]	40.93	2.25[11]	7.96[-14]
$3d2$	3P_1	$3d7f$	3P_1	2.89[12]	2.89[12]	20.244	5.94[11]	1.76[11]	40.90	1.64[11]	5.68[-14]
$3d2$	3P_2	$3d7f$	3D_3	5.88[12]	5.88[12]	20.061	1.46[12]	2.04[11]	40.96	1.97[11]	6.95[-14]
$3d2$	3P_2	$3d7f$	3P_2	1.98[12]	1.98[12]	20.210	9.79[11]	4.40[11]	40.94	4.00[11]	1.39[-13]
$3d2$	3P_2	$3d7f$	1F_3	2.86[13]	2.86[13]	20.247	1.59[12]	5.61[11]	40.93	5.56[11]	1.92[-13]
$3d2$	3P_2	$3d8f$	1F_3	1.50[13]	4.81[13]	34.970	1.08[12]	3.78[11]	39.04	1.17[11]	9.28[-15]
$3d2$	1S_0	$3d7f$	1P_1	2.37[12]	2.37[12]	20.567	6.29[11]	2.66[11]	42.12	2.44[11]	8.18[-14]
$3p4f$	3G_5	$3p10g$	3H_6	3.19[13]	3.19[13]	5.117	5.01[11]	1.19[11]	75.30	1.19[11]	1.87[-13]
$3d4d$	1F_3	$3d7f$	3H_4	4.59[11]	4.59[11]	19.381	9.89[11]	1.67[11]	87.48	1.35[11]	5.08[-14]
$3d4d$	3D_1	$3d7f$	3F_2	2.85[12]	2.85[12]	19.484	8.00[11]	1.39[11]	87.67	1.32[11]	4.91[-14]
$3d4d$	3D_2	$3d7f$	3F_3	3.15[12]	3.15[12]	19.551	1.16[12]	1.85[11]	87.75	1.76[11]	6.51[-14]
$3d4d$	3D_3	$3d7f$	3F_4	2.28[12]	2.28[12]	19.809	1.29[12]	1.95[11]	87.71	1.83[11]	6.62[-14]
$3d4d$	3G_3	$3d7f$	3H_4	4.59[11]	4.59[11]	19.381	9.89[11]	1.70[11]	88.07	1.37[11]	5.18[-14]
$3d4d$	3G_3	$3d7f$	3H_4	4.59[11]	4.59[11]	19.483	9.89[11]	1.35[11]	88.00	1.09[11]	4.07[-14]
$3d4d$	3G_3	$3d8f$	3H_4	6.88[11]	6.88[11]	34.275	7.36[11]	1.19[11]	79.64	1.06[11]	9.02[-15]
$3d4d$	3G_4	$3d7f$	3H_5	5.31[11]	5.31[11]	19.558	1.24[12]	4.21[11]	88.08	3.47[11]	1.29[-13]
$3d4d$	3G_5	$3d7f$	3H_6	2.97[11]	2.97[11]	19.820	1.22[12]	5.32[11]	88.09	4.04[11]	1.46[-13]
$3d4d$	3F_2	$3d7f$	3G_3	8.59[12]	8.59[12]	19.743	1.70[12]	1.54[11]	89.25	1.50[11]	5.44[-14]
$3d4d$	3F_3	$3d7f$	3G_4	4.37[11]	4.37[11]	20.006	2.12[12]	2.19[11]	89.20	1.43[11]	5.05[-14]
$3d4d$	3F_3	$3d8f$	3G_4	9.29[11]	9.29[11]	34.811	1.04[12]	1.23[11]	80.62	1.09[11]	8.81[-15]

Low level Conf.	Upper level Conf.	A_a s ⁻¹	ΣA_a s ⁻¹	E_S eV	ΣgA_r s ⁻¹	gA_r s ⁻¹	λ Å	Q_d s ⁻¹	C_S^{eff} cm ³ /s		
3d4d	³ P ₂	3d7f	¹ F ₃	2.86[13]	2.86[13]	20.247	1.59[12]	1.19[11]	90.38	1.18[11]	4.08[-14]
3d4d	¹ G ₄	3d7f	¹ H ₅	3.41[12]	3.41[12]	20.535	3.30[12]	4.24[11]	90.49	3.89[11]	1.31[-13]
3d5d	³ G ₃	3d7f	³ H ₄	4.59[11]	4.59[11]	19.483	9.89[11]	1.30[11]	189.56	1.05[11]	3.91[-14]
3d5d	³ G ₄	3d7f	³ H ₅	5.31[11]	5.31[11]	19.558	1.24[12]	2.29[11]	189.81	1.89[11]	7.00[-14]
3d5d	³ D ₃	3d7f	³ F ₄	2.28[12]	2.28[12]	19.809	1.29[12]	1.34[11]	189.17	1.26[11]	4.57[-14]
3d5d	³ G ₅	3d7f	³ H ₆	2.97[11]	2.97[11]	19.820	1.22[12]	2.77[11]	189.82	2.11[11]	7.60[-14]
3d5d	¹ G ₄	3d7f	¹ H ₅	3.41[12]	3.41[12]	20.535	3.30[12]	2.27[11]	192.21	2.08[11]	6.99[-14]
3s10i	¹ I ₆	3p10i	¹ K ₇	1.96[13]	1.96[13]	5.172	3.20[11]	1.07[11]	334.54	1.06[11]	1.66[-13]
3s10i	³ I ₇	3p10i	³ K ₈	1.96[13]	1.96[13]	5.172	3.62[11]	1.22[11]	334.55	1.22[11]	1.91[-13]
3p7f	³ G ₃	3d7f	³ H ₄	4.59[11]	4.59[11]	19.381	9.89[11]	1.32[11]	251.92	1.07[11]	4.03[-14]
3p7f	³ G ₄	3d7f	³ H ₅	5.31[11]	5.31[11]	19.558	1.24[12]	1.39[11]	251.76	1.15[11]	4.25[-14]
3p7h	³ I ₅	3d7h	³ K ₆	2.93[12]	2.93[12]	20.068	6.03[11]	1.95[11]	251.19	1.92[11]	6.76[-14]
3p7h	³ G ₅	3d7h	³ G ₅	2.16[12]	2.16[12]	19.997	5.06[11]	1.18[11]	251.58	1.16[11]	4.10[-14]
3p7h	³ G ₅	3d7h	³ F ₄	2.48[11]	2.48[11]	20.106	4.15[11]	1.29[11]	251.02	1.09[11]	3.81[-14]
3p7h	³ I ₆	3d7h	³ I ₆	1.01[12]	1.01[12]	19.963	6.10[11]	1.20[11]	251.77	1.14[11]	4.06[-14]
3p7h	³ I ₆	3d7h	³ K ₇	2.95[12]	2.95[12]	20.081	6.94[11]	2.31[11]	251.17	2.27[11]	7.98[-14]
3p7f	³ G ₅	3d7f	³ H ₆	2.97[11]	2.97[11]	19.820	1.22[12]	2.11[11]	262.97	1.60[11]	5.78[-14]
3p7f	¹ G ₄	3d7f	¹ H ₅	3.41[12]	3.41[12]	20.535	3.30[12]	1.53[11]	260.25	1.41[11]	4.72[-14]
3p7h	¹ H ₅	3d7h	¹ I ₆	1.12[12]	1.12[12]	20.396	5.79[11]	1.46[11]	262.01	1.41[11]	4.79[-14]
3p7h	³ H ₆	3d7h	³ I ₇	1.20[12]	1.20[12]	20.404	6.67[11]	1.72[11]	261.99	1.65[11]	5.62[-14]
3p7h	³ I ₇	3d7h	³ K ₈	4.22[12]	4.22[12]	20.517	7.62[11]	1.99[11]	261.51	1.97[11]	6.62[-14]
3p7h	¹ I ₆	3d7h	¹ K ₇	4.35[12]	4.35[12]	20.528	6.70[11]	1.71[11]	261.47	1.69[11]	5.68[-14]
3p7h	³ G ₅	3d7h	³ G ₅	2.16[12]	2.16[12]	20.414	5.06[11]	1.13[11]	262.43	1.11[11]	3.76[-14]
3s11g	³ G ₅	3p11g	³ H ₆	2.24[13]	2.24[13]	10.442	3.97[11]	1.18[11]	334.97	1.18[11]	1.09[-13]
3s11i	³ I ₇	3p11i	³ K ₈	1.56[13]	1.56[13]	10.478	2.98[11]	1.62[11]	336.12	1.61[11]	1.48[-13]
3s11i	¹ I ₆	3p11i	¹ K ₇	1.56[13]	1.56[13]	10.478	2.63[11]	1.41[11]	336.14	1.40[11]	1.29[-13]
3s12g	³ G ₅	3p12g	³ H ₆	1.62[13]	1.62[13]	14.491	3.21[11]	1.01[11]	334.80	1.01[11]	6.19[-14]
3s12i	¹ I ₆	3p12i	¹ K ₇	1.23[13]	1.23[13]	14.516	2.24[11]	1.13[11]	334.86	1.13[11]	6.90[-14]
3s12i	³ I ₇	3p12i	³ K ₈	1.23[13]	1.23[13]	14.517	2.54[11]	1.30[11]	334.86	1.30[11]	7.95[-14]
3p8p	³ D ₂	3d8p	³ F ₃	8.62[11]	8.62[11]	31.515	5.17[11]	1.13[11]	250.99	1.04[11]	1.16[-14]
3p8f	³ G ₃	3d8f	³ H ₄	6.88[11]	6.88[11]	34.275	7.36[11]	1.30[11]	251.75	1.16[11]	9.86[-15]
3d5d	³ G ₅	3d7f	³ H ₆	2.97[11]	2.97[11]	19.820	1.22[12]	1.42[11]	491.07	1.08[11]	3.89[-14]
3d6g	¹ H ₅	3d7h	³ I ₆	1.01[12]	1.01[12]	19.963	6.10[11]	3.06[11]	542.60	2.92[11]	1.04[-13]
3d6g	³ G ₃	3d7h	³ H ₄	1.82[12]	1.82[12]	19.990	4.18[11]	2.03[11]	543.01	1.98[11]	7.02[-14]
3d6g	³ H ₄	3d7h	³ I ₅	1.15[12]	1.15[12]	19.961	5.10[11]	2.18[11]	543.77	2.10[11]	7.46[-14]
3d6g	³ G ₄	3d7h	³ G ₅	2.16[12]	2.16[12]	19.997	5.06[11]	1.90[11]	544.50	1.86[11]	6.59[-14]
3d6g	³ I ₅	3d7h	³ K ₆	2.93[12]	2.93[12]	20.068	6.03[11]	3.18[11]	544.75	3.13[11]	1.10[-13]
3d6g	³ I ₆	3d7h	³ K ₇	2.95[12]	2.95[12]	20.081	6.94[11]	2.17[11]	545.64	2.14[11]	7.52[-14]
3d6g	³ H ₅	3d7h	¹ I ₆	1.12[12]	1.12[12]	20.396	5.79[11]	2.29[11]	538.86	2.20[11]	7.49[-14]
3d6g	³ I ₇	3d7h	³ K ₈	4.22[12]	4.22[12]	20.517	7.62[11]	2.90[11]	536.37	2.87[11]	9.66[-14]
3d6g	³ H ₆	3d7h	³ I ₇	1.20[12]	1.20[12]	20.404	6.67[11]	2.42[11]	539.70	2.34[11]	7.95[-14]
3d6g	¹ F ₃	3d7h	³ F ₄	2.48[11]	2.48[11]	20.106	4.15[11]	2.01[11]	547.27	1.69[11]	5.94[-14]
3d6g	³ G ₅	3d7h	³ H ₆	2.28[12]	2.28[12]	20.382	5.77[11]	2.36[11]	540.94	2.31[11]	7.89[-14]
3d6g	¹ G ₄	3d7h	³ H ₅	2.76[12]	2.76[12]	20.383	4.87[11]	1.76[11]	542.52	1.74[11]	5.92[-14]
3d6g	¹ I ₆	3d7h	¹ K ₇	4.35[12]	4.35[12]	20.528	6.70[11]	1.08[11]	539.68	1.07[11]	3.58[-14]
3d6g	³ F ₃	3d7h	³ H ₄	1.82[12]	1.82[12]	20.407	4.18[11]	1.19[11]	543.34	1.16[11]	3.94[-14]
3d6g	³ F ₄	3d7h	³ G ₅	2.16[12]	2.16[12]	20.414	5.06[11]	1.35[11]	544.68	1.32[11]	4.48[-14]
3d6g	³ D ₃	3d7h	³ F ₄	2.48[11]	2.48[11]	20.485	4.15[11]	1.71[11]	549.14	1.44[11]	4.87[-14]
3p9h	³ H ₆	3d7h	³ I ₇	1.20[12]	1.20[12]	20.404	6.67[11]	1.06[11]	556.25	1.02[11]	3.46[-14]
3p9h	³ I ₇	3d7h	³ K ₈	4.22[12]	4.22[12]	20.517	7.62[11]	1.74[11]	557.60	1.73[11]	5.80[-14]
3p9h	¹ I ₆	3d7h	¹ K ₇	4.35[12]	4.35[12]	20.528	6.70[11]	1.96[11]	560.91	1.94[11]	6.53[-14]

Table IX: Autoionization rates (A_a in s^{-1}) and excitation energies (E_S in eV) for even-parity states. Wavelengths (λ in \AA), weighted radiative rates (gA_r in s^{-1}), factor intensities (Q_d in s^{-1}) and effective emission rate coefficients (C_S^{eff} in cm^3/s) for transitions between the excited odd-parity and the $3lnl'$ autoionization even-parity states of Mg-like iron.

Low level Conf.	Upper level Conf.	A_a s^{-1}	ΣA_a s^{-1}	E_S eV	ΣgA_r s^{-1}	gA_r s^{-1}	λ \AA	Q_d s^{-1}	C_S^{eff} cm^3/s		
$3p3d$	3F_2	$3p10f$	3G_3	8.81[12]	8.81[12]	2.460	4.93[11]	2.02[11]	36.05	2.01[11]	4.10[-13]
$3p3d$	3F_2	$3p11f$	3G_3	5.68[12]	5.68[12]	7.828	3.80[11]	1.51[11]	35.49	1.50[11]	1.79[-13]
$3p3d$	3F_2	$3p12f$	3G_3	3.79[12]	3.79[12]	11.908	3.12[11]	1.23[11]	35.08	1.22[11]	9.67[-14]
$3p3d$	3F_2	$3d7d$	1F_3	1.65[12]	1.65[12]	17.928	9.77[11]	2.45[11]	34.49	2.26[11]	9.85[-14]
$3p3d$	3F_2	$3d7d$	3G_3	2.68[12]	2.68[12]	18.025	9.59[11]	1.94[11]	34.49	1.85[11]	7.96[-14]
$3p3d$	3F_2	$3d8d$	1F_3	1.19[12]	1.19[12]	33.313	7.15[11]	1.79[11]	33.08	1.65[11]	1.54[-14]
$3p3d$	3F_2	$3d8d$	3G_3	1.53[12]	1.53[12]	33.375	7.07[11]	1.16[11]	33.07	1.09[11]	1.01[-14]
$3p3d$	3F_3	$3p10f$	3G_4	1.62[13]	1.62[13]	2.507	6.23[11]	1.61[11]	36.17	1.61[11]	3.27[-13]
$3p3d$	3F_3	$3p11f$	3G_4	1.09[13]	1.09[13]	7.863	4.88[11]	1.19[11]	35.61	1.18[11]	1.41[-13]
$3p3d$	3F_3	$3d7d$	3G_4	5.01[12]	5.01[12]	18.123	1.22[12]	4.75[11]	34.59	4.63[11]	1.98[-13]
$3p3d$	3F_3	$3d7d$	3F_3	1.07[12]	1.07[12]	18.451	9.97[11]	1.56[11]	34.56	1.38[11]	5.71[-14]
$3p3d$	3F_3	$3d8d$	3G_4	3.90[12]	3.90[12]	33.451	9.01[11]	2.82[11]	33.17	2.75[11]	2.54[-14]
$3p3d$	3F_3	$3d9d$	3G_4	3.03[12]	3.87[12]	43.894	6.98[11]	1.79[11]	32.27	1.37[11]	4.46[-15]
$3p3d$	1D_2	$3p10f$	1F_3	3.12[12]	3.12[12]	4.928	4.88[11]	1.04[11]	36.04	1.02[11]	1.62[-13]
$3p3d$	1D_2	$3d7d$	3G_3	2.68[12]	2.68[12]	18.025	9.59[11]	1.25[11]	34.72	1.19[11]	5.12[-14]
$3p3d$	1D_2	$3d7d$	1D_2	1.08[13]	1.08[13]	18.639	6.81[11]	1.62[11]	34.66	1.60[11]	6.48[-14]
$3p3d$	3F_4	$3p10f$	3G_5	1.20[13]	1.20[13]	4.964	7.95[11]	3.53[11]	36.05	3.51[11]	5.59[-13]
$3p3d$	3F_4	$3p11f$	3G_5	7.67[12]	7.67[12]	10.329	6.26[11]	2.65[11]	35.50	2.63[11]	2.45[-13]
$3p3d$	3F_4	$3d7s$	3D_3	2.00[12]	2.00[12]	13.090	7.64[11]	1.17[11]	35.22	1.11[11]	7.82[-14]
$3p3d$	3F_4	$3p12f$	3G_5	5.09[12]	5.09[12]	14.407	5.26[11]	2.19[11]	35.09	2.17[11]	1.34[-13]
$3p3d$	3F_4	$3d7d$	3G_5	3.54[12]	3.54[12]	18.425	1.44[12]	7.56[11]	34.69	7.29[11]	3.02[-13]
$3p3d$	3F_4	$3d7d$	3F_4	8.27[11]	8.27[11]	18.531	1.27[12]	2.43[11]	34.68	2.08[11]	8.51[-14]
$3p3d$	3F_4	$3d8d$	3G_5	2.12[12]	2.12[12]	33.778	1.07[12]	5.07[11]	33.27	4.85[11]	4.33[-14]
$3p3d$	3F_4	$3d8d$	3F_4	6.56[11]	6.56[11]	33.837	9.25[11]	1.62[11]	33.26	1.40[11]	1.24[-14]
$3p3d$	3F_4	$3d9d$	3G_5	1.35[12]	2.32[12]	44.241	8.27[11]	3.57[11]	32.36	2.01[11]	6.32[-15]
$3p3d$	3F_4	$3d10d$	3G_5	9.19[11]	1.18[12]	51.690	6.61[11]	2.59[11]	31.74	1.92[11]	2.86[-15]
$3p3d$	3F_4	$3d11d$	3G_5	5.77[11]	6.86[11]	57.181	5.42[11]	1.91[11]	31.30	1.50[11]	1.29[-15]
$3p3d$	3F_4	$3d12d$	3G_5	5.72[11]	6.00[11]	61.347	4.46[11]	1.36[11]	30.97	1.21[11]	6.88[-16]
$3p3d$	3D_1	$3d7d$	3D_1	3.94[12]	3.94[12]	17.958	4.39[11]	1.28[11]	35.09	1.24[11]	5.38[-14]
$3p3d$	3D_1	$3d7d$	3F_2	3.87[12]	3.87[12]	18.188	7.15[11]	1.41[11]	35.06	1.36[11]	5.78[-14]
$3p3d$	3P_2	$3p10f$	3D_3	5.89[12]	5.89[12]	2.490	4.86[11]	1.25[11]	36.71	1.24[11]	2.53[-13]
$3p3d$	3P_2	$3d7d$	3F_3	1.07[12]	1.07[12]	18.451	9.97[11]	1.41[11]	35.05	1.24[11]	5.14[-14]
$3p3d$	3P_2	$3d7d$	3P_1	4.91[12]	4.91[12]	18.737	4.14[11]	1.86[11]	35.02	1.81[11]	7.26[-14]
$3p3d$	3P_2	$3d8d$	3P_1	4.06[12]	4.06[12]	33.959	3.06[11]	1.28[11]	33.58	1.25[11]	1.10[-14]
$3p3d$	3D_3	$3p10f$	3F_4	4.23[12]	4.23[12]	4.943	6.26[11]	1.63[11]	36.59	1.60[11]	2.55[-13]
$3p3d$	3D_3	$3p11f$	3F_4	2.68[12]	2.68[12]	10.313	4.88[11]	1.18[11]	36.02	1.15[11]	1.07[-13]
$3p3d$	3D_3	$3d7d$	3D_3	3.36[12]	3.36[12]	18.338	9.75[11]	1.40[11]	35.20	1.34[11]	5.61[-14]
$3p3d$	3D_3	$3d7d$	3F_3	1.07[12]	1.07[12]	18.451	9.97[11]	1.34[11]	35.19	1.18[11]	4.88[-14]
$3p3d$	3D_3	$3d7d$	3F_4	8.27[11]	8.27[11]	18.531	1.27[12]	4.21[11]	35.18	3.60[11]	1.48[-13]
$3p3d$	3D_3	$3d8d$	3F_4	6.56[11]	6.56[11]	33.837	9.25[11]	2.57[11]	33.72	2.22[11]	1.97[-14]
$3p3d$	3D_3	$3d9d$	3F_4	4.79[11]	6.87[11]	44.277	6.99[11]	1.67[11]	32.79	1.04[11]	3.26[-15]
$3p3d$	3P_1	$3d7d$	3D_2	3.78[12]	3.78[12]	18.055	7.09[11]	2.24[11]	35.23	2.16[11]	9.30[-14]
$3p3d$	3P_1	$3d8d$	3D_2	2.13[12]	2.13[12]	33.397	5.19[11]	1.55[11]	33.76	1.48[11]	1.37[-14]
$3p3d$	3D_2	$3p10f$	3D_3	5.89[12]	5.89[12]	4.970	4.86[11]	1.26[11]	36.61	1.25[11]	1.98[-13]
$3p3d$	3D_2	$3d7d$	3G_3	2.68[12]	2.68[12]	18.025	9.59[11]	1.24[11]	35.25	1.18[11]	5.09[-14]
$3p3d$	3D_2	$3d7d$	3D_3	3.36[12]	3.36[12]	18.338	9.75[11]	1.78[11]	35.22	1.71[11]	7.13[-14]
$3p3d$	3D_2	$3d7d$	3P_2	7.03[12]	7.03[12]	18.824	6.64[11]	1.14[11]	35.17	1.11[11]	4.44[-14]
$3p3d$	3D_2	$3d8d$	3D_3	2.08[12]	2.08[12]	33.717	7.20[11]	1.13[11]	33.74	1.08[11]	9.71[-15]
$3p3d$	1F_3	$3p10f$	1G_4	2.64[13]	2.64[13]	5.041	6.34[11]	1.88[11]	37.43	1.88[11]	2.97[-13]
$3p3d$	1F_3	$3p11f$	1G_4	1.75[13]	1.75[13]	10.385	4.98[11]	1.33[11]	36.83	1.33[11]	1.23[-13]
$3p3d$	1F_3	$3d7d$	1G_4	1.94[13]	1.94[13]	18.788	1.36[12]	7.12[11]	35.94	7.07[11]	2.83[-13]
$3p3d$	1F_3	$3d8d$	1G_4	1.16[13]	1.16[13]	33.992	9.82[11]	4.39[11]	34.42	4.35[11]	3.80[-14]

Low level	Upper level	A_a	ΣA_a	E_S	ΣgA_r	gA_r	λ	Q_d	C_S^{eff}		
Conf.	LSJ	Conf.	LSJ	s^{-1}	s^{-1}	eV	s^{-1}	s^{-1}	\AA	s^{-1}	cm^3/s
3p3d	1F_3	3d9d	1G_4	6.96[12]	7.50[12]	44.378	7.45[11]	2.85[11]	33.45	2.62[11]	8.10[-15]
3p3d	1F_3	3d10d	1G_4	4.36[12]	4.95[12]	51.783	4.65[11]	1.93[11]	32.80	1.68[11]	2.47[-15]
3p4d	3D_3	3p10f	3G_4	1.62[13]	1.62[13]	2.507	6.23[11]	1.19[11]	71.83	1.18[11]	2.41[-13]
3p4d	3F_4	3p10f	3G_5	1.20[13]	1.20[13]	4.964	7.95[11]	1.53[11]	71.95	1.52[11]	2.42[-13]
3p4d	3F_4	3p11f	3G_5	7.67[12]	7.67[12]	10.329	6.26[11]	1.12[11]	69.78	1.12[11]	1.04[-13]
3p4d	1F_3	3p10f	1G_4	2.64[13]	2.64[13]	5.041	6.34[11]	1.28[11]	71.95	1.28[11]	2.02[-13]
3d4p	1D_2	3d7d	1F_3	1.65[12]	1.65[12]	17.928	9.77[11]	1.15[11]	78.76	1.06[11]	4.62[-14]
3d4p	3F_2	3d7d	3G_3	2.68[12]	2.68[12]	18.025	9.59[11]	1.48[11]	79.22	1.41[11]	6.08[-14]
3d4p	3D_3	3d7d	3G_4	5.01[12]	5.01[12]	18.123	1.22[12]	1.50[11]	79.35	1.46[11]	6.24[-14]
3d4p	3F_4	3d7d	3G_5	3.54[12]	3.54[12]	18.425	1.44[12]	2.74[11]	79.40	2.64[11]	1.09[-13]
3d4p	3F_4	3d8d	3G_5	2.12[12]	2.12[12]	33.778	1.07[12]	1.87[11]	72.29	1.78[11]	1.59[-14]
3d4p	1F_3	3d7d	1G_4	1.94[13]	1.94[13]	18.788	1.36[12]	1.99[11]	80.17	1.98[11]	7.90[-14]
3d4p	1F_3	3d8d	1G_4	1.16[13]	1.16[13]	33.992	9.82[11]	1.29[11]	72.99	1.28[11]	1.12[-14]
3d4f	3H_4	3d7g	3I_5	2.31[12]	2.31[12]	19.943	1.15[12]	3.07[11]	92.62	2.94[11]	1.05[-13]
3d4f	1G_4	3d7g	1H_5	1.66[12]	1.66[12]	19.849	1.14[12]	1.35[11]	92.85	1.27[11]	4.57[-14]
3d4f	1G_4	3d7g	1H_5	1.66[12]	1.66[12]	20.259	1.14[12]	1.66[11]	92.57	1.56[11]	5.39[-14]
3d4f	3H_5	3d7g	3I_6	2.54[12]	2.54[12]	20.018	1.31[12]	3.01[11]	92.75	2.90[11]	1.02[-13]
3d4f	3H_6	3d7g	3I_7	3.17[12]	3.17[12]	20.384	1.55[12]	5.59[11]	92.66	5.42[11]	1.85[-13]
3d4f	3F_2	3d7g	3G_3	4.15[12]	4.15[12]	19.894	7.36[11]	1.73[11]	93.36	1.68[11]	6.03[-14]
3d4f	3F_3	3d7g	3H_4	2.69[12]	2.69[12]	19.882	9.16[11]	1.04[11]	93.43	1.00[11]	3.59[-14]
3d4f	3F_4	3d7g	1H_5	1.66[12]	1.66[12]	20.259	1.14[12]	1.90[11]	93.26	1.79[11]	6.17[-14]
3d4f	3G_3	3d7g	3H_4	2.69[12]	2.69[12]	19.882	9.16[11]	1.69[11]	95.03	1.63[11]	5.84[-14]
3d4f	3G_4	3d7g	3H_5	2.39[12]	2.39[12]	20.290	1.11[12]	1.55[11]	94.85	1.48[11]	5.10[-14]
3d4f	3G_5	3d7g	3H_6	9.43[11]	9.43[11]	20.318	1.29[12]	2.70[11]	94.94	2.44[11]	8.38[-14]
3d4f	3D_1	3d7g	3F_2	1.52[12]	1.52[12]	20.102	4.90[11]	1.09[11]	95.42	1.02[11]	3.58[-14]
3d4f	3P_2	3d7g	3D_3	3.15[11]	3.15[11]	20.466	7.25[11]	1.36[11]	95.42	1.02[11]	3.46[-14]
3d4f	1F_3	3d7g	1G_4	1.65[13]	1.65[13]	20.392	9.01[11]	1.80[11]	95.69	1.79[11]	6.10[-14]
3d4f	1H_5	3d7g	1I_6	5.06[12]	5.06[12]	20.559	1.17[12]	2.54[11]	96.96	2.50[11]	8.37[-14]
3d5p	3F_4	3d7d	3G_5	3.54[12]	3.54[12]	18.425	1.44[12]	1.12[11]	171.66	1.08[11]	4.47[-14]
3d5f	1G_4	3d7g	1H_5	1.66[12]	1.66[12]	19.849	1.14[12]	1.20[11]	200.13	1.13[11]	4.06[-14]
3d5f	1G_4	3d7g	3I_5	2.31[12]	2.31[12]	19.943	1.15[12]	1.56[11]	199.83	1.49[11]	5.31[-14]
3d5f	3H_4	3d7g	3I_5	2.31[12]	2.31[12]	19.943	1.15[12]	1.05[11]	200.42	1.00[11]	3.58[-14]
3d5f	3H_5	3d7g	3I_6	2.54[12]	2.54[12]	20.018	1.31[12]	2.43[11]	200.47	2.34[11]	8.27[-14]
3d5f	3F_2	3d7g	3G_3	4.15[12]	4.15[12]	19.894	7.36[11]	1.47[11]	201.05	1.43[11]	5.12[-14]
3d5f	3H_6	3d7g	3I_7	3.17[12]	3.17[12]	20.384	1.55[12]	4.12[11]	200.05	3.99[11]	1.36[-13]
3d5f	3F_4	3d7g	1H_5	1.66[12]	1.66[12]	20.259	1.14[12]	1.97[11]	200.68	1.86[11]	6.41[-14]
3d5f	3G_3	3d7g	3H_4	2.69[12]	2.69[12]	19.882	9.16[11]	1.22[11]	204.03	1.17[11]	4.21[-14]
3d5f	3G_4	3d7g	3H_5	2.39[12]	2.39[12]	20.290	1.11[12]	1.53[11]	203.28	1.47[11]	5.05[-14]
3d5f	3G_5	3d7g	3H_6	9.43[11]	9.43[11]	20.318	1.29[12]	2.38[11]	203.60	2.16[11]	7.40[-14]
3d5f	3D_3	3d7g	3G_4	6.49[12]	6.49[12]	20.312	9.16[11]	1.06[11]	204.00	1.04[11]	3.57[-14]
3d5f	1F_3	3d7g	1G_4	1.65[13]	1.65[13]	20.392	9.01[11]	1.74[11]	204.71	1.73[11]	5.89[-14]
3d5f	1H_5	3d7g	1I_6	5.06[12]	5.06[12]	20.559	1.17[12]	1.50[11]	207.56	1.47[11]	4.92[-14]
3s9h	1H_5	3d7g	1I_6	5.06[12]	5.06[12]	20.559	1.17[12]	1.10[11]	208.25	1.08[11]	3.60[-14]
3p7s	3P_2	3d7s	3D_3	2.00[12]	2.00[12]	13.090	7.64[11]	1.11[11]	261.93	1.05[11]	7.42[-14]
3s10h	3H_6	3p10h	3I_7	3.15[13]	3.15[13]	5.165	4.04[11]	1.09[11]	334.53	1.09[11]	1.71[-13]
3s10k	1K_7	3p10k	1L_8	8.67[12]	8.67[12]	5.170	2.84[11]	1.14[11]	334.68	1.14[11]	1.78[-13]
3s10k	3K_8	3p10k	3L_9	8.67[12]	8.67[12]	5.171	3.18[11]	1.29[11]	334.68	1.28[11]	2.00[-13]
3p7d	3F_3	3d7d	3G_4	5.01[12]	5.01[12]	18.123	1.22[12]	1.15[11]	251.20	1.12[11]	4.78[-14]
3p7g	3H_4	3d7g	3I_5	2.31[12]	2.31[12]	19.943	1.15[12]	1.39[11]	251.37	1.33[11]	4.75[-14]
3p7g	3H_5	3d7g	3I_6	2.54[12]	2.54[12]	20.018	1.31[12]	2.21[11]	251.51	2.13[11]	7.52[-14]
3p7i	3K_6	3d7i	3L_7	1.25[12]	1.25[12]	20.123	8.37[11]	2.17[11]	251.25	2.07[11]	7.25[-14]
3p7i	3K_7	3d7i	3K_7	1.35[11]	1.35[11]	20.049	8.45[11]	1.46[11]	251.64	1.03[11]	3.62[-14]
3p7i	3K_7	3d7i	3L_8	1.26[12]	1.26[12]	20.126	9.48[11]	2.49[11]	251.25	2.39[11]	8.35[-14]
3p7i	3H_6	3d7i	3H_6	1.85[11]	1.85[11]	20.065	7.33[11]	1.45[11]	251.56	1.11[11]	3.91[-14]

Low level Conf.	Upper level Conf.	A_a s^{-1}	ΣA_a s^{-1}	E_S eV	ΣgA_r s^{-1}	gA_r s^{-1}	λ \AA	Q_d s^{-1}	C_S^{eff} cm^3/s		
3p7d	³ F ₄	3d7d	³ G ₅	3.54[12]	3.54[12]	18.425	1.44[12]	1.77[11]	262.70	1.70[11]	7.06[-14]
3p7d	¹ F ₃	3d7d	¹ G ₄	1.94[13]	1.94[13]	18.788	1.36[12]	1.15[11]	261.16	1.14[11]	4.56[-14]
3p7g	³ G ₅	3d7g	³ H ₆	9.43[11]	9.43[11]	20.318	1.29[12]	1.77[11]	262.01	1.60[11]	5.48[-14]
3p7g	³ H ₆	3d7g	³ I ₇	3.17[12]	3.17[12]	20.384	1.55[12]	2.10[11]	261.91	2.03[11]	6.92[-14]
3p7g	¹ H ₅	3d7g	¹ I ₆	5.06[12]	5.06[12]	20.559	1.17[12]	1.42[11]	261.48	1.39[11]	4.66[-14]
3p7i	¹ I ₆	3d7i	¹ K ₇	3.75[11]	3.75[11]	20.479	8.17[11]	1.51[11]	262.15	1.32[11]	4.45[-14]
3p7i	³ I ₇	3d7i	³ K ₈	3.77[11]	3.77[11]	20.481	9.25[11]	1.74[11]	262.15	1.52[11]	5.13[-14]
3p7i	¹ K ₇	3d7i	¹ L ₈	1.69[12]	1.69[12]	20.556	9.16[11]	1.86[11]	261.79	1.80[11]	6.03[-14]
3p7i	³ K ₈	3d7i	³ L ₉	1.69[12]	1.69[12]	20.559	1.02[12]	2.09[11]	261.79	2.02[11]	6.78[-14]
3p7i	³ H ₆	3d7i	³ H ₆	1.85[11]	1.85[11]	20.479	7.33[11]	1.35[11]	262.46	1.04[11]	3.50[-14]
3s11k	¹ K ₇	3p11k	¹ L ₈	8.24[12]	8.24[12]	10.482	2.47[11]	1.34[11]	335.73	1.34[11]	1.23[-13]
3s11k	³ K ₈	3p11k	³ L ₉	8.24[12]	8.24[12]	10.483	2.76[11]	1.51[11]	335.73	1.50[11]	1.38[-13]
3s11h	³ H ₆	3p11h	³ I ₇	2.31[13]	2.31[13]	10.472	3.25[11]	1.52[11]	335.95	1.52[11]	1.39[-13]
3s11h	¹ H ₅	3p11h	¹ I ₆	2.37[13]	2.37[13]	10.476	2.80[11]	1.18[11]	336.67	1.18[11]	1.09[-13]
3s11h	¹ H ₅	3d7g	¹ I ₆	5.06[12]	5.06[12]	20.559	1.17[12]	1.09[11]	264.30	1.07[11]	3.58[-14]
3s12h	³ H ₆	3p12h	³ I ₇	1.71[13]	1.71[13]	14.512	2.72[11]	1.17[11]	334.86	1.17[11]	7.15[-14]
3s12k	¹ K ₇	3p12k	¹ L ₈	7.30[12]	7.30[12]	14.523	2.20[11]	1.26[11]	334.82	1.26[11]	7.71[-14]
3s12k	³ K ₈	3p12k	³ L ₉	7.30[12]	7.30[12]	14.523	2.46[11]	1.42[11]	334.82	1.42[11]	8.69[-14]
3p8d	³ F ₃	3d8d	³ G ₄	3.90[12]	3.90[12]	33.451	9.01[11]	1.31[11]	251.06	1.28[11]	1.18[-14]
3p8d	¹ F ₃	3d8d	¹ G ₄	1.16[13]	1.16[13]	33.992	9.82[11]	1.31[11]	261.35	1.30[11]	1.14[-14]
3p8d	³ F ₄	3d8d	³ G ₅	2.12[12]	2.12[12]	33.778	1.07[12]	1.86[11]	262.54	1.78[11]	1.59[-14]
3d6f	³ H ₅	3d7g	³ I ₆	2.54[12]	2.54[12]	20.018	1.31[12]	1.70[11]	528.83	1.64[11]	5.78[-14]
3d6f	³ F ₄	3d7g	¹ H ₅	1.66[12]	1.66[12]	20.259	1.14[12]	1.36[11]	527.29	1.28[11]	4.41[-14]
3d6f	³ H ₆	3d7g	³ I ₇	3.17[12]	3.17[12]	20.384	1.55[12]	2.68[11]	524.80	2.60[11]	8.86[-14]
3d6f	³ G ₄	3d7g	³ H ₅	2.39[12]	2.39[12]	20.290	1.11[12]	1.14[11]	535.65	1.09[11]	3.77[-14]
3d6f	³ G ₅	3d7g	³ H ₆	9.43[11]	9.43[11]	20.318	1.29[12]	1.60[11]	536.86	1.45[11]	4.97[-14]
3d6h	³ I ₅	3d7i	³ K ₆	1.34[11]	1.34[11]	20.047	7.34[11]	4.47[11]	544.89	3.15[11]	1.11[-13]
3d6h	³ I ₆	3d7i	³ K ₇	1.35[11]	1.35[11]	20.049	8.45[11]	5.24[11]	544.90	3.69[11]	1.30[-13]
3d6h	³ H ₄	3d7i	³ I ₅	1.88[11]	1.88[11]	20.062	6.20[11]	3.69[11]	545.17	2.84[11]	1.00[-13]
3d6h	³ H ₅	3d7i	³ H ₆	1.85[11]	1.85[11]	20.065	7.33[11]	4.43[11]	545.31	3.40[11]	1.20[-13]
3d6h	³ K ₆	3d7i	³ L ₇	1.25[12]	1.25[12]	20.123	8.37[11]	5.32[11]	547.92	5.09[11]	1.78[-13]
3d6h	³ K ₇	3d7i	³ L ₈	1.26[12]	1.26[12]	20.126	9.48[11]	6.04[11]	548.18	5.78[11]	2.02[-13]
3d6h	¹ I ₆	3d7i	¹ K ₇	3.75[11]	3.75[11]	20.479	8.17[11]	3.63[11]	541.06	3.17[11]	1.07[-13]
3d6h	³ I ₇	3d7i	³ K ₈	3.77[11]	3.77[11]	20.481	9.25[11]	3.88[11]	541.13	3.39[11]	1.14[-13]
3d6h	³ K ₈	3d7i	³ L ₉	1.69[12]	1.69[12]	20.559	1.02[12]	3.79[11]	539.58	3.67[11]	1.23[-13]
3d6h	¹ K ₇	3d7i	¹ L ₈	1.69[12]	1.69[12]	20.556	9.16[11]	3.13[11]	539.69	3.04[11]	1.02[-13]
3d6h	¹ H ₅	3d7i	¹ I ₆	2.61[11]	2.61[11]	20.460	7.10[11]	3.33[11]	543.17	2.76[11]	9.33[-14]
3d6h	³ H ₆	3d7i	³ I ₇	2.36[11]	2.36[11]	20.462	8.19[11]	3.99[11]	543.11	3.24[11]	1.10[-13]
3d6h	¹ G ₄	3d7i	³ I ₅	1.88[11]	1.88[11]	20.477	6.20[11]	3.15[11]	545.19	2.42[11]	8.18[-14]
3d6h	³ G ₅	3d7i	³ H ₆	1.85[11]	1.85[11]	20.479	7.33[11]	3.78[11]	545.28	2.90[11]	9.79[-14]
3p9i	¹ I ₆	3d7i	¹ K ₇	3.75[11]	3.75[11]	20.479	8.17[11]	1.70[11]	554.99	1.48[11]	5.01[-14]
3p9i	³ I ₇	3d7i	³ K ₈	3.77[11]	3.77[11]	20.481	9.25[11]	1.98[11]	555.07	1.73[11]	5.84[-14]
3p9i	³ K ₈	3d7i	³ L ₉	1.69[12]	1.69[12]	20.559	1.02[12]	3.43[11]	557.86	3.32[11]	1.11[-13]
3p9i	¹ K ₇	3d7i	¹ L ₈	1.69[12]	1.69[12]	20.556	9.16[11]	3.08[11]	558.05	2.98[11]	1.00[-13]
3d6f	¹ H ₅	3d7g	¹ I ₆	5.06[12]	5.06[12]	20.559	1.17[12]	1.31[11]	561.16	1.29[11]	4.30[-14]

Table X: Autoionization rates (A_a in s^{-1}) and excitation energies (E_S in eV) for even-parity states. Wavelengths (λ in \AA), weighted radiative rates (gA_r in s^{-1}), factor intensities (Q_d in s^{-1}) and effective emission rate coefficients (C_S^{eff} in cm^3/s) for transitions between the excited even-parity and the $4lnl'$ autoionization odd-parity states of Mg-like iron.

Low level Conf.	LSJ	Upper level Conf.	LSJ	A_a s^{-1}	ΣA_a s^{-1}	E_S eV	ΣgA_r s^{-1}	gA_r s^{-1}	λ \AA	Q_d s^{-1}	C_S^{eff} cm^3/s
3s4s	3S_1	4s4p	3P_1	2.48[13]	2.48[13]	0.967	1.63[12]	5.38[11]	51.75	5.27[11]	1.25[-12]
3s4s	3S_1	4s4p	3P_2	2.44[13]	2.44[13]	1.622	2.72[12]	9.11[11]	51.61	8.91[11]	1.98[-12]
3s4s	1S_0	4s4p	1P_1	8.93[13]	8.93[13]	7.146	1.68[12]	4.76[11]	50.99	4.73[11]	6.05[-13]
3s4d	3D_3	4s4f	3F_4	2.12[13]	2.12[13]	29.871	1.04[13]	4.27[11]	52.78	4.05[11]	5.34[-14]
3p4p	3D_3	4s4f	3F_4	2.12[13]	2.12[13]	29.871	1.04[13]	5.75[11]	57.33	5.46[11]	7.20[-14]
3d4s	3D_2	4s4f	3F_2	2.11[13]	2.11[13]	29.668	5.59[12]	4.85[11]	68.11	4.61[11]	6.20[-14]
3d4s	3D_3	4s4f	3F_3	2.13[13]	2.13[13]	29.761	7.93[12]	5.24[11]	68.18	4.97[11]	6.63[-14]
3d4s	1D_2	4s4f	1F_3	9.06[13]	9.06[13]	30.199	7.83[12]	4.59[12]	68.32	4.53[12]	5.79[-13]
3p4p	1D_2	4s4f	1F_3	9.06[13]	9.06[13]	30.199	7.83[12]	7.11[11]	57.94	7.02[11]	8.97[-14]
3p4f	3G_4	4s4f	3F_4	2.12[13]	2.12[13]	29.871	1.04[13]	4.57[11]	64.83	4.33[11]	5.72[-14]
3p4f	3D_3	4s4f	3F_4	2.12[13]	2.12[13]	29.871	1.04[13]	6.83[11]	65.91	6.48[11]	8.55[-14]
3p4f	3D_2	4s4f	3F_3	2.13[13]	2.13[13]	29.761	7.93[12]	5.11[11]	66.06	4.85[11]	6.47[-14]
3p4f	3D_1	4s4f	3F_2	2.11[13]	2.11[13]	29.668	5.59[12]	4.99[11]	66.23	4.74[11]	6.39[-14]
3p4f	1G_4	4s4f	1F_3	9.06[13]	9.06[13]	30.199	7.83[12]	6.79[11]	66.44	6.70[11]	8.56[-14]
3p4f	1D_2	4s4f	1F_3	9.06[13]	9.06[13]	30.199	7.83[12]	4.80[11]	66.68	4.74[11]	6.05[-14]
3d4s	3D_1	4s4f	3F_2	2.11[13]	2.11[13]	29.668	5.59[12]	2.74[12]	68.07	2.60[12]	3.51[-13]
3d4s	3D_2	4s4f	3F_3	2.13[13]	2.13[13]	29.761	7.93[12]	4.06[12]	68.08	3.85[12]	5.14[-13]
3d4s	3D_3	4s4f	3F_4	2.12[13]	2.12[13]	29.871	1.04[13]	6.45[12]	68.14	6.12[12]	8.07[-13]
3p4f	1G_4	4d4f	1H_5	6.12[13]	1.08[14]	66.844	1.49[13]	3.27[12]	55.53	1.83[12]	5.97[-15]
3p4f	3G_5	4d4f	3H_6	1.32[11]	1.35[11]	60.942	1.67[13]	5.60[12]	56.24	5.20[11]	3.07[-15]
3p4f	3F_4	4d4f	3F_4	7.60[11]	1.37[12]	61.417	1.17[13]	1.48[12]	56.14	4.21[11]	2.37[-15]
3p4f	1D_2	4d4f	1F_3	4.03[13]	5.42[13]	65.350	9.22[12]	7.38[11]	56.08	5.36[11]	2.04[-15]
3d4d	1F_3	4d4f	1F_3	4.03[13]	5.42[13]	65.350	9.22[12]	1.70[12]	66.05	1.23[12]	4.69[-15]
3d4d	3D_2	4d4f	3F_3	7.61[11]	1.37[12]	61.353	9.14[12]	3.80[12]	67.71	1.08[12]	6.12[-15]
3d4d	3D_3	4d4f	3F_4	7.60[11]	1.37[12]	61.417	1.17[13]	5.15[12]	67.76	1.46[12]	8.23[-15]
3d4d	1D_2	4d4f	1F_3	4.03[13]	5.42[13]	65.350	9.22[12]	3.77[12]	67.83	2.74[12]	1.04[-14]
3d4d	1G_4	4d4f	1H_5	6.12[13]	1.08[14]	66.844	1.49[13]	1.12[13]	67.59	6.24[12]	2.04[-14]
3d4d	3D_1	4d4f	3F_2	7.53[11]	1.35[12]	61.303	6.55[12]	2.45[12]	67.66	6.94[11]	3.95[-15]
3d4d	3G_3	4d4f	3H_4	1.23[11]	1.31[11]	60.751	1.16[13]	6.44[12]	68.05	5.55[11]	3.34[-15]
3d4d	3G_4	4d4f	3H_5	1.35[11]	1.42[11]	60.830	1.42[13]	8.43[12]	68.09	7.97[11]	4.76[-15]
3d4d	3G_5	4d4f	3H_6	1.32[11]	1.35[11]	60.942	1.67[13]	1.04[13]	68.16	9.68[11]	5.72[-15]
3d4d	3F_3	4d4f	3F_3	7.61[11]	1.37[12]	61.353	9.14[12]	1.54[12]	68.74	4.37[11]	2.47[-15]
3d4d	3F_4	4d4f	3F_4	7.60[11]	1.37[12]	61.417	1.17[13]	2.23[12]	68.80	6.34[11]	3.57[-15]
3d4d	3P_2	4d4f	1F_3	4.03[13]	5.42[13]	65.350	9.22[12]	9.03[11]	68.00	6.57[11]	2.49[-15]
3d4d	1S_0	4d4f	1P_1	5.05[12]	1.53[13]	68.594	3.86[12]	1.34[12]	68.08	4.09[11]	1.12[-15]
3d4s	3D_1	4s5f	3F_2	1.97[13]	4.15[13]	103.721	3.90[12]	1.37[12]	48.39	6.37[11]	5.22[-17]
3d4s	3D_2	4s5f	3F_3	1.98[13]	4.15[13]	103.742	4.62[12]	1.98[12]	48.41	9.29[11]	7.59[-17]
3d4s	3D_2	4s6f	3F_3	1.49[13]	3.06[13]	143.294	3.44[12]	9.95[11]	41.94	4.76[11]	7.45[-19]
3d4s	3D_3	4s5f	3F_4	1.97[13]	4.13[13]	103.771	7.23[12]	2.95[12]	48.46	1.38[12]	1.13[-16]
3d4s	1D_2	4s5f	1F_3	5.62[13]	1.17[14]	103.958	4.58[12]	2.16[12]	48.58	1.04[12]	8.30[-17]
3d4s	3D_3	4s6f	3F_4	1.48[13]	3.05[13]	143.307	5.16[12]	1.49[12]	41.97	7.09[11]	1.11[-18]
3d4s	3D_3	4s7f	3F_4	8.73[12]	1.77[13]	166.776	4.31[12]	8.49[11]	38.88	4.07[11]	6.09[-20]
3d4s	1D_2	4s6f	1F_3	4.26[13]	9.28[13]	143.516	3.52[12]	1.07[12]	42.06	4.87[11]	7.46[-19]
3s5g	1G_4	4p5g	1H_5	1.36[13]	4.40[13]	121.415	5.15[12]	1.67[12]	50.52	5.10[11]	7.12[-18]
3d4d	1G_4	4d5f	1H_5	6.81[11]	2.39[12]	135.579	1.13[13]	2.36[12]	49.17	4.70[11]	1.59[-18]
3p5p	3D_3	4d5p	3F_4	4.55[12]	1.27[13]	122.227	7.50[12]	2.19[12]	55.41	7.37[11]	9.49[-18]
3p5f	3G_5	4s5f	3F_4	1.97[13]	4.13[13]	103.771	7.23[12]	9.75[11]	64.42	4.56[11]	3.72[-17]
3s7g	1G_4	4p7g	1H_5	6.35[12]	1.51[13]	182.247	5.05[12]	1.20[12]	50.39	4.91[11]	1.56[-20]
3s7i	3I_7	4p7i	3I_7	6.77[11]	2.56[12]	181.755	4.51[12]	2.00[12]	50.50	4.72[11]	1.58[-20]
3d5s	3D_3	4d5p	3F_4	4.55[12]	1.27[13]	122.227	7.50[12]	3.45[12]	67.69	1.16[12]	1.50[-17]
3d5s	3D_2	4d5p	3F_3	4.30[12]	1.31[13]	122.035	5.07[12]	1.44[12]	67.58	4.47[11]	5.87[-18]
3d5s	3D_3	4f5s	3F_4	1.48[12]	9.56[12]	125.551	8.28[12]	5.02[12]	66.48	7.06[11]	6.52[-18]

Low level		Upper level		A_a	ΣA_a	E_S	ΣgA_r	gA_r	λ	Q_d	C_S^{eff}
Conf.	LSJ	Conf.	LSJ	s^{-1}	s^{-1}	eV	s^{-1}	s^{-1}	\AA	s^{-1}	cm^3/s
<i>3d5s</i>	1D_2	<i>4f5s</i>	1F_3	2.32[13]	7.59[13]	122.690	5.27[12]	1.60[12]	67.56	4.85[11]	5.95[-18]
<i>3p6p</i>	3D_3	<i>4d6p</i>	3F_4	1.25[12]	8.17[12]	168.142	4.98[12]	3.25[12]	54.96	4.64[11]	6.06[-20]
<i>3p6f</i>	3G_5	<i>4s6f</i>	3F_4	1.48[13]	3.05[13]	143.307	5.16[12]	1.05[12]	64.04	4.99[11]	7.80[-19]
<i>3p6f</i>	3G_5	<i>4d6f</i>	3H_6	7.75[11]	5.34[12]	175.416	8.15[12]	4.78[12]	54.93	6.21[11]	3.91[-20]
<i>3p6h</i>	3I_7	<i>4d6h</i>	3K_8	1.95[12]	1.22[13]	176.623	8.21[12]	3.80[12]	54.78	5.87[11]	3.28[-20]
<i>3d5d</i>	1G_4	<i>4f5d</i>	1H_5	3.10[13]	1.56[14]	142.264	1.28[13]	7.69[12]	66.56	1.52[12]	2.63[-18]
<i>3d5d</i>	3G_4	<i>4f5d</i>	3H_5	1.98[11]	3.49[12]	139.742	1.32[13]	9.62[12]	66.84	4.06[11]	9.06[-19]
<i>3d5d</i>	3D_3	<i>4f5d</i>	3F_4	3.97[11]	2.72[12]	139.408	1.11[13]	5.12[12]	66.97	5.15[11]	1.19[-18]
<i>3d5d</i>	3G_5	<i>4f5d</i>	3H_6	1.97[11]	3.48[12]	139.814	1.56[13]	1.20[13]	66.91	5.05[11]	1.12[-18]
<i>3d5d</i>	1G_4	<i>4d5f</i>	1H_5	6.81[11]	2.39[12]	135.579	1.13[13]	2.47[12]	69.04	4.92[11]	1.67[-18]
<i>3p7f</i>	3G_5	<i>4d7f</i>	3H_6	8.89[11]	3.83[12]	198.859	7.09[12]	5.21[12]	54.82	1.06[12]	6.40[-21]
<i>3p7f</i>	3F_4	<i>4d7f</i>	3H_5	5.96[11]	2.94[12]	198.785	6.20[12]	3.43[12]	54.83	5.83[11]	3.55[-21]
<i>3p7f</i>	3G_5	<i>4s7f</i>	3F_4	8.73[12]	1.77[13]	166.776	4.31[12]	1.13[12]	63.89	5.41[11]	8.09[-20]
<i>3p7h</i>	1H_5	<i>4d7h</i>	3K_6	1.33[12]	9.95[12]	199.646	6.11[12]	3.13[12]	54.74	4.00[11]	2.24[-21]
<i>3p7h</i>	3I_7	<i>4d7h</i>	3K_8	1.62[12]	1.16[13]	199.774	7.89[12]	6.80[12]	54.74	9.12[11]	5.03[-21]
<i>3p7h</i>	1I_6	<i>4d7h</i>	1K_7	3.40[12]	2.92[13]	200.352	7.04[12]	3.89[12]	54.60	4.45[11]	2.32[-21]
<i>3d6s</i>	3D_1	<i>4f6s</i>	3F_2	2.48[12]	7.74[12]	171.977	5.16[12]	3.85[12]	66.52	1.09[12]	9.68[-20]
<i>3d6s</i>	3D_2	<i>4f6s</i>	3F_3	2.62[12]	8.08[12]	172.009	7.18[12]	5.02[12]	66.53	1.44[12]	1.28[-19]
<i>3d6s</i>	3D_3	<i>4f6s</i>	3F_4	2.43[12]	7.74[12]	172.059	9.64[12]	7.92[12]	66.64	2.18[12]	1.92[-19]
<i>3d6s</i>	1D_2	<i>4f6s</i>	1F_3	1.42[13]	3.29[13]	172.249	6.98[12]	5.06[12]	66.64	2.12[12]	1.83[-19]
<i>3d6d</i>	3G_5	<i>4f6d</i>	3H_6	7.17[11]	5.53[12]	180.626	1.48[13]	1.24[13]	66.64	1.33[12]	4.98[-20]
<i>3d6g</i>	3G_5	<i>4f6g</i>	3H_6	1.80[12]	4.69[12]	183.078	1.34[13]	4.34[12]	66.83	1.37[12]	4.01[-20]
<i>3d6g</i>	3I_7	<i>4f6g</i>	3K_8	4.25[11]	3.32[12]	183.471	1.26[13]	1.02[13]	66.76	1.07[12]	3.01[-20]
<i>3d6d</i>	3G_3	<i>4f6d</i>	3H_4	8.35[11]	6.58[12]	180.506	9.61[12]	5.52[12]	66.54	6.03[11]	2.29[-20]
<i>3d6d</i>	3G_4	<i>4f6d</i>	3H_5	7.87[11]	6.37[12]	180.557	1.22[13]	8.94[12]	66.57	9.40[11]	3.54[-20]
<i>3d6d</i>	1G_4	<i>4f6d</i>	1H_5	7.27[12]	6.87[13]	181.355	9.96[12]	6.21[12]	66.61	6.49[11]	2.26[-20]
<i>3d6d</i>	1G_4	<i>4p7g</i>	1H_5	6.35[12]	1.51[13]	182.247	5.05[12]	9.90[11]	66.30	4.04[11]	1.29[-20]
<i>3d6g</i>	1H_5	<i>4f6g</i>	3H_5	1.58[12]	4.14[12]	183.071	1.03[13]	1.54[12]	66.68	4.80[11]	1.41[-20]
<i>3d6g</i>	1H_5	<i>4f6g</i>	1H_5	2.73[13]	9.52[13]	184.384	1.26[13]	1.76[12]	66.21	4.98[11]	1.28[-20]
<i>3d6g</i>	3H_4	<i>4f6g</i>	3H_4	1.43[12]	3.70[12]	183.061	7.66[12]	2.67[12]	66.69	8.42[11]	2.47[-20]
<i>3d6g</i>	3G_3	<i>4f6g</i>	3H_4	1.43[12]	3.70[12]	183.061	7.66[12]	2.87[12]	66.71	9.05[11]	2.66[-20]
<i>3d6g</i>	3G_4	<i>4f6g</i>	3H_5	1.58[12]	4.14[12]	183.071	1.03[13]	1.96[12]	66.73	6.13[11]	1.80[-20]
<i>3d6g</i>	3G_4	<i>4f6g</i>	3H_5	1.58[12]	4.14[12]	183.071	1.03[13]	2.06[12]	66.85	6.43[11]	1.88[-20]
<i>3d6g</i>	3H_6	<i>4f6g</i>	3H_6	1.80[12]	4.69[12]	183.078	1.34[13]	1.73[12]	66.76	5.46[11]	1.60[-20]
<i>3d6g</i>	3H_6	<i>4f6g</i>	3K_7	5.32[11]	3.92[12]	183.401	1.12[13]	3.99[12]	66.64	4.55[11]	1.29[-20]
<i>3d6g</i>	3H_6	<i>4f6g</i>	3H_6	1.80[12]	4.69[12]	183.078	1.34[13]	2.77[12]	66.86	8.72[11]	2.55[-20]
<i>3d6g</i>	3H_6	<i>4f6g</i>	3K_7	5.32[11]	3.92[12]	183.401	1.12[13]	3.54[12]	66.74	4.04[11]	1.15[-20]
<i>3d6g</i>	3G_5	<i>4f6g</i>	1H_5	2.73[13]	9.52[13]	184.384	1.26[13]	1.65[12]	66.36	4.68[11]	1.20[-20]
<i>3d6g</i>	3H_5	<i>4f6g</i>	3H_6	1.80[12]	4.69[12]	183.078	1.34[13]	1.85[12]	66.84	5.82[11]	1.70[-20]
<i>3d6g</i>	1G_4	<i>4f6g</i>	1H_5	2.73[13]	9.52[13]	184.384	1.26[13]	3.12[12]	66.42	8.84[11]	2.27[-20]
<i>3d6g</i>	3I_7	<i>4p7i</i>	3K_8	9.86[11]	5.96[12]	182.672	9.21[12]	6.20[12]	67.05	9.41[11]	2.87[-20]
<i>3d6g</i>	1D_2	<i>4f6g</i>	1P_1	3.58[12]	1.53[13]	185.635	3.34[12]	2.20[12]	66.13	4.79[11]	1.09[-20]

Table XI: Autoionization rates (A_a in s^{-1}) and excitation energies (E_S in eV) for even-parity states. Wavelengths (λ in \AA), weighted radiative rates (gA_r in s^{-1}), factor intensities (Q_d in s^{-1}) and effective emission rate coefficients (C_S^{eff} in cm^3/s) for transitions between the excited odd-parity and the $4lnl'$ autoionization even-parity states of Mg-like iron.

Low level Conf.	Upper level Conf.	A_a s^{-1}	ΣA_a s^{-1}	E_S eV	ΣgA_r s^{-1}	gA_r s^{-1}	λ \AA	Q_d s^{-1}	C_S^{eff} cm^3/s		
$3p4s$	3P_1	$4s4d$	3D_2	4.89[13]	4.89[13]	21.193	3.44[12]	1.30[12]	55.46	1.28[12]	4.04[-13]
$3p4s$	3P_2	$4s4d$	3D_3	4.93[13]	4.93[13]	21.290	4.77[12]	2.69[12]	55.95	2.65[12]	8.25[-13]
$3p4s$	3P_0	$4s4d$	3D_1	4.85[13]	4.85[13]	21.130	2.07[12]	6.52[11]	55.38	6.43[11]	2.03[-13]
$3p4s$	3P_1	$4s4d$	3D_1	4.85[13]	4.85[13]	21.130	2.07[12]	4.29[11]	55.48	4.23[11]	1.34[-13]
$3p4s$	3P_2	$4s4d$	3D_2	4.89[13]	4.89[13]	21.193	3.44[12]	4.76[11]	55.97	4.69[11]	1.47[-13]
$3p4d$	3D_3	$4s4d$	3D_3	4.93[13]	4.93[13]	21.290	4.77[12]	5.13[11]	64.78	5.06[11]	1.57[-13]
$3p4d$	3F_2	$4s4d$	3D_1	4.85[13]	4.85[13]	21.130	2.07[12]	3.16[11]	65.46	3.12[11]	9.86[-14]
$3p4d$	3D_3	$4s4d$	3D_2	4.89[13]	4.89[13]	21.193	3.44[12]	4.83[11]	65.49	4.76[11]	1.50[-13]
$3p4s$	1P_1	$4s4d$	1D_2	6.88[13]	6.88[13]	26.264	3.23[12]	1.33[12]	55.07	1.32[12]	2.49[-13]
$3s4f$	3F_4	$4p4f$	3G_5	2.91[12]	3.61[12]	44.840	1.29[13]	2.02[12]	51.48	1.23[12]	3.64[-14]
$3d4p$	3F_4	$4p4f$	3G_5	2.91[12]	3.61[12]	44.840	1.29[13]	9.99[12]	67.89	6.09[12]	1.80[-13]
$3d4p$	3F_2	$4p4f$	3G_3	2.07[12]	1.07[13]	44.342	8.23[12]	4.84[12]	67.80	8.43[11]	2.62[-14]
$3d4p$	3D_3	$4p4f$	3G_4	2.25[12]	1.92[13]	44.511	1.05[13]	5.84[12]	67.87	6.43[11]	1.96[-14]
$3d4f$	1G_4	$4f2$	1G_4	7.28[13]	1.53[14]	71.940	1.64[13]	4.16[12]	66.79	1.96[12]	3.85[-15]
$3d4f$	3F_4	$4f2$	3F_4	8.35[11]	2.12[12]	71.623	1.68[13]	7.34[12]	67.27	1.54[12]	3.12[-15]
$3d4f$	3D_3	$4f2$	3F_4	8.35[11]	2.12[12]	71.623	1.68[13]	7.19[12]	68.33	1.51[12]	3.06[-15]
$3d4f$	1F_3	$4f2$	1G_4	7.28[13]	1.53[14]	71.940	1.64[13]	9.38[12]	68.44	4.42[12]	8.68[-15]
$3d4f$	3H_4	$4f2$	1G_4	7.28[13]	1.53[14]	71.940	1.64[13]	1.44[12]	66.71	6.77[11]	1.33[-15]
$3d4f$	1H_5	$4f2$	1I_6	2.37[13]	3.06[14]	73.171	2.28[13]	2.23[13]	68.69	1.72[12]	2.99[-15]
$3d4f$	1D_2	$4f2$	1D_2	1.02[13]	2.12[13]	73.804	9.18[12]	5.25[12]	66.84	2.32[12]	3.78[-15]
$3d4f$	1F_3	$4f2$	1D_2	1.02[13]	2.12[13]	73.804	9.18[12]	1.33[12]	67.75	5.84[11]	9.53[-16]
$3d4f$	1P_1	$4f2$	1D_2	1.02[13]	2.12[13]	73.804	9.18[12]	2.12[12]	68.63	9.36[11]	1.53[-15]
$3d4f$	1P_1	$4f2$	1S_0	2.03[13]	7.68[13]	79.942	1.77[12]	1.69[12]	66.38	4.36[11]	3.85[-16]
$3p5s$	3P_2	$4s5s$	3S_1	2.18[12]	2.19[12]	83.236	1.66[12]	4.93[11]	64.71	3.92[11]	2.49[-16]
$3p4s$	3P_1	$4s5d$	3D_2	2.81[13]	4.06[13]	99.081	2.95[12]	7.09[11]	41.13	4.83[11]	6.30[-17]
$3p4s$	3P_2	$4s5d$	3D_3	2.87[13]	4.15[13]	99.195	3.74[12]	1.37[12]	41.40	9.36[11]	1.20[-16]
$3p4s$	1P_1	$4s5d$	1D_2	3.28[13]	4.97[13]	99.220	2.79[12]	8.54[11]	41.59	5.58[11]	7.17[-17]
$3p5d$	3F_4	$4s5d$	3D_3	2.87[13]	4.15[13]	99.195	3.74[12]	8.50[11]	64.68	5.80[11]	7.47[-17]
$3s5p$	3P_2	$4p5p$	3D_3	6.09[12]	1.35[13]	105.561	3.02[12]	1.14[12]	50.83	4.97[11]	3.38[-17]
$3p4s$	3P_1	$4s6d$	3D_2	2.16[13]	2.89[13]	140.800	2.45[12]	4.46[11]	36.13	3.28[11]	6.59[-19]
$3p4s$	3P_2	$4s6d$	3D_3	2.17[13]	2.89[13]	140.838	3.18[12]	8.73[11]	36.34	6.44[11]	1.29[-18]
$3p4s$	3P_2	$4s7d$	3D_3	1.44[13]	1.81[13]	165.311	2.84[12]	5.55[11]	33.91	4.33[11]	7.50[-20]
$3p4s$	1P_1	$4s6d$	1D_2	2.50[13]	3.72[13]	140.991	2.27[12]	4.57[11]	36.48	3.04[11]	5.99[-19]
$3p4d$	3F_4	$4d5d$	3G_5	1.42[12]	3.23[12]	132.975	9.83[12]	1.27[12]	41.28	4.35[11]	1.91[-18]
$3d4f$	3H_5	$4f5f$	3I_6	2.71[12]	2.46[13]	143.224	1.72[13]	3.50[12]	48.26	3.65[11]	5.75[-19]
$3d4f$	3H_6	$4f5f$	3I_7	2.72[12]	2.47[13]	143.270	1.98[13]	4.15[12]	48.30	4.34[11]	6.81[-19]
$3p5s$	3P_1	$4d5s$	3D_2	1.61[13]	4.63[13]	116.253	2.75[12]	1.22[12]	54.63	4.18[11]	9.78[-18]
$3p5s$	3P_2	$4d5s$	3D_3	1.57[13]	4.41[13]	116.359	4.02[12]	2.58[12]	55.18	9.08[11]	2.10[-17]
$3p5d$	3F_4	$4d5d$	3G_5	1.42[12]	3.23[12]	132.975	9.83[12]	2.05[12]	54.99	7.03[11]	3.09[-18]
$3p5g$	3H_4	$4d5g$	3I_5	3.10[12]	1.96[13]	136.693	7.51[12]	2.45[12]	54.67	3.74[11]	1.13[-18]
$3p5g$	3H_5	$4s5g$	3G_5	8.07[12]	1.34[13]	105.498	6.36[12]	5.62[11]	63.45	3.24[11]	2.22[-17]
$3p5g$	3H_5	$4d5g$	3I_6	3.19[12]	2.00[13]	136.763	8.84[12]	2.36[12]	54.70	3.64[11]	1.10[-18]
$3p5g$	3H_6	$4s5g$	3G_5	8.07[12]	1.34[13]	105.498	6.36[12]	8.35[11]	64.04	4.81[11]	3.29[-17]
$3p5g$	3H_6	$4d5g$	3I_7	3.20[12]	1.99[13]	136.860	1.01[13]	3.91[12]	55.11	6.08[11]	1.81[-18]
$3p5g$	3G_5	$4s5g$	3G_5	8.07[12]	1.34[13]	105.498	6.36[12]	5.29[11]	64.15	3.05[11]	2.09[-17]
$3s6h$	3H_5	$4p6h$	3I_6	1.98[12]	6.23[12]	159.292	4.67[12]	1.66[12]	50.61	4.98[11]	1.58[-19]
$3s6h$	3H_6	$4d5g$	3I_7	3.20[12]	1.99[13]	136.860	1.01[13]	1.96[12]	55.80	3.05[11]	9.09[-19]
$3s6h$	3H_6	$4p6h$	3H_6	9.23[11]	3.78[12]	158.407	4.68[12]	1.38[12]	50.87	3.08[11]	1.06[-19]
$3s6h$	3H_6	$4p6h$	3I_7	2.46[12]	7.32[12]	159.553	5.37[12]	1.98[12]	50.63	6.35[11]	1.96[-19]
$3s6h$	1H_5	$4p6h$	1I_6	5.48[12]	1.56[13]	160.089	4.75[12]	1.60[12]	50.57	5.48[11]	1.60[-19]
$3p6s$	3P_1	$4d6s$	3D_2	6.31[12]	2.82[13]	164.166	2.41[12]	1.55[12]	54.37	3.42[11]	6.63[-20]
$3p6s$	3P_2	$4d6s$	3D_3	8.60[12]	3.00[13]	164.333	3.49[12]	2.74[12]	54.90	7.71[11]	1.47[-19]

Low level		Upper level		A_a	ΣA_a	E_S	ΣgA_r	gA_r	λ	Q_d	C_S^{eff}
Conf.	LSJ	Conf.	LSJ	s^{-1}	s^{-1}	eV	s^{-1}	s^{-1}	\AA	s^{-1}	cm^3/s
3p6d	3D_3	4s6d	3D_2	2.16[13]	2.89[13]	140.800	2.45[12]	4.59[11]	64.11	3.37[11]	6.78[-19]
3p6d	3F_4	4s6d	3D_3	2.17[13]	2.89[13]	140.838	3.18[12]	8.59[11]	64.12	6.34[11]	1.27[-18]
3p6g	3H_4	4s6g	3G_3	6.39[12]	9.52[12]	144.246	2.36[12]	4.82[11]	63.13	3.12[11]	4.45[-19]
3p6g	3H_5	4s6g	3G_5	6.38[12]	9.49[12]	144.259	5.31[12]	5.70[11]	63.15	3.65[11]	5.18[-19]
3p6g	3F_4	4s6g	3G_5	6.38[12]	9.49[12]	144.259	5.31[12]	5.62[11]	63.16	3.59[11]	5.11[-19]
3p6g	3F_4	4s6g	3G_4	6.39[12]	9.51[12]	144.252	3.12[12]	3.53[11]	63.95	2.28[11]	3.25[-19]
3p6g	3G_5	4s6g	3G_4	6.39[12]	9.51[12]	144.252	3.12[12]	5.80[11]	63.87	3.75[11]	5.34[-19]
3p6g	3G_5	4s6g	3G_5	6.38[12]	9.49[12]	144.259	5.31[12]	3.82[11]	63.87	2.45[11]	3.48[-19]
3p6g	3H_6	4s6g	3G_5	6.38[12]	9.49[12]	144.259	5.31[12]	8.66[11]	63.87	5.54[11]	7.87[-19]
3d5p	3F_4	4d5d	3G_5	1.42[12]	3.23[12]	132.975	9.83[12]	4.87[12]	66.37	1.67[12]	7.35[-18]
3d5f	3H_5	4f5f	3I_6	2.71[12]	2.46[13]	143.224	1.72[13]	1.16[13]	67.00	1.21[12]	1.90[-18]
3d5f	3H_6	4f5f	3I_7	2.72[12]	2.47[13]	143.270	1.98[13]	1.38[13]	67.07	1.45[12]	2.27[-18]
3d5f	1G_4	4f5f	3I_5	2.70[12]	2.46[13]	143.186	1.46[13]	4.06[12]	66.92	4.23[11]	6.70[-19]
3d5f	3H_4	4f5f	3I_5	2.70[12]	2.46[13]	143.186	1.46[13]	5.66[12]	66.98	5.90[11]	9.33[-19]
3d5f	3F_3	4f5f	3G_4	8.43[11]	9.06[12]	142.754	1.20[13]	4.41[12]	67.23	3.58[11]	5.91[-19]
3d5f	3F_4	4f5f	3G_5	8.50[11]	9.08[12]	142.790	1.53[13]	5.65[12]	67.27	4.59[11]	7.55[-19]
3d5f	1F_3	4f5f	1G_4	4.96[13]	3.09[14]	145.327	1.20[13]	4.70[12]	66.88	7.51[11]	9.59[-19]
3p7s	3P_1	4d7s	3D_2	5.44[12]	1.90[13]	191.888	2.29[12]	1.59[12]	54.26	4.44[11]	5.39[-21]
3p7s	3P_2	4s7s	3S_1	1.92[12]	2.08[12]	159.814	1.19[12]	5.20[11]	63.90	4.03[11]	1.21[-19]
3p7s	3P_2	4d7s	3D_3	5.61[12]	1.81[13]	192.030	3.21[12]	2.82[12]	54.80	8.51[11]	1.02[-20]
3p7s	1P_1	4d7s	1D_2	4.54[12]	2.36[13]	192.137	2.25[12]	1.81[12]	54.80	3.41[11]	4.04[-21]
3p7g	3H_4	4s7g	3G_3	4.97[12]	7.16[12]	167.331	2.27[12]	5.26[11]	63.03	3.49[11]	4.94[-20]
3p7g	3F_4	4s7g	3G_5	4.98[12]	7.17[12]	167.338	4.60[12]	6.34[11]	63.04	4.16[11]	5.87[-20]
3p7g	3F_4	4s7g	3G_4	4.97[12]	7.18[12]	167.334	2.96[12]	4.55[11]	63.84	3.02[11]	4.27[-20]
3p7g	3G_3	4s7g	3G_3	4.97[12]	7.16[12]	167.331	2.27[12]	5.08[11]	63.85	3.37[11]	4.77[-20]
3p7g	3H_5	4s7g	3G_5	4.98[12]	7.17[12]	167.338	4.60[12]	5.70[11]	63.06	3.74[11]	5.28[-20]
3p7d	3D_3	4s7d	3D_2	1.44[13]	1.80[13]	165.292	2.13[12]	4.42[11]	63.86	3.45[11]	5.99[-20]
3p7d	3F_4	4s7d	3D_3	1.44[13]	1.81[13]	165.311	2.84[12]	9.25[11]	63.89	7.23[11]	1.25[-19]
3p7g	3G_5	4s7g	3G_4	4.97[12]	7.18[12]	167.334	2.96[12]	6.08[11]	63.82	4.03[11]	5.70[-20]
3p7g	3G_5	4s7g	3G_5	4.98[12]	7.17[12]	167.338	4.60[12]	5.30[11]	63.82	3.47[11]	4.91[-20]
3p7g	3H_6	4s7g	3G_5	4.98[12]	7.17[12]	167.338	4.60[12]	1.37[12]	63.86	8.96[11]	1.27[-19]
3p7g	3F_2	4s7g	3G_3	4.97[12]	7.16[12]	167.331	2.27[12]	5.06[11]	63.90	3.36[11]	4.75[-20]
3d6p	3F_4	4f6p	3G_5	5.63[11]	1.06[13]	176.231	1.07[13]	8.16[12]	66.56	3.95[11]	2.30[-20]
3d6p	1F_3	4f6p	1G_4	1.46[13]	1.08[14]	176.840	7.51[12]	4.81[12]	66.43	6.43[11]	3.52[-20]
3d6f	3H_5	4f6f	3I_6	3.18[12]	2.61[13]	182.809	1.45[13]	1.07[13]	66.58	1.25[12]	3.76[-20]
3d6f	3H_6	4f6f	3I_7	3.53[12]	2.26[13]	182.873	1.58[13]	1.20[13]	66.64	1.79[12]	5.34[-20]
3d6f	3H_4	4f6f	3I_5	2.82[12]	2.34[13]	182.757	1.29[13]	4.91[12]	66.52	5.62[11]	1.70[-20]
3d6f	3H_4	4f6f	3I_5	2.82[12]	2.34[13]	182.757	1.29[13]	4.49[12]	66.57	5.15[11]	1.56[-20]
3d6f	3H_6	4p7h	3I_7	5.54[11]	4.09[12]	182.429	7.81[12]	2.78[12]	66.80	3.34[11]	1.04[-20]
3d6h	3I_5	4f6h	3I_5	1.28[12]	1.41[13]	183.745	1.19[13]	4.78[12]	66.50	4.01[11]	1.10[-20]
3d6h	3I_6	4f6h	3I_6	1.45[12]	1.59[13]	183.770	1.40[13]	3.56[12]	66.49	3.05[11]	8.33[-21]
3d6h	3H_4	4f6h	3I_5	1.28[12]	1.41[13]	183.745	1.19[13]	4.24[12]	66.52	3.55[11]	9.73[-21]
3d6h	3I_7	4f6h	3I_7	1.51[12]	1.56[13]	183.802	1.61[13]	4.04[12]	66.65	3.66[11]	9.97[-21]
3d6f	1F_3	4f6f	1G_4	2.15[13]	1.35[14]	183.447	9.49[12]	3.13[12]	66.70	4.95[11]	1.40[-20]
3d6h	3H_6	4f6h	3I_7	1.51[12]	1.56[13]	183.802	1.61[13]	6.85[12]	66.63	6.20[11]	1.69[-20]

Table XII: DR rate coefficients (α_d in cm^3/s) for excited even-parity states of Mg-like iron.

T_e eV	$3s^2$ 1S_0	$3p^2$ 3P_0	$3p^2$ 1D_2	$3p^2$ 3P_1	$3p^2$ 3P_2	$3p^2$ 1S_0	$3s3d$ 3D_1	$3s3d$ 3D_2	$3s3d$ 3D_3	$3s3d$ 1D_2
0.100	4.12[-16]	2.32[-12]	6.11[-12]	4.69[-12]	2.07[-13]	7.89[-13]	4.17[-15]	9.14[-16]	2.22[-19]	1.05[-12]
0.130	4.46[-16]	2.50[-12]	6.61[-12]	4.92[-12]	2.23[-13]	8.52[-13]	5.82[-15]	1.40[-15]	6.73[-18]	1.13[-12]
0.169	4.40[-16]	2.43[-12]	6.40[-12]	4.67[-12]	2.17[-13]	8.26[-13]	8.56[-15]	2.76[-15]	8.90[-17]	1.09[-12]
0.220	4.36[-16]	2.17[-12]	5.72[-12]	4.10[-12]	1.97[-13]	7.37[-13]	1.23[-14]	5.65[-15]	6.20[-16]	9.78[-13]
0.286	5.60[-16]	1.86[-12]	4.85[-12]	3.46[-12]	1.74[-13]	6.22[-13]	1.63[-14]	1.02[-14]	2.62[-15]	8.29[-13]
0.371	1.02[-15]	1.58[-12]	4.06[-12]	2.92[-12]	1.65[-13]	5.14[-13]	1.95[-14]	1.57[-14]	7.47[-15]	6.95[-13]
0.483	1.95[-15]	1.41[-12]	3.55[-12]	2.60[-12]	1.88[-13]	4.36[-13]	2.14[-14]	2.11[-14]	1.57[-14]	6.07[-13]
0.627	3.24[-15]	1.36[-12]	3.30[-12]	2.50[-12]	2.71[-13]	3.99[-13]	2.20[-14]	2.58[-14]	2.58[-14]	5.71[-13]
0.816	4.66[-15]	1.35[-12]	3.22[-12]	2.51[-12]	4.30[-13]	4.01[-13]	2.17[-14]	2.89[-14]	3.54[-14]	5.71[-13]
1.060	5.91[-15]	1.33[-12]	3.17[-12]	2.53[-12]	6.63[-13]	4.33[-13]	2.09[-14]	3.08[-14]	4.25[-14]	5.88[-13]
1.379	6.88[-15]	1.27[-12]	3.07[-12]	2.46[-12]	9.28[-13]	4.79[-13]	2.04[-14]	3.20[-14]	4.68[-14]	6.02[-13]
1.792	7.49[-15]	1.16[-12]	2.89[-12]	2.33[-12]	1.17[-12]	5.20[-13]	2.13[-14]	3.52[-14]	5.14[-14]	6.08[-13]
2.330	7.79[-15]	1.02[-12]	2.66[-12]	2.14[-12]	1.33[-12]	5.43[-13]	2.74[-14]	4.71[-14]	6.47[-14]	6.07[-13]
3.029	7.80[-15]	8.86[-13]	2.42[-12]	1.92[-12]	1.41[-12]	5.46[-13]	4.32[-14]	7.74[-14]	9.78[-14]	6.12[-13]
3.937	7.59[-15]	7.61[-13]	2.16[-12]	1.70[-12]	1.43[-12]	5.29[-13]	7.02[-14]	1.30[-13]	1.55[-13]	6.33[-13]
5.119	7.22[-15]	6.51[-13]	1.93[-12]	1.50[-12]	1.39[-12]	4.99[-13]	1.04[-13]	1.94[-13]	2.27[-13]	6.63[-13]
6.654	6.72[-15]	5.56[-13]	1.72[-12]	1.31[-12]	1.31[-12]	4.62[-13]	1.34[-13]	2.54[-13]	2.93[-13]	6.86[-13]
8.650	6.10[-15]	4.72[-13]	1.51[-12]	1.14[-12]	1.20[-12]	4.17[-13]	1.56[-13]	2.96[-13]	3.37[-13]	6.88[-13]
11.245	5.40[-15]	3.98[-13]	1.30[-12]	9.71[-13]	1.07[-12]	3.69[-13]	1.63[-13]	3.11[-13]	3.50[-13]	6.57[-13]
14.619	4.63[-15]	3.29[-13]	1.10[-12]	8.13[-13]	9.26[-13]	3.16[-13]	1.57[-13]	3.01[-13]	3.34[-13]	5.98[-13]
19.005	3.83[-15]	2.66[-13]	9.04[-13]	6.62[-13]	7.74[-13]	2.63[-13]	1.42[-13]	2.72[-13]	2.97[-13]	5.18[-13]
24.706	3.08[-15]	2.09[-13]	7.20[-13]	5.24[-13]	6.23[-13]	2.11[-13]	1.21[-13]	2.33[-13]	2.51[-13]	4.30[-13]
32.118	2.40[-15]	1.60[-13]	5.58[-13]	4.04[-13]	4.88[-13]	1.64[-13]	9.89[-14]	1.90[-13]	2.02[-13]	3.43[-13]
41.754	1.83[-15]	1.20[-13]	4.20[-13]	3.05[-13]	3.71[-13]	1.25[-13]	7.76[-14]	1.49[-13]	1.57[-13]	2.66[-13]
54.280	1.36[-15]	8.81[-14]	3.10[-13]	2.24[-13]	2.75[-13]	9.24[-14]	5.90[-14]	1.14[-13]	1.18[-13]	2.00[-13]
70.564	1.00[-15]	6.35[-14]	2.25[-13]	1.62[-13]	2.00[-13]	6.71[-14]	4.37[-14]	8.41[-14]	8.73[-14]	1.47[-13]
91.733	7.31[-16]	4.51[-14]	1.61[-13]	1.15[-13]	1.43[-13]	4.81[-14]	3.18[-14]	6.11[-14]	6.31[-14]	1.06[-13]
119.253	5.29[-16]	3.18[-14]	1.13[-13]	8.13[-14]	1.01[-13]	3.40[-14]	2.28[-14]	4.38[-14]	4.50[-14]	7.54[-14]
155.029	3.80[-16]	2.21[-14]	7.91[-14]	5.67[-14]	7.08[-14]	2.38[-14]	1.61[-14]	3.09[-14]	3.16[-14]	5.30[-14]
201.538	2.71[-16]	1.53[-14]	5.48[-14]	3.93[-14]	4.92[-14]	1.65[-14]	1.13[-14]	2.16[-14]	2.20[-14]	3.69[-14]
261.999	1.92[-16]	1.05[-14]	3.78[-14]	2.70[-14]	3.39[-14]	1.14[-14]	7.82[-15]	1.50[-14]	1.53[-14]	2.56[-14]
340.599	1.35[-16]	7.22[-15]	2.59[-14]	1.85[-14]	2.33[-14]	7.82[-15]	5.40[-15]	1.03[-14]	1.05[-14]	1.76[-14]
442.779	9.42[-17]	4.93[-15]	1.77[-14]	1.27[-14]	1.59[-14]	5.35[-15]	3.70[-15]	7.10[-15]	7.21[-15]	1.21[-14]
575.612	6.54[-17]	3.36[-15]	1.21[-14]	8.62[-15]	1.08[-14]	3.65[-15]	2.53[-15]	4.85[-15]	4.93[-15]	8.25[-15]
748.296	4.51[-17]	2.28[-15]	8.20[-15]	5.86[-15]	7.37[-15]	2.48[-15]	1.73[-15]	3.31[-15]	3.35[-15]	5.61[-15]
972.784	3.09[-17]	1.55[-15]	5.56[-15]	3.97[-15]	5.00[-15]	1.69[-15]	1.17[-15]	2.25[-15]	2.28[-15]	3.82[-15]
1264.620	2.12[-17]	1.05[-15]	3.77[-15]	2.69[-15]	3.39[-15]	1.14[-15]	7.97[-16]	1.53[-15]	1.55[-15]	2.59[-15]
1644.005	1.45[-17]	7.09[-16]	2.55[-15]	1.82[-15]	2.30[-15]	7.74[-16]	5.39[-16]	1.03[-15]	1.05[-15]	1.76[-15]
T_e eV	$3d^2$ 3F_2	$3d^2$ 3F_3	$3d^2$ 3F_4	$3d^2$ 1D_2	$3d^2$ 3P_0	$3d^2$ 3P_1	$3d^2$ 3P_2	$3d^2$ 1G_4	$3d^2$ 1S_0	$3s4s$ 3S_1
0.100	2.59[-16]	4.62[-21]	2.83[-21]	3.50[-14]	1.14[-16]	1.00[-15]	1.15[-14]	1.41[-20]	4.43[-14]	5.67[-13]
0.130	2.80[-16]	3.03[-19]	1.92[-19]	3.78[-14]	1.43[-16]	1.19[-15]	1.24[-14]	9.73[-19]	4.79[-14]	2.13[-12]
0.169	2.79[-16]	7.13[-18]	4.71[-18]	3.67[-14]	2.11[-16]	1.43[-15]	1.21[-14]	2.48[-17]	4.65[-14]	5.73[-12]
0.220	3.31[-16]	7.75[-17]	5.41[-17]	3.31[-14]	4.17[-16]	1.90[-15]	1.09[-14]	3.05[-16]	4.17[-14]	1.18[-11]
0.286	7.27[-16]	4.70[-16]	3.50[-16]	2.96[-14]	1.03[-15]	3.15[-15]	9.48[-15]	2.14[-15]	3.60[-14]	1.99[-11]
0.371	2.11[-15]	1.81[-15]	1.44[-15]	2.90[-14]	2.47[-15]	6.11[-15]	8.41[-15]	9.50[-15]	3.18[-14]	2.85[-11]
0.483	5.21[-15]	4.87[-15]	4.13[-15]	3.37[-14]	5.01[-15]	1.14[-14]	8.11[-15]	2.87[-14]	3.05[-14]	3.56[-11]
0.627	1.01[-14]	9.87[-15]	8.82[-15]	4.30[-14]	8.25[-15]	1.82[-14]	8.83[-15]	6.39[-14]	3.21[-14]	3.98[-11]
0.816	1.59[-14]	1.60[-14]	1.50[-14]	5.39[-14]	1.14[-14]	2.47[-14]	1.07[-14]	1.12[-13]	3.53[-14]	4.03[-11]
1.060	2.12[-14]	2.20[-14]	2.17[-14]	6.30[-14]	1.34[-14]	2.93[-14]	1.36[-14]	1.64[-13]	3.86[-14]	3.76[-11]
1.379	2.51[-14]	2.68[-14]	2.75[-14]	6.84[-14]	1.41[-14]	3.12[-14]	1.71[-14]	2.09[-13]	4.11[-14]	3.29[-11]
1.792	2.80[-14]	3.08[-14]	3.25[-14]	7.05[-14]	1.37[-14]	3.11[-14]	2.10[-14]	2.42[-13]	4.22[-14]	2.72[-11]
2.330	3.54[-14]	3.95[-14]	4.00[-14]	7.52[-14]	1.37[-14]	3.23[-14]	2.90[-14]	2.71[-13]	4.27[-14]	2.15[-11]
3.029	6.22[-14]	6.92[-14]	6.07[-14]	9.76[-14]	1.67[-14]	4.35[-14]	5.41[-14]	3.19[-13]	4.53[-14]	1.64[-11]

T_e eV	$3d^2$ 3F_2	$3d^2$ 3F_3	$3d^2$ 3F_4	$3d^2$ 1D_2	$3d^2$ 3P_0	$3d^2$ 3P_1	$3d^2$ 3P_2	$3d^2$ 1G_4	$3d^2$ 1S_0	$3s4s$ 3S_1
3.937	1.29[-13]	1.44[-13]	1.08[-13]	1.59[-13]	2.68[-14]	7.68[-14]	1.16[-13]	4.24[-13]	5.41[-14]	1.22[-11]
5.119	2.42[-13]	2.72[-13]	1.88[-13]	2.66[-13]	4.52[-14]	1.37[-13]	2.24[-13]	6.04[-13]	7.13[-14]	8.86[-12]
6.654	3.80[-13]	4.34[-13]	2.85[-13]	3.99[-13]	6.78[-14]	2.10[-13]	3.57[-13]	8.23[-13]	9.33[-14]	6.33[-12]
8.650	5.03[-13]	5.88[-13]	3.71[-13]	5.18[-13]	8.75[-14]	2.76[-13]	4.79[-13]	1.01[-12]	1.12[-13]	4.47[-12]
11.245	5.79[-13]	6.95[-13]	4.24[-13]	5.91[-13]	9.86[-14]	3.13[-13]	5.55[-13]	1.12[-12]	1.23[-13]	3.12[-12]
14.619	5.98[-13]	7.33[-13]	4.35[-13]	6.09[-13]	9.95[-14]	3.18[-13]	5.77[-13]	1.13[-12]	1.23[-13]	2.16[-12]
19.005	5.68[-13]	7.10[-13]	4.10[-13]	5.78[-13]	9.18[-14]	2.96[-13]	5.50[-13]	1.04[-12]	1.12[-13]	1.49[-12]
24.706	5.04[-13]	6.38[-13]	3.61[-13]	5.13[-13]	7.90[-14]	2.57[-13]	4.90[-13]	8.99[-13]	9.62[-14]	1.03[-12]
32.118	4.25[-13]	5.41[-13]	3.00[-13]	4.34[-13]	6.45[-14]	2.11[-13]	4.15[-13]	7.39[-13]	7.84[-14]	7.10[-13]
41.754	3.44[-13]	4.39[-13]	2.41[-13]	3.52[-13]	5.04[-14]	1.66[-13]	3.36[-13]	5.83[-13]	6.14[-14]	4.93[-13]
54.280	2.68[-13]	3.42[-13]	1.85[-13]	2.75[-13]	3.83[-14]	1.27[-13]	2.62[-13]	4.45[-13]	4.65[-14]	3.45[-13]
70.564	2.03[-13]	2.59[-13]	1.39[-13]	2.09[-13]	2.83[-14]	9.42[-14]	2.00[-13]	3.31[-13]	3.44[-14]	2.45[-13]
91.733	1.50[-13]	1.92[-13]	1.02[-13]	1.55[-13]	2.05[-14]	6.86[-14]	1.48[-13]	2.41[-13]	2.50[-14]	1.74[-13]
119.253	1.09[-13]	1.39[-13]	7.34[-14]	1.13[-13]	1.46[-14]	4.90[-14]	1.08[-13]	1.72[-13]	1.79[-14]	1.25[-13]
155.029	7.81[-14]	9.89[-14]	5.21[-14]	8.09[-14]	1.03[-14]	3.47[-14]	7.74[-14]	1.22[-13]	1.27[-14]	8.93[-14]
201.538	5.52[-14]	6.97[-14]	3.66[-14]	5.72[-14]	7.16[-15]	2.42[-14]	5.47[-14]	8.52[-14]	8.92[-15]	6.37[-14]
261.999	3.86[-14]	4.86[-14]	2.55[-14]	4.01[-14]	4.96[-15]	1.68[-14]	3.83[-14]	5.91[-14]	6.22[-15]	4.52[-14]
340.599	2.67[-14]	3.37[-14]	1.77[-14]	2.79[-14]	3.42[-15]	1.16[-14]	2.66[-14]	4.08[-14]	4.31[-15]	3.18[-14]
442.779	1.84[-14]	2.32[-14]	1.21[-14]	1.93[-14]	2.34[-15]	7.98[-15]	1.84[-14]	2.80[-14]	2.97[-15]	2.22[-14]
575.612	1.26[-14]	1.59[-14]	8.30[-15]	1.32[-14]	1.60[-15]	5.45[-15]	1.26[-14]	1.92[-14]	2.04[-15]	1.54[-14]
748.296	8.64[-15]	1.08[-14]	5.66[-15]	9.02[-15]	1.09[-15]	3.72[-15]	8.63[-15]	1.30[-14]	1.40[-15]	1.07[-14]
972.784	5.88[-15]	7.38[-15]	3.85[-15]	6.15[-15]	7.42[-16]	2.53[-15]	5.89[-15]	8.88[-15]	9.51[-16]	7.35[-15]
1264.620	4.01[-15]	5.02[-15]	2.62[-15]	4.18[-15]	5.03[-16]	1.71[-15]	4.00[-15]	6.02[-15]	6.47[-16]	5.03[-15]
1644.005	2.72[-15]	3.41[-15]	1.77[-15]	2.84[-15]	3.41[-16]	1.16[-15]	2.71[-15]	4.09[-15]	4.40[-16]	3.44[-15]
T_e eV	$3s4s$ 1S_0	$3s4d$ 3D_1	$3s4d$ 3D_2	$3s4d$ 3D_3	$3s4d$ 1D_2	$3d4s$ 3D_1	$3d4s$ 3D_2	$3d4s$ 3D_3	$3d4s$ 1D_2	$3d4p$ 1P_1
0.100	5.01[-16]	8.14[-14]	3.01[-14]	9.42[-18]	3.84[-14]	1.60[-13]	3.01[-14]	5.39[-17]	1.72[-14]	2.55[-17]
0.130	2.30[-15]	1.63[-13]	5.25[-14]	2.68[-16]	4.17[-14]	5.33[-13]	1.37[-13]	1.53[-15]	1.94[-14]	1.85[-16]
0.169	8.14[-15]	3.18[-13]	1.19[-13]	3.23[-15]	4.11[-14]	1.27[-12]	4.85[-13]	1.84[-14]	2.19[-14]	7.74[-16]
0.220	2.03[-14]	5.34[-13]	2.58[-13]	2.00[-14]	3.82[-14]	2.31[-12]	1.22[-12]	1.14[-13]	2.66[-14]	2.13[-15]
0.286	3.76[-14]	7.60[-13]	4.63[-13]	7.39[-14]	3.52[-14]	3.39[-12]	2.30[-12]	4.22[-13]	3.47[-14]	4.24[-15]
0.371	5.53[-14]	9.31[-13]	6.83[-13]	1.85[-13]	3.33[-14]	4.21[-12]	3.46[-12]	1.05[-12]	4.52[-14]	6.61[-15]
0.483	6.81[-14]	1.01[-12]	8.57[-13]	3.43[-13]	3.32[-14]	4.57[-12]	4.37[-12]	1.95[-12]	5.55[-14]	8.57[-15]
0.627	7.38[-14]	9.84[-13]	9.43[-13]	5.05[-13]	3.41[-14]	4.48[-12]	4.81[-12]	2.85[-12]	6.32[-14]	9.76[-15]
0.816	7.85[-14]	8.88[-13]	9.36[-13]	6.20[-13]	3.57[-14]	4.04[-12]	4.76[-12]	3.50[-12]	6.98[-14]	1.02[-14]
1.060	1.05[-13]	7.53[-13]	8.54[-13]	6.64[-13]	4.05[-14]	3.41[-12]	4.33[-12]	3.73[-12]	8.65[-14]	1.02[-14]
1.379	1.87[-13]	6.08[-13]	7.32[-13]	6.41[-13]	5.28[-14]	2.74[-12]	3.69[-12]	3.58[-12]	1.33[-13]	9.99[-15]
1.792	3.43[-13]	4.72[-13]	5.96[-13]	5.71[-13]	7.51[-14]	2.12[-12]	3.00[-12]	3.18[-12]	2.19[-13]	1.00[-14]
2.330	5.43[-13]	3.56[-13]	4.67[-13]	4.80[-13]	1.04[-13]	1.60[-12]	2.33[-12]	2.65[-12]	3.31[-13]	1.18[-14]
3.029	7.24[-13]	2.63[-13]	3.57[-13]	3.85[-13]	1.29[-13]	1.17[-12]	1.77[-12]	2.11[-12]	4.43[-13]	1.81[-14]
3.937	8.32[-13]	1.93[-13]	2.69[-13]	3.01[-13]	1.45[-13]	8.70[-13]	1.35[-12]	1.67[-12]	5.38[-13]	3.20[-14]
5.119	8.48[-13]	1.45[-13]	2.08[-13]	2.38[-13]	1.50[-13]	6.81[-13]	1.09[-12]	1.39[-12]	6.40[-13]	5.43[-14]
6.654	7.87[-13]	1.17[-13]	1.73[-13]	1.97[-13]	1.50[-13]	6.05[-13]	1.00[-12]	1.31[-12]	7.79[-13]	8.12[-14]
8.650	6.79[-13]	1.06[-13]	1.62[-13]	1.78[-13]	1.48[-13]	6.19[-13]	1.06[-12]	1.41[-12]	9.62[-13]	1.06[-13]
11.245	5.54[-13]	1.04[-13]	1.64[-13]	1.72[-13]	1.46[-13]	6.71[-13]	1.17[-12]	1.58[-12]	1.14[-12]	1.24[-13]
14.619	4.32[-13]	1.04[-13]	1.67[-13]	1.67[-13]	1.42[-13]	7.11[-13]	1.24[-12]	1.69[-12]	1.25[-12]	1.31[-13]
19.005	3.27[-13]	1.01[-13]	1.64[-13]	1.58[-13]	1.34[-13]	7.07[-13]	1.24[-12]	1.70[-12]	1.26[-12]	1.29[-13]
24.706	2.42[-13]	9.23[-14]	1.52[-13]	1.43[-13]	1.21[-13]	6.57[-13]	1.16[-12]	1.58[-12]	1.19[-12]	1.20[-13]
32.118	1.77[-13]	8.03[-14]	1.33[-13]	1.23[-13]	1.04[-13]	5.77[-13]	1.02[-12]	1.40[-12]	1.04[-12]	1.05[-13]
41.754	1.29[-13]	6.69[-14]	1.12[-13]	1.03[-13]	8.65[-14]	4.85[-13]	8.60[-13]	1.18[-12]	8.79[-13]	8.85[-14]
54.280	9.36[-14]	5.38[-14]	9.03[-14]	8.41[-14]	6.97[-14]	3.94[-13]	6.98[-13]	9.54[-13]	7.13[-13]	7.20[-14]
70.564	6.83[-14]	4.21[-14]	7.11[-14]	6.70[-14]	5.48[-14]	3.12[-13]	5.52[-13]	7.55[-13]	5.63[-13]	5.69[-14]
91.733	5.00[-14]	3.23[-14]	5.45[-14]	5.24[-14]	4.22[-14]	2.42[-13]	4.27[-13]	5.86[-13]	4.36[-13]	4.37[-14]
119.253	3.65[-14]	2.42[-14]	4.11[-14]	4.02[-14]	3.18[-14]	1.84[-13]	3.25[-13]	4.45[-13]	3.31[-13]	3.29[-14]
155.029	2.66[-14]	1.79[-14]	3.03[-14]	3.03[-14]	2.35[-14]	1.38[-13]	2.42[-13]	3.33[-13]	2.47[-13]	2.43[-14]

T_e eV	$3s4s$ 1S_0	$3s4d$ 3D_1	$3s4d$ 3D_2	$3s4d$ 3D_3	$3s4d$ 1D_2	$3d4s$ 3D_1	$3d4s$ 3D_2	$3d4s$ 3D_3	$3d4s$ 1D_2	$3d4p$ 1P_1
201.538	1.93[-14]	1.30[-14]	2.21[-14]	2.24[-14]	1.72[-14]	1.01[-13]	1.78[-13]	2.45[-13]	1.81[-13]	1.75[-14]
261.999	1.38[-14]	9.31[-15]	1.58[-14]	1.63[-14]	1.23[-14]	7.35[-14]	1.28[-13]	1.77[-13]	1.31[-13]	1.26[-14]
340.599	9.79[-15]	6.60[-15]	1.12[-14]	1.17[-14]	8.74[-15]	5.26[-14]	9.20[-14]	1.26[-13]	9.35[-14]	8.89[-15]
442.779	6.89[-15]	4.63[-15]	7.87[-15]	8.29[-15]	6.14[-15]	3.72[-14]	6.51[-14]	8.95[-14]	6.60[-14]	6.23[-15]
575.612	4.81[-15]	3.23[-15]	5.48[-15]	5.82[-15]	4.28[-15]	2.61[-14]	4.56[-14]	6.27[-14]	4.62[-14]	4.33[-15]
748.296	3.33[-15]	2.23[-15]	3.79[-15]	4.05[-15]	2.96[-15]	1.81[-14]	3.16[-14]	4.36[-14]	3.21[-14]	2.99[-15]
972.784	2.30[-15]	1.53[-15]	2.61[-15]	2.80[-15]	2.03[-15]	1.25[-14]	2.18[-14]	3.00[-14]	2.22[-14]	2.05[-15]
1264.620	1.58[-15]	1.05[-15]	1.78[-15]	1.92[-15]	1.40[-15]	8.59[-15]	1.50[-14]	2.07[-14]	1.52[-14]	1.40[-15]
1644.005	1.08[-15]	7.17[-16]	1.22[-15]	1.32[-15]	9.53[-16]	5.88[-15]	1.03[-14]	1.42[-14]	1.04[-14]	9.58[-16]
T_e eV	$3p4p$ 1P_1	$3p4p$ 3D_1	$3p4p$ 3D_2	$3p4p$ 3P_0	$3p4p$ 3P_1	$3p4p$ 3D_3	$3p4p$ 3P_2	$3p4p$ 3S_1	$3p4p$ 1D_2	$3p4p$ 1S_0
0.100	2.61[-12]	2.30[-12]	3.18[-12]	8.00[-13]	1.18[-12]	1.70[-16]	6.93[-13]	2.94[-13]	5.09[-13]	2.00[-13]
0.130	3.35[-12]	2.71[-12]	3.67[-12]	9.37[-13]	1.85[-12]	4.84[-15]	9.41[-13]	8.27[-13]	5.50[-13]	2.18[-13]
0.169	4.45[-12]	3.23[-12]	4.35[-12]	1.15[-12]	2.95[-12]	5.81[-14]	1.57[-12]	1.97[-12]	5.39[-13]	2.18[-13]
0.220	5.98[-12]	3.93[-12]	5.67[-12]	1.57[-12]	4.36[-12]	3.59[-13]	2.88[-12]	3.74[-12]	5.09[-13]	2.09[-13]
0.286	7.60[-12]	4.73[-12]	7.77[-12]	2.17[-12]	5.76[-12]	1.33[-12]	4.92[-12]	5.82[-12]	5.16[-13]	1.97[-13]
0.371	8.88[-12]	5.48[-12]	1.03[-11]	2.80[-12]	6.85[-12]	3.34[-12]	7.24[-12]	7.67[-12]	6.07[-13]	1.87[-13]
0.483	9.46[-12]	6.00[-12]	1.25[-11]	3.25[-12]	7.46[-12]	6.17[-12]	9.23[-12]	8.81[-12]	7.85[-13]	1.79[-13]
0.627	9.25[-12]	6.18[-12]	1.37[-11]	3.39[-12]	7.55[-12]	9.06[-12]	1.04[-11]	9.09[-12]	9.93[-13]	1.71[-13]
0.816	8.43[-12]	5.98[-12]	1.39[-11]	3.24[-12]	7.15[-12]	1.11[-11]	1.06[-11]	8.59[-12]	1.17[-12]	1.66[-13]
1.060	7.26[-12]	5.45[-12]	1.30[-11]	2.89[-12]	6.39[-12]	1.20[-11]	9.93[-12]	7.60[-12]	1.28[-12]	1.66[-13]
1.379	5.98[-12]	4.74[-12]	1.13[-11]	2.42[-12]	5.45[-12]	1.15[-11]	8.70[-12]	6.38[-12]	1.34[-12]	1.76[-13]
1.792	4.79[-12]	3.97[-12]	9.36[-12]	1.94[-12]	4.47[-12]	1.03[-11]	7.25[-12]	5.14[-12]	1.37[-12]	1.94[-13]
2.330	3.78[-12]	3.24[-12]	7.46[-12]	1.51[-12]	3.56[-12]	8.62[-12]	5.79[-12]	4.03[-12]	1.39[-12]	2.18[-13]
3.029	2.95[-12]	2.61[-12]	5.76[-12]	1.15[-12]	2.77[-12]	6.89[-12]	4.49[-12]	3.09[-12]	1.37[-12]	2.36[-13]
3.937	2.30[-12]	2.07[-12]	4.37[-12]	8.56[-13]	2.12[-12]	5.32[-12]	3.41[-12]	2.34[-12]	1.31[-12]	2.43[-13]
5.119	1.79[-12]	1.64[-12]	3.25[-12]	6.32[-13]	1.61[-12]	4.01[-12]	2.55[-12]	1.75[-12]	1.22[-12]	2.37[-13]
6.654	1.38[-12]	1.27[-12]	2.42[-12]	4.67[-13]	1.20[-12]	2.99[-12]	1.90[-12]	1.31[-12]	1.10[-12]	2.20[-13]
8.650	1.07[-12]	9.93[-13]	1.82[-12]	3.45[-13]	9.05[-13]	2.22[-12]	1.41[-12]	9.71[-13]	9.82[-13]	1.98[-13]
11.245	8.28[-13]	7.72[-13]	1.37[-12]	2.56[-13]	6.78[-13]	1.65[-12]	1.05[-12]	7.25[-13]	8.67[-13]	1.73[-13]
14.619	6.41[-13]	6.00[-13]	1.05[-12]	1.89[-13]	5.08[-13]	1.23[-12]	7.82[-13]	5.41[-13]	7.53[-13]	1.48[-13]
19.005	4.92[-13]	4.64[-13]	8.08[-13]	1.40[-13]	3.80[-13]	9.15[-13]	5.83[-13]	4.03[-13]	6.38[-13]	1.25[-13]
24.706	3.75[-13]	3.55[-13]	6.18[-13]	1.03[-13]	2.82[-13]	6.80[-13]	4.33[-13]	2.98[-13]	5.26[-13]	1.02[-13]
32.118	2.81[-13]	2.68[-13]	4.68[-13]	7.56[-14]	2.09[-13]	5.03[-13]	3.19[-13]	2.19[-13]	4.22[-13]	8.18[-14]
41.754	2.08[-13]	2.01[-13]	3.51[-13]	5.49[-14]	1.52[-13]	3.68[-13]	2.33[-13]	1.60[-13]	3.30[-13]	6.40[-14]
54.280	1.53[-13]	1.47[-13]	2.59[-13]	3.96[-14]	1.11[-13]	2.68[-13]	1.70[-13]	1.16[-13]	2.53[-13]	4.92[-14]
70.564	1.11[-13]	1.08[-13]	1.90[-13]	2.85[-14]	7.98[-14]	1.94[-13]	1.23[-13]	8.36[-14]	1.90[-13]	3.70[-14]
91.733	7.95[-14]	7.76[-14]	1.37[-13]	2.03[-14]	5.72[-14]	1.40[-13]	8.81[-14]	5.99[-14]	1.41[-13]	2.76[-14]
119.253	5.66[-14]	5.56[-14]	9.83[-14]	1.44[-14]	4.08[-14]	9.93[-14]	6.30[-14]	4.25[-14]	1.03[-13]	2.03[-14]
155.029	4.01[-14]	3.94[-14]	6.98[-14]	1.02[-14]	2.88[-14]	7.02[-14]	4.47[-14]	3.01[-14]	7.39[-14]	1.48[-14]
201.538	2.81[-14]	2.77[-14]	4.93[-14]	7.14[-15]	2.03[-14]	4.95[-14]	3.15[-14]	2.12[-14]	5.28[-14]	1.06[-14]
261.999	1.96[-14]	1.94[-14]	3.45[-14]	4.98[-15]	1.42[-14]	3.45[-14]	2.21[-14]	1.48[-14]	3.72[-14]	7.55[-15]
340.599	1.35[-14]	1.35[-14]	2.40[-14]	3.46[-15]	9.85[-15]	2.40[-14]	1.54[-14]	1.03[-14]	2.61[-14]	5.32[-15]
442.779	9.35[-15]	9.31[-15]	1.66[-14]	2.39[-15]	6.80[-15]	1.66[-14]	1.07[-14]	7.11[-15]	1.81[-14]	3.73[-15]
575.612	6.42[-15]	6.40[-15]	1.14[-14]	1.64[-15]	4.68[-15]	1.14[-14]	7.35[-15]	4.89[-15]	1.25[-14]	2.59[-15]
748.296	4.39[-15]	4.39[-15]	7.79[-15]	1.13[-15]	3.21[-15]	7.82[-15]	5.05[-15]	3.34[-15]	8.61[-15]	1.79[-15]
972.784	2.99[-15]	2.99[-15]	5.32[-15]	7.69[-16]	2.19[-15]	5.34[-15]	3.45[-15]	2.28[-15]	5.90[-15]	1.23[-15]
1264.620	2.04[-15]	2.04[-15]	3.62[-15]	5.23[-16]	1.49[-15]	3.63[-15]	2.35[-15]	1.56[-15]	4.03[-15]	8.39[-16]
1644.005	1.38[-15]	1.39[-15]	2.46[-15]	3.55[-16]	1.02[-15]	2.47[-15]	1.60[-15]	1.06[-15]	2.75[-15]	5.73[-16]
T_e eV	$3p4f$ 3G_3	$3p4f$ 3F_3	$3p4f$ 3G_4	$3p4f$ 3F_2	$3p4f$ 1F_3	$3p4f$ 3G_5	$3p4f$ 3F_4	$3p4f$ 3D_3	$3p4f$ 3D_2	$3p4f$ 3D_1
0.100	1.43[-20]	1.15[-19]	9.34[-21]	2.13[-17]	1.91[-20]	1.53[-24]	1.89[-22]	8.55[-19]	8.05[-16]	4.77[-15]
0.130	9.20[-19]	3.77[-18]	8.03[-19]	1.35[-16]	5.75[-19]	4.42[-22]	1.30[-20]	2.44[-17]	2.88[-15]	1.44[-14]
0.169	3.14[-17]	6.31[-17]	3.04[-17]	5.23[-16]	7.93[-18]	3.15[-20]	3.26[-19]	2.96[-16]	9.62[-15]	3.32[-14]
0.220	5.64[-16]	7.02[-16]	5.67[-16]	1.60[-15]	6.56[-17]	7.74[-19]	3.91[-18]	1.88[-15]	2.38[-14]	5.97[-14]

T_e eV	$3p4f$ 3G_3	$3p4f$ 3F_3	$3p4f$ 3G_4	$3p4f$ 3F_2	$3p4f$ 1F_3	$3p4f$ 3G_5	$3p4f$ 3F_4	$3p4f$ 3D_3	$3p4f$ 3D_2	$3p4f$ 3D_1
0.286	5.28[-15]	5.25[-15]	5.45[-15]	5.20[-15]	3.80[-16]	9.39[-18]	2.77[-17]	7.42[-15]	4.50[-14]	8.74[-14]
0.371	2.79[-14]	2.54[-14]	2.95[-14]	1.81[-14]	1.60[-15]	9.73[-17]	1.59[-16]	2.06[-14]	6.89[-14]	1.08[-13]
0.483	9.32[-14]	8.17[-14]	1.00[-13]	5.28[-14]	5.18[-15]	9.83[-16]	1.03[-15]	4.42[-14]	9.09[-14]	1.18[-13]
0.627	2.16[-13]	1.87[-13]	2.37[-13]	1.17[-13]	1.42[-14]	6.75[-15]	6.04[-15]	7.87[-14]	1.09[-13]	1.17[-13]
0.816	3.79[-13]	3.26[-13]	4.22[-13]	2.04[-13]	3.46[-14]	2.88[-14]	2.44[-14]	1.23[-13]	1.27[-13]	1.11[-13]
1.060	5.35[-13]	4.62[-13]	6.06[-13]	2.90[-13]	7.33[-14]	8.17[-14]	6.78[-14]	1.77[-13]	1.49[-13]	1.08[-13]
1.379	6.42[-13]	5.60[-13]	7.39[-13]	3.53[-13]	1.30[-13]	1.68[-13]	1.38[-13]	2.36[-13]	1.77[-13]	1.14[-13]
1.792	6.87[-13]	6.05[-13]	8.03[-13]	3.84[-13]	1.93[-13]	2.73[-13]	2.22[-13]	2.91[-13]	2.05[-13]	1.25[-13]
2.330	6.76[-13]	6.04[-13]	8.04[-13]	3.86[-13]	2.51[-13]	3.70[-13]	3.00[-13]	3.33[-13]	2.28[-13]	1.38[-13]
3.029	6.30[-13]	5.71[-13]	7.62[-13]	3.69[-13]	2.90[-13]	4.42[-13]	3.56[-13]	3.57[-13]	2.42[-13]	1.46[-13]
3.937	5.70[-13]	5.24[-13]	7.00[-13]	3.41[-13]	3.13[-13]	4.85[-13]	3.91[-13]	3.66[-13]	2.49[-13]	1.52[-13]
5.119	5.13[-13]	4.78[-13]	6.39[-13]	3.14[-13]	3.25[-13]	5.09[-13]	4.10[-13]	3.72[-13]	2.55[-13]	1.57[-13]
6.654	4.70[-13]	4.46[-13]	5.93[-13]	2.95[-13]	3.35[-13]	5.28[-13]	4.26[-13]	3.85[-13]	2.68[-13]	1.67[-13]
8.650	4.41[-13]	4.28[-13]	5.63[-13]	2.85[-13]	3.47[-13]	5.45[-13]	4.43[-13]	4.08[-13]	2.87[-13]	1.81[-13]
11.245	4.20[-13]	4.15[-13]	5.38[-13]	2.78[-13]	3.55[-13]	5.56[-13]	4.54[-13]	4.31[-13]	3.08[-13]	1.96[-13]
14.619	3.97[-13]	4.00[-13]	5.12[-13]	2.69[-13]	3.55[-13]	5.48[-13]	4.51[-13]	4.42[-13]	3.16[-13]	2.03[-13]
19.005	3.65[-13]	3.75[-13]	4.71[-13]	2.51[-13]	3.38[-13]	5.18[-13]	4.30[-13]	4.30[-13]	3.09[-13]	1.98[-13]
24.706	3.24[-13]	3.40[-13]	4.21[-13]	2.27[-13]	3.12[-13]	4.68[-13]	3.91[-13]	3.98[-13]	2.86[-13]	1.83[-13]
32.118	2.78[-13]	2.96[-13]	3.62[-13]	1.96[-13]	2.74[-13]	4.05[-13]	3.40[-13]	3.52[-13]	2.51[-13]	1.60[-13]
41.754	2.32[-13]	2.48[-13]	3.01[-13]	1.64[-13]	2.31[-13]	3.37[-13]	2.84[-13]	2.97[-13]	2.11[-13]	1.35[-13]
54.280	1.87[-13]	2.02[-13]	2.43[-13]	1.33[-13]	1.89[-13]	2.73[-13]	2.30[-13]	2.43[-13]	1.72[-13]	1.10[-13]
70.564	1.48[-13]	1.60[-13]	1.92[-13]	1.04[-13]	1.50[-13]	2.16[-13]	1.81[-13]	1.93[-13]	1.36[-13]	8.64[-14]
91.733	1.15[-13]	1.23[-13]	1.49[-13]	8.04[-14]	1.16[-13]	1.68[-13]	1.40[-13]	1.49[-13]	1.05[-13]	6.65[-14]
119.253	8.72[-14]	9.36[-14]	1.14[-13]	6.05[-14]	8.84[-14]	1.29[-13]	1.06[-13]	1.13[-13]	7.90[-14]	5.03[-14]
155.029	6.54[-14]	6.96[-14]	8.53[-14]	4.48[-14]	6.60[-14]	9.79[-14]	7.88[-14]	8.40[-14]	5.86[-14]	3.73[-14]
201.538	4.83[-14]	5.10[-14]	6.31[-14]	3.27[-14]	4.84[-14]	7.31[-14]	5.76[-14]	6.16[-14]	4.29[-14]	2.73[-14]
261.999	3.51[-14]	3.68[-14]	4.59[-14]	2.34[-14]	3.50[-14]	5.37[-14]	4.17[-14]	4.44[-14]	3.09[-14]	1.96[-14]
340.599	2.53[-14]	2.63[-14]	3.30[-14]	1.67[-14]	2.50[-14]	3.88[-14]	2.98[-14]	3.16[-14]	2.20[-14]	1.40[-14]
442.779	1.80[-14]	1.85[-14]	2.35[-14]	1.17[-14]	1.77[-14]	2.78[-14]	2.10[-14]	2.23[-14]	1.55[-14]	9.85[-15]
575.612	1.26[-14]	1.29[-14]	1.65[-14]	8.15[-15]	1.24[-14]	1.97[-14]	1.47[-14]	1.56[-14]	1.08[-14]	6.88[-15]
748.296	8.78[-15]	8.97[-15]	1.15[-14]	5.65[-15]	8.61[-15]	1.38[-14]	1.02[-14]	1.08[-14]	7.50[-15]	4.77[-15]
972.784	6.08[-15]	6.18[-15]	7.98[-15]	3.89[-15]	5.94[-15]	9.56[-15]	7.04[-15]	7.45[-15]	5.17[-15]	3.29[-15]
1264.620	4.18[-15]	4.25[-15]	5.49[-15]	2.67[-15]	4.08[-15]	6.59[-15]	4.84[-15]	5.12[-15]	3.55[-15]	2.26[-15]
1644.005	2.87[-15]	2.90[-15]	3.76[-15]	1.82[-15]	2.80[-15]	4.53[-15]	3.30[-15]	3.49[-15]	2.42[-15]	1.54[-15]
T_e eV	$3d4d$ 1F_3	$3d4d$ 3D_1	$3d4d$ 3D_2	$3d4d$ 3D_3	$3d4d$ 3G_3	$3d4d$ 1P_1	$3d4d$ 3G_4	$3d4d$ 3G_5	$3d4d$ 3S_1	$3d4d$ 1S_0
0.100	1.19[-21]	3.12[-15]	2.60[-15]	1.32[-20]	1.87[-21]	2.25[-15]	1.46[-18]	7.40[-25]	1.86[-14]	2.91[-16]
0.130	5.31[-20]	3.39[-15]	2.84[-15]	3.80[-19]	9.95[-20]	2.40[-15]	5.03[-18]	2.14[-22]	1.98[-14]	3.20[-16]
0.169	1.02[-18]	3.43[-15]	2.85[-15]	4.67[-18]	2.05[-18]	2.30[-15]	1.32[-17]	1.53[-20]	1.91[-14]	3.31[-16]
0.220	9.69[-18]	3.34[-15]	2.74[-15]	2.98[-17]	1.99[-17]	2.05[-15]	3.48[-17]	3.75[-19]	1.71[-14]	3.43[-16]
0.286	5.30[-17]	3.24[-15]	2.68[-15]	1.16[-16]	1.07[-16]	1.76[-15]	1.07[-16]	4.02[-18]	1.45[-14]	3.78[-16]
0.371	1.87[-16]	3.23[-15]	2.73[-15]	3.07[-16]	3.63[-16]	1.57[-15]	3.07[-16]	2.31[-17]	1.20[-14]	4.54[-16]
0.483	4.67[-16]	3.33[-15]	2.91[-15]	6.09[-16]	8.66[-16]	1.55[-15]	7.09[-16]	8.47[-17]	1.01[-14]	5.72[-16]
0.627	8.89[-16]	3.51[-15]	3.15[-15]	9.68[-16]	1.58[-15]	1.69[-15]	1.30[-15]	2.26[-16]	8.61[-15]	7.19[-16]
0.816	1.36[-15]	3.65[-15]	3.32[-15]	1.30[-15]	2.31[-15]	1.89[-15]	1.98[-15]	4.77[-16]	7.53[-15]	8.80[-16]
1.060	1.79[-15]	3.62[-15]	3.34[-15]	1.55[-15]	2.92[-15]	2.04[-15]	2.60[-15]	8.43[-16]	6.70[-15]	1.08[-15]
1.379	2.09[-15]	3.40[-15]	3.21[-15]	1.71[-15]	3.33[-15]	2.10[-15]	3.12[-15]	1.31[-15]	5.97[-15]	1.39[-15]
1.792	2.57[-15]	3.22[-15]	3.19[-15]	2.08[-15]	3.87[-15]	2.16[-15]	3.96[-15]	2.16[-15]	5.41[-15]	1.91[-15]
2.330	4.85[-15]	3.95[-15]	4.61[-15]	4.32[-15]	6.15[-15]	2.94[-15]	7.16[-15]	5.12[-15]	5.68[-15]	2.76[-15]
3.029	1.36[-14]	7.84[-15]	1.11[-14]	1.32[-14]	1.44[-14]	6.48[-15]	1.80[-14]	1.53[-14]	8.81[-15]	4.41[-15]
3.937	3.49[-14]	1.79[-14]	2.73[-14]	3.51[-14]	3.43[-14]	1.57[-14]	4.33[-14]	3.94[-14]	1.76[-14]	7.56[-15]
5.119	7.11[-14]	3.49[-14]	5.46[-14]	7.23[-14]	6.82[-14]	3.22[-14]	8.41[-14]	7.94[-14]	3.29[-14]	1.23[-14]
6.654	1.17[-13]	5.62[-14]	8.79[-14]	1.19[-13]	1.11[-13]	5.36[-14]	1.32[-13]	1.27[-13]	5.17[-14]	1.80[-14]
8.650	1.60[-13]	7.73[-14]	1.20[-13]	1.64[-13]	1.52[-13]	7.60[-14]	1.75[-13]	1.71[-13]	6.90[-14]	2.32[-14]
11.245	1.96[-13]	9.52[-14]	1.45[-13]	2.02[-13]	1.86[-13]	9.59[-14]	2.01[-13]	2.02[-13]	8.11[-14]	2.74[-14]

T_e eV	$3d4d$ 1F_3	$3d4d$ 3D_1	$3d4d$ 3D_2	$3d4d$ 3D_3	$3d4d$ 3G_3	$3d4d$ 1P_1	$3d4d$ 3G_4	$3d4d$ 3G_5	$3d4d$ 3S_1	$3d4d$ 1S_0
14.619	2.21[-13]	1.09[-13]	1.65[-13]	2.34[-13]	2.06[-13]	1.13[-13]	2.08[-13]	2.19[-13]	8.75[-14]	3.11[-14]
19.005	2.36[-13]	1.18[-13]	1.79[-13]	2.57[-13]	2.13[-13]	1.24[-13]	2.00[-13]	2.24[-13]	8.94[-14]	3.48[-14]
24.706	2.39[-13]	1.22[-13]	1.85[-13]	2.69[-13]	2.07[-13]	1.30[-13]	1.83[-13]	2.19[-13]	8.75[-14]	3.79[-14]
32.118	2.30[-13]	1.19[-13]	1.82[-13]	2.68[-13]	1.92[-13]	1.29[-13]	1.59[-13]	2.04[-13]	8.28[-14]	3.92[-14]
41.754	2.10[-13]	1.10[-13]	1.69[-13]	2.50[-13]	1.70[-13]	1.21[-13]	1.34[-13]	1.84[-13]	7.59[-14]	3.86[-14]
54.280	1.83[-13]	9.72[-14]	1.50[-13]	2.23[-13]	1.46[-13]	1.10[-13]	1.11[-13]	1.62[-13]	6.72[-14]	3.58[-14]
70.564	1.52[-13]	8.23[-14]	1.27[-13]	1.90[-13]	1.21[-13]	9.57[-14]	8.92[-14]	1.38[-13]	5.77[-14]	3.17[-14]
91.733	1.23[-13]	6.73[-14]	1.04[-13]	1.56[-13]	9.82[-14]	8.11[-14]	7.01[-14]	1.16[-13]	4.80[-14]	2.69[-14]
119.253	9.55[-14]	5.35[-14]	8.20[-14]	1.23[-13]	7.78[-14]	6.68[-14]	5.41[-14]	9.52[-14]	3.87[-14]	2.19[-14]
155.029	7.24[-14]	4.13[-14]	6.29[-14]	9.52[-14]	6.03[-14]	5.34[-14]	4.09[-14]	7.61[-14]	3.02[-14]	1.74[-14]
201.538	5.37[-14]	3.12[-14]	4.71[-14]	7.16[-14]	4.56[-14]	4.15[-14]	3.03[-14]	5.94[-14]	2.30[-14]	1.33[-14]
261.999	3.91[-14]	2.31[-14]	3.45[-14]	5.27[-14]	3.40[-14]	3.15[-14]	2.21[-14]	4.51[-14]	1.71[-14]	1.00[-14]
340.599	2.81[-14]	1.67[-14]	2.49[-14]	3.81[-14]	2.48[-14]	2.34[-14]	1.59[-14]	3.36[-14]	1.25[-14]	7.38[-15]
442.779	1.99[-14]	1.19[-14]	1.78[-14]	2.72[-14]	1.79[-14]	1.70[-14]	1.13[-14]	2.46[-14]	9.00[-15]	5.34[-15]
575.612	1.39[-14]	8.44[-15]	1.25[-14]	1.92[-14]	1.27[-14]	1.22[-14]	7.94[-15]	1.77[-14]	6.38[-15]	3.80[-15]
748.296	9.67[-15]	5.91[-15]	8.71[-15]	1.34[-14]	8.91[-15]	8.64[-15]	5.53[-15]	1.25[-14]	4.47[-15]	2.68[-15]
972.784	6.68[-15]	4.10[-15]	6.02[-15]	9.27[-15]	6.20[-15]	6.05[-15]	3.83[-15]	8.79[-15]	3.11[-15]	1.87[-15]
1264.620	4.59[-15]	2.83[-15]	4.14[-15]	6.38[-15]	4.29[-15]	4.20[-15]	2.63[-15]	6.11[-15]	2.15[-15]	1.29[-15]
1644.005	3.14[-15]	1.94[-15]	2.84[-15]	4.38[-15]	2.95[-15]	2.90[-15]	1.81[-15]	4.22[-15]	1.48[-15]	8.90[-16]
T_e eV	$3d4d$ 3F_2	$3d4d$ 3F_3	$3d4d$ 3F_4	$3d4d$ 1D_2	$3d4d$ 3P_0	$3d4d$ 3P_1	$3d4d$ 3P_2	$3d4d$ 1G_4	$3p4f$ 1G_4	$3p4f$ 1D_2
0.100	5.54[-22]	3.70[-22]	2.08[-22]	4.57[-19]	1.07[-15]	3.82[-15]	2.06[-15]	8.36[-22]	5.23[-21]	2.32[-15]
0.130	3.51[-20]	2.42[-20]	1.41[-20]	2.98[-18]	1.16[-15]	4.05[-15]	2.23[-15]	5.83[-20]	3.78[-19]	2.73[-15]
0.169	7.92[-19]	5.63[-19]	3.40[-19]	1.31[-17]	1.16[-15]	3.95[-15]	2.18[-15]	1.52[-18]	1.07[-17]	3.40[-15]
0.220	8.13[-18]	5.99[-18]	3.83[-18]	4.92[-17]	1.10[-15]	3.62[-15]	2.00[-15]	1.93[-17]	1.51[-16]	4.76[-15]
0.286	4.61[-17]	3.52[-17]	2.41[-17]	1.67[-16]	1.05[-15]	3.24[-15]	1.79[-15]	1.40[-16]	1.21[-15]	7.17[-15]
0.371	1.65[-16]	1.31[-16]	9.67[-17]	4.66[-16]	1.04[-15]	2.95[-15]	1.63[-15]	6.37[-16]	5.94[-15]	1.13[-14]
0.483	4.16[-16]	3.42[-16]	2.70[-16]	1.02[-15]	1.09[-15]	2.81[-15]	1.56[-15]	1.96[-15]	1.95[-14]	1.88[-14]
0.627	7.94[-16]	6.72[-16]	5.66[-16]	1.77[-15]	1.17[-15]	2.81[-15]	1.56[-15]	4.40[-15]	4.78[-14]	3.17[-14]
0.816	1.22[-15]	1.06[-15]	9.47[-16]	2.56[-15]	1.24[-15]	2.82[-15]	1.62[-15]	7.72[-15]	9.53[-14]	5.28[-14]
1.060	1.59[-15]	1.43[-15]	1.34[-15]	3.19[-15]	1.25[-15]	2.77[-15]	1.69[-15]	1.12[-14]	1.64[-13]	8.42[-14]
1.379	1.85[-15]	1.72[-15]	1.68[-15]	3.60[-15]	1.19[-15]	2.63[-15]	1.77[-15]	1.42[-14]	2.49[-13]	1.25[-13]
1.792	2.24[-15]	2.16[-15]	2.16[-15]	4.00[-15]	1.14[-15]	2.54[-15]	2.06[-15]	1.65[-14]	3.35[-13]	1.66[-13]
2.330	4.06[-15]	4.10[-15]	3.84[-15]	5.63[-15]	1.34[-15]	3.23[-15]	3.68[-15]	1.99[-14]	4.08[-13]	2.03[-13]
3.029	1.07[-14]	1.13[-14]	9.38[-15]	1.18[-14]	2.46[-15]	6.66[-15]	9.88[-15]	2.98[-14]	4.58[-13]	2.29[-13]
3.937	2.69[-14]	2.92[-14]	2.21[-14]	2.70[-14]	5.29[-15]	1.54[-14]	2.51[-14]	5.31[-14]	4.87[-13]	2.44[-13]
5.119	5.40[-14]	5.96[-14]	4.29[-14]	5.26[-14]	1.00[-14]	3.02[-14]	5.09[-14]	9.25[-14]	5.01[-13]	2.54[-13]
6.654	8.68[-14]	9.81[-14]	6.80[-14]	8.44[-14]	1.56[-14]	4.79[-14]	8.26[-14]	1.42[-13]	5.12[-13]	2.65[-13]
8.650	1.18[-13]	1.36[-13]	9.19[-14]	1.17[-13]	2.05[-14]	6.36[-14]	1.13[-13]	1.93[-13]	5.22[-13]	2.79[-13]
11.245	1.39[-13]	1.66[-13]	1.11[-13]	1.50[-13]	2.34[-14]	7.36[-14]	1.36[-13]	2.46[-13]	5.29[-13]	2.92[-13]
14.619	1.51[-13]	1.83[-13]	1.24[-13]	1.86[-13]	2.43[-14]	7.70[-14]	1.55[-13]	3.13[-13]	5.28[-13]	2.97[-13]
19.005	1.54[-13]	1.88[-13]	1.31[-13]	2.25[-13]	2.34[-14]	7.48[-14]	1.68[-13]	3.92[-13]	5.16[-13]	2.92[-13]
24.706	1.48[-13]	1.82[-13]	1.33[-13]	2.59[-13]	2.15[-14]	6.91[-14]	1.75[-13]	4.68[-13]	4.90[-13]	2.74[-13]
32.118	1.36[-13]	1.67[-13]	1.27[-13]	2.78[-13]	1.93[-14]	6.18[-14]	1.74[-13]	5.16[-13]	4.50[-13]	2.48[-13]
41.754	1.20[-13]	1.46[-13]	1.17[-13]	2.77[-13]	1.72[-14]	5.37[-14]	1.64[-13]	5.24[-13]	3.97[-13]	2.16[-13]
54.280	1.01[-13]	1.24[-13]	1.03[-13]	2.58[-13]	1.51[-14]	4.57[-14]	1.48[-13]	4.93[-13]	3.39[-13]	1.80[-13]
70.564	8.25[-14]	1.01[-13]	8.84[-14]	2.26[-13]	1.31[-14]	3.81[-14]	1.27[-13]	4.35[-13]	2.80[-13]	1.47[-13]
91.733	6.55[-14]	8.10[-14]	7.37[-14]	1.88[-13]	1.11[-14]	3.10[-14]	1.04[-13]	3.64[-13]	2.25[-13]	1.17[-13]
119.253	5.06[-14]	6.34[-14]	5.99[-14]	1.50[-13]	9.10[-15]	2.46[-14]	8.26[-14]	2.91[-13]	1.75[-13]	9.03[-14]
155.029	3.83[-14]	4.87[-14]	4.75[-14]	1.16[-13]	7.27[-15]	1.91[-14]	6.37[-14]	2.25[-13]	1.34[-13]	6.85[-14]
201.538	2.84[-14]	3.67[-14]	3.67[-14]	8.71[-14]	5.64[-15]	1.45[-14]	4.79[-14]	1.69[-13]	1.00[-13]	5.10[-14]
261.999	2.06[-14]	2.71[-14]	2.78[-14]	6.39[-14]	4.27[-15]	1.07[-14]	3.52[-14]	1.24[-13]	7.37[-14]	3.73[-14]
340.599	1.48[-14]	1.97[-14]	2.05[-14]	4.61[-14]	3.16[-15]	7.81[-15]	2.53[-14]	8.93[-14]	5.32[-14]	2.68[-14]
442.779	1.05[-14]	1.41[-14]	1.49[-14]	3.28[-14]	2.28[-15]	5.60[-15]	1.80[-14]	6.35[-14]	3.80[-14]	1.92[-14]

Table XIII: DR rate coefficients (α_d in cm^3/s) for excited odd-parity states of Mg-like iron.

T_e eV	$3s3p$ 3P_0	$3s3p$ 3P_1	$3s3p$ 3P_2	$3s3p$ 1P_1	$3s4p$ 3P_0	$3s4p$ 3P_1	$3s4p$ 3P_2	$3s4p$ 1P_1	$3p3d$ 1F_3	$3p3d$ 1P_1
0.100	5.38[-15]	1.02[-14]	2.89[-18]	4.44[-15]	6.15[-18]	8.35[-19]	6.14[-19]	3.77[-17]	1.78[-16]	3.36[-16]
0.130	3.33[-14]	6.56[-14]	1.85[-17]	2.83[-14]	3.86[-17]	5.28[-18]	4.08[-18]	2.44[-16]	1.26[-15]	2.44[-15]
0.169	1.24[-13]	2.53[-13]	7.14[-17]	1.08[-13]	1.46[-16]	2.01[-17]	1.62[-17]	9.46[-16]	5.18[-15]	1.03[-14]
0.220	3.14[-13]	6.56[-13]	2.05[-16]	2.80[-13]	3.72[-16]	5.23[-17]	4.43[-17]	2.46[-15]	1.45[-14]	2.86[-14]
0.286	5.86[-13]	1.25[-12]	8.59[-16]	5.31[-13]	7.00[-16]	1.06[-16]	1.02[-16]	4.71[-15]	3.28[-14]	5.86[-14]
0.371	8.67[-13]	1.88[-12]	6.02[-15]	7.98[-13]	1.04[-15]	1.91[-16]	2.29[-16]	7.11[-15]	7.01[-14]	9.87[-14]
0.483	1.07[-12]	2.35[-12]	3.22[-14]	1.01[-12]	1.29[-15]	3.42[-16]	5.10[-16]	8.94[-15]	1.45[-13]	1.49[-13]
0.627	1.15[-12]	2.57[-12]	1.12[-13]	1.14[-12]	1.40[-15]	6.01[-16]	1.01[-15]	9.81[-15]	2.73[-13]	2.11[-13]
0.816	1.11[-12]	2.52[-12]	2.67[-13]	1.19[-12]	1.37[-15]	9.76[-16]	1.72[-15]	9.76[-15]	4.53[-13]	2.87[-13]
1.060	9.90[-13]	2.29[-12]	4.81[-13]	1.20[-12]	1.27[-15]	1.43[-15]	2.48[-15]	9.11[-15]	6.69[-13]	3.75[-13]
1.379	8.33[-13]	1.98[-12]	6.94[-13]	1.18[-12]	1.14[-15]	2.08[-15]	3.17[-15]	8.48[-15]	8.92[-13]	4.66[-13]
1.792	6.76[-13]	1.65[-12]	8.53[-13]	1.13[-12]	1.04[-15]	4.72[-15]	3.85[-15]	1.09[-14]	1.09[-12]	5.46[-13]
2.330	5.38[-13]	1.35[-12]	9.34[-13]	1.04[-12]	9.77[-16]	1.68[-14]	5.17[-15]	2.73[-14]	1.23[-12]	6.04[-13]
3.029	4.25[-13]	1.10[-12]	9.46[-13]	9.52[-13]	9.79[-16]	5.23[-14]	8.45[-15]	7.86[-14]	1.34[-12]	6.41[-13]
3.937	3.38[-13]	9.01[-13]	9.08[-13]	8.55[-13]	1.08[-15]	1.20[-13]	1.46[-14]	1.80[-13]	1.41[-12]	6.67[-13]
5.119	2.72[-13]	7.41[-13]	8.44[-13]	7.61[-13]	1.28[-15]	2.13[-13]	2.29[-14]	3.23[-13]	1.48[-12]	6.86[-13]
6.654	2.21[-13]	6.15[-13]	7.67[-13]	6.73[-13]	1.52[-15]	3.04[-13]	3.08[-14]	4.67[-13]	1.54[-12]	6.98[-13]
8.650	1.81[-13]	5.11[-13]	6.84[-13]	5.89[-13]	1.70[-15]	3.66[-13]	3.60[-14]	5.73[-13]	1.57[-12]	6.94[-13]
11.245	1.47[-13]	4.24[-13]	5.97[-13]	5.07[-13]	1.79[-15]	3.87[-13]	3.75[-14]	6.15[-13]	1.54[-12]	6.66[-13]
14.619	1.19[-13]	3.46[-13]	5.08[-13]	4.28[-13]	1.81[-15]	3.69[-13]	3.59[-14]	5.96[-13]	1.44[-12]	6.12[-13]
19.005	9.49[-14]	2.77[-13]	4.18[-13]	3.50[-13]	1.90[-15]	3.25[-13]	3.27[-14]	5.34[-13]	1.30[-12]	5.37[-13]
24.706	7.36[-14]	2.17[-13]	3.35[-13]	2.78[-13]	2.17[-15]	2.72[-13]	2.97[-14]	4.49[-13]	1.13[-12]	4.52[-13]
32.118	5.59[-14]	1.65[-13]	2.60[-13]	2.15[-13]	2.63[-15]	2.18[-13]	2.75[-14]	3.61[-13]	9.42[-13]	3.66[-13]
41.754	4.15[-14]	1.24[-13]	1.97[-13]	1.63[-13]	3.08[-15]	1.70[-13]	2.60[-14]	2.81[-13]	7.59[-13]	2.86[-13]
54.280	3.02[-14]	9.04[-14]	1.45[-13]	1.20[-13]	3.38[-15]	1.29[-13]	2.43[-14]	2.12[-13]	5.92[-13]	2.17[-13]
70.564	2.18[-14]	6.51[-14]	1.06[-13]	8.71[-14]	3.40[-15]	9.65[-14]	2.21[-14]	1.58[-13]	4.50[-13]	1.61[-13]
91.733	1.54[-14]	4.63[-14]	7.55[-14]	6.23[-14]	3.18[-15]	7.12[-14]	1.92[-14]	1.15[-13]	3.34[-13]	1.17[-13]
119.253	1.08[-14]	3.25[-14]	5.33[-14]	4.39[-14]	2.78[-15]	5.19[-14]	1.61[-14]	8.26[-14]	2.43[-13]	8.38[-14]
155.029	7.54[-15]	2.26[-14]	3.73[-14]	3.07[-14]	2.31[-15]	3.73[-14]	1.30[-14]	5.89[-14]	1.75[-13]	5.92[-14]
201.538	5.21[-15]	1.57[-14]	2.59[-14]	2.13[-14]	1.82[-15]	2.65[-14]	1.01[-14]	4.15[-14]	1.23[-13]	4.15[-14]
261.999	3.58[-15]	1.08[-14]	1.78[-14]	1.47[-14]	1.39[-15]	1.87[-14]	7.57[-15]	2.90[-14]	8.64[-14]	2.88[-14]
340.599	2.45[-15]	7.38[-15]	1.22[-14]	1.01[-14]	1.04[-15]	1.31[-14]	5.58[-15]	2.01[-14]	5.99[-14]	1.98[-14]
442.779	1.67[-15]	5.04[-15]	8.36[-15]	6.89[-15]	7.58[-16]	9.06[-15]	4.03[-15]	1.39[-14]	4.14[-14]	1.36[-14]
575.612	1.14[-15]	3.44[-15]	5.70[-15]	4.70[-15]	5.43[-16]	6.25[-15]	2.87[-15]	9.54[-15]	2.85[-14]	9.31[-15]
748.296	7.74[-16]	2.33[-15]	3.88[-15]	3.20[-15]	3.84[-16]	4.29[-15]	2.02[-15]	6.53[-15]	1.94[-14]	6.35[-15]
972.784	5.25[-16]	1.58[-15]	2.63[-15]	2.17[-15]	2.68[-16]	2.94[-15]	1.41[-15]	4.45[-15]	1.32[-14]	4.31[-15]
1264.620	3.55[-16]	1.07[-15]	1.78[-15]	1.47[-15]	1.86[-16]	2.00[-15]	9.70[-16]	3.03[-15]	9.01[-15]	2.93[-15]
1644.005	2.41[-16]	7.26[-16]	1.21[-15]	9.96[-16]	1.29[-16]	1.36[-15]	6.68[-16]	2.06[-15]	6.11[-15]	1.99[-15]
T_e eV	$3p3d$ 3F_2	$3p3d$ 3F_3	$3p3d$ 1D_2	$3p3d$ 3F_4	$3p3d$ 3D_1	$3p3d$ 3P_2	$3p3d$ 3P_0	$3p3d$ 3D_3	$3p3d$ 3P_1	$3p3d$ 3D_2
0.100	2.01[-15]	6.75[-16]	3.49[-16]	5.37[-24]	3.48[-16]	5.09[-16]	3.14[-17]	1.53[-16]	5.29[-17]	4.15[-17]
0.130	1.15[-14]	4.76[-15]	2.40[-15]	1.21[-21]	2.46[-15]	3.50[-15]	2.14[-16]	1.08[-15]	3.70[-16]	2.81[-16]
0.169	4.04[-14]	1.96[-14]	9.73[-15]	8.86[-20]	1.02[-14]	1.42[-14]	8.57[-16]	4.45[-15]	1.51[-15]	1.13[-15]
0.220	9.90[-14]	5.44[-14]	2.66[-14]	3.26[-18]	2.85[-14]	3.89[-14]	2.27[-15]	1.24[-14]	4.08[-15]	3.05[-15]
0.286	1.94[-13]	1.19[-13]	5.72[-14]	6.74[-17]	6.25[-14]	8.46[-14]	4.41[-15]	2.78[-14]	8.00[-15]	6.29[-15]
0.371	3.52[-13]	2.35[-13]	1.12[-13]	8.37[-16]	1.24[-13]	1.70[-13]	6.76[-15]	5.82[-14]	1.24[-14]	1.14[-14]
0.483	6.22[-13]	4.45[-13]	2.09[-13]	6.77[-15]	2.34[-13]	3.26[-13]	9.05[-15]	1.19[-13]	1.74[-14]	2.12[-14]
0.627	1.02[-12]	7.73[-13]	3.63[-13]	3.63[-14]	4.04[-13]	5.70[-13]	1.27[-14]	2.24[-13]	2.74[-14]	4.43[-14]
0.816	1.48[-12]	1.18[-12]	5.62[-13]	1.31[-13]	6.06[-13]	8.66[-13]	2.20[-14]	3.80[-13]	5.51[-14]	9.91[-14]
1.060	1.88[-12]	1.57[-12]	7.73[-13]	3.35[-13]	7.89[-13]	1.14[-12]	4.20[-14]	5.81[-13]	1.15[-13]	2.04[-13]
1.379	2.11[-12]	1.87[-12]	9.61[-13]	6.46[-13]	9.10[-13]	1.34[-12]	7.32[-14]	8.02[-13]	2.07[-13]	3.58[-13]
1.792	2.16[-12]	2.04[-12]	1.10[-12]	1.00[-12]	9.57[-13]	1.44[-12]	1.10[-13]	1.00[-12]	3.14[-13]	5.30[-13]
2.330	2.07[-12]	2.08[-12]	1.18[-12]	1.33[-12]	9.45[-13]	1.45[-12]	1.44[-13]	1.16[-12]	4.15[-13]	6.88[-13]
3.029	1.93[-12]	2.07[-12]	1.21[-12]	1.59[-12]	9.02[-13]	1.42[-12]	1.72[-13]	1.27[-12]	4.97[-13]	8.15[-13]

T_e eV	$3p3d$ 3F_2	$3p3d$ 3F_3	$3p3d$ 1D_2	$3p3d$ 3F_4	$3p3d$ 3D_1	$3p3d$ 3P_2	$3p3d$ 3P_0	$3p3d$ 3D_3	$3p3d$ 3P_1	$3p3d$ 3D_2
3.937	1.78[-12]	2.02[-12]	1.23[-12]	1.79[-12]	8.55[-13]	1.36[-12]	1.94[-13]	1.35[-12]	5.63[-13]	9.16[-13]
5.119	1.64[-12]	1.97[-12]	1.23[-12]	1.93[-12]	8.15[-13]	1.32[-12]	2.11[-13]	1.41[-12]	6.13[-13]	9.96[-13]
6.654	1.53[-12]	1.91[-12]	1.22[-12]	2.03[-12]	7.83[-13]	1.28[-12]	2.23[-13]	1.45[-12]	6.49[-13]	1.05[-12]
8.650	1.42[-12]	1.82[-12]	1.19[-12]	2.05[-12]	7.47[-13]	1.22[-12]	2.26[-13]	1.46[-12]	6.60[-13]	1.07[-12]
11.245	1.29[-12]	1.71[-12]	1.13[-12]	1.98[-12]	6.95[-13]	1.15[-12]	2.19[-13]	1.41[-12]	6.42[-13]	1.04[-12]
14.619	1.14[-12]	1.55[-12]	1.03[-12]	1.85[-12]	6.26[-13]	1.04[-12]	2.02[-13]	1.31[-12]	5.93[-13]	9.69[-13]
19.005	9.79[-13]	1.36[-12]	8.96[-13]	1.65[-12]	5.41[-13]	8.99[-13]	1.78[-13]	1.17[-12]	5.23[-13]	8.58[-13]
24.706	8.10[-13]	1.15[-12]	7.49[-13]	1.42[-12]	4.50[-13]	7.49[-13]	1.50[-13]	9.96[-13]	4.41[-13]	7.26[-13]
32.118	6.49[-13]	9.37[-13]	6.04[-13]	1.17[-12]	3.61[-13]	6.02[-13]	1.21[-13]	8.19[-13]	3.57[-13]	5.92[-13]
41.754	5.05[-13]	7.40[-13]	4.71[-13]	9.37[-13]	2.80[-13]	4.69[-13]	9.45[-14]	6.50[-13]	2.79[-13]	4.65[-13]
54.280	3.82[-13]	5.70[-13]	3.58[-13]	7.28[-13]	2.11[-13]	3.55[-13]	7.15[-14]	5.02[-13]	2.11[-13]	3.55[-13]
70.564	2.83[-13]	4.28[-13]	2.65[-13]	5.50[-13]	1.56[-13]	2.63[-13]	5.29[-14]	3.77[-13]	1.56[-13]	2.65[-13]
91.733	2.05[-13]	3.15[-13]	1.92[-13]	4.07[-13]	1.13[-13]	1.90[-13]	3.83[-14]	2.78[-13]	1.14[-13]	1.93[-13]
119.253	1.47[-13]	2.28[-13]	1.38[-13]	2.96[-13]	8.06[-14]	1.36[-13]	2.74[-14]	2.01[-13]	8.13[-14]	1.39[-13]
155.029	1.04[-13]	1.62[-13]	9.74[-14]	2.12[-13]	5.68[-14]	9.59[-14]	1.93[-14]	1.43[-13]	5.74[-14]	9.82[-14]
201.538	7.29[-14]	1.14[-13]	6.81[-14]	1.50[-13]	3.97[-14]	6.70[-14]	1.35[-14]	1.01[-13]	4.00[-14]	6.88[-14]
261.999	5.06[-14]	7.95[-14]	4.72[-14]	1.05[-13]	2.75[-14]	4.65[-14]	9.35[-15]	7.02[-14]	2.78[-14]	4.78[-14]
340.599	3.49[-14]	5.50[-14]	3.26[-14]	7.26[-14]	1.89[-14]	3.21[-14]	6.44[-15]	4.86[-14]	1.92[-14]	3.30[-14]
442.779	2.40[-14]	3.79[-14]	2.23[-14]	5.00[-14]	1.30[-14]	2.20[-14]	4.41[-15]	3.35[-14]	1.31[-14]	2.27[-14]
575.612	1.64[-14]	2.60[-14]	1.53[-14]	3.43[-14]	8.87[-15]	1.51[-14]	3.02[-15]	2.29[-14]	8.98[-15]	1.55[-14]
748.296	1.12[-14]	1.77[-14]	1.04[-14]	2.35[-14]	6.05[-15]	1.02[-14]	2.05[-15]	1.56[-14]	6.11[-15]	1.06[-14]
972.784	7.60[-15]	1.21[-14]	7.09[-15]	1.60[-14]	4.11[-15]	6.96[-15]	1.40[-15]	1.07[-14]	4.16[-15]	7.21[-15]
1264.620	5.16[-15]	8.21[-15]	4.81[-15]	1.09[-14]	2.79[-15]	4.72[-15]	9.48[-16]	7.25[-15]	2.82[-15]	4.89[-15]
1644.005	3.50[-15]	5.57[-15]	3.26[-15]	7.39[-15]	1.89[-15]	3.20[-15]	6.42[-16]	4.92[-15]	1.92[-15]	3.31[-15]
T_e eV	$3p4s$ 3P_0	$3p4s$ 3P_1	$3p4s$ 3P_2	$3p4s$ 1P_1	$3s4f$ 3F_2	$3s4f$ 3F_3	$3s4f$ 3F_4	$3s4f$ 1F_3	$3p4d$ 3P_0	$3p4d$ 1F_3
0.100	2.22[-15]	5.12[-15]	4.76[-19]	4.31[-16]	5.68[-18]	1.87[-18]	7.67[-23]	3.37[-20]	8.15[-18]	2.62[-17]
0.130	1.36[-14]	3.29[-14]	3.17[-18]	2.73[-15]	3.24[-17]	1.32[-17]	1.62[-20]	2.54[-19]	4.80[-17]	1.88[-16]
0.169	5.06[-14]	1.27[-13]	1.27[-17]	1.04[-14]	1.13[-16]	5.45[-17]	9.14[-19]	1.97[-18]	1.72[-16]	7.84[-16]
0.220	1.28[-13]	3.28[-13]	4.25[-17]	2.68[-14]	2.77[-16]	1.56[-16]	1.86[-17]	2.34[-17]	4.23[-16]	2.16[-15]
0.286	2.38[-13]	6.26[-13]	2.77[-16]	5.08[-14]	5.34[-16]	3.76[-16]	1.72[-16]	2.02[-16]	7.75[-16]	4.40[-15]
0.371	3.51[-13]	9.40[-13]	2.34[-15]	7.71[-14]	9.36[-16]	9.00[-16]	8.73[-16]	1.02[-15]	1.17[-15]	7.43[-15]
0.483	4.33[-13]	1.17[-12]	1.29[-14]	1.02[-13]	1.60[-15]	2.05[-15]	2.80[-15]	3.30[-15]	1.78[-15]	1.18[-14]
0.627	4.64[-13]	1.28[-12]	4.48[-14]	1.27[-13]	2.64[-15]	4.06[-15]	6.34[-15]	7.59[-15]	3.52[-15]	2.01[-14]
0.816	4.48[-13]	1.24[-12]	1.07[-13]	1.60[-13]	4.09[-15]	6.83[-15]	1.11[-14]	1.36[-14]	8.51[-15]	3.80[-14]
1.060	3.99[-13]	1.12[-12]	1.93[-13]	1.99[-13]	5.88[-15]	1.00[-14]	1.63[-14]	2.05[-14]	1.90[-14]	7.13[-14]
1.379	3.36[-13]	9.49[-13]	2.78[-13]	2.36[-13]	7.89[-15]	1.33[-14]	2.11[-14]	2.74[-14]	3.47[-14]	1.19[-13]
1.792	2.72[-13]	7.77[-13]	3.42[-13]	2.61[-13]	9.97[-15]	1.65[-14]	2.55[-14]	3.39[-14]	5.26[-14]	1.73[-13]
2.330	2.18[-13]	6.27[-13]	3.82[-13]	2.73[-13]	1.22[-14]	1.98[-14]	2.99[-14]	4.03[-14]	6.88[-14]	2.22[-13]
3.029	1.80[-13]	5.24[-13]	4.21[-13]	2.83[-13]	1.48[-14]	2.37[-14]	3.50[-14]	4.72[-14]	8.11[-14]	2.59[-13]
3.937	1.67[-13]	4.88[-13]	5.11[-13]	3.07[-13]	1.80[-14]	2.83[-14]	4.10[-14]	5.49[-14]	9.00[-14]	2.87[-13]
5.119	1.83[-13]	5.34[-13]	6.88[-13]	3.64[-13]	2.18[-14]	3.34[-14]	4.80[-14]	6.28[-14]	9.67[-14]	3.08[-13]
6.654	2.17[-13]	6.35[-13]	9.25[-13]	4.53[-13]	2.60[-14]	3.84[-14]	5.83[-14]	6.99[-14]	1.02[-13]	3.24[-13]
8.650	2.54[-13]	7.42[-13]	1.15[-12]	5.48[-13]	3.07[-14]	4.32[-14]	7.63[-14]	7.50[-14]	1.04[-13]	3.32[-13]
11.245	2.75[-13]	8.04[-13]	1.28[-12]	6.17[-13]	3.58[-14]	4.75[-14]	1.04[-13]	7.75[-14]	1.01[-13]	3.27[-13]
14.619	2.73[-13]	8.01[-13]	1.29[-12]	6.37[-13]	4.03[-14]	5.06[-14]	1.36[-13]	7.64[-14]	9.37[-14]	3.09[-13]
19.005	2.51[-13]	7.41[-13]	1.21[-12]	6.07[-13]	4.29[-14]	5.14[-14]	1.63[-13]	7.19[-14]	8.22[-14]	2.80[-13]
24.706	2.18[-13]	6.45[-13]	1.05[-12]	5.44[-13]	4.28[-14]	4.94[-14]	1.76[-13]	6.44[-14]	6.89[-14]	2.43[-13]
32.118	1.81[-13]	5.39[-13]	8.82[-13]	4.64[-13]	3.98[-14]	4.48[-14]	1.74[-13]	5.52[-14]	5.54[-14]	2.03[-13]
41.754	1.47[-13]	4.37[-13]	7.18[-13]	3.83[-13]	3.51[-14]	3.87[-14]	1.59[-13]	4.58[-14]	4.32[-14]	1.63[-13]
54.280	1.18[-13]	3.50[-13]	5.76[-13]	3.10[-13]	2.95[-14]	3.22[-14]	1.36[-13]	3.72[-14]	3.29[-14]	1.28[-13]
70.564	9.30[-14]	2.77[-13]	4.56[-13]	2.47[-13]	2.39[-14]	2.58[-14]	1.12[-13]	2.97[-14]	2.45[-14]	9.75[-14]
91.733	7.29[-14]	2.17[-13]	3.58[-13]	1.93[-13]	1.89[-14]	2.03[-14]	8.83[-14]	2.37[-14]	1.80[-14]	7.28[-14]
119.253	5.64[-14]	1.68[-13]	2.78[-13]	1.49[-13]	1.46[-14]	1.57[-14]	6.77[-14]	1.88[-14]	1.31[-14]	5.34[-14]
155.029	4.30[-14]	1.28[-13]	2.13[-13]	1.13[-13]	1.10[-14]	1.18[-14]	5.07[-14]	1.47[-14]	9.38[-15]	3.85[-14]

T_e eV	$3p4s$ 3P_0	$3p4s$ 3P_1	$3p4s$ 3P_2	$3p4s$ 1P_1	$3s4f$ 3F_2	$3s4f$ 3F_3	$3s4f$ 3F_4	$3s4f$ 1F_3	$3p4d$ 3P_0	$3p4d$ 1F_3
201.538	3.22[-14]	9.58[-14]	1.60[-13]	8.43[-14]	8.16[-15]	8.81[-15]	3.71[-14]	1.13[-14]	6.67[-15]	2.75[-14]
261.999	2.38[-14]	7.06[-14]	1.17[-13]	6.17[-14]	5.96[-15]	6.45[-15]	2.68[-14]	8.57[-15]	4.70[-15]	1.94[-14]
340.599	1.73[-14]	5.12[-14]	8.52[-14]	4.47[-14]	4.29[-15]	4.66[-15]	1.91[-14]	6.37[-15]	3.29[-15]	1.36[-14]
442.779	1.23[-14]	3.66[-14]	6.10[-14]	3.19[-14]	3.05[-15]	3.32[-15]	1.34[-14]	4.64[-15]	2.29[-15]	9.41[-15]
575.612	8.73[-15]	2.59[-14]	4.32[-14]	2.24[-14]	2.14[-15]	2.34[-15]	9.36[-15]	3.33[-15]	1.58[-15]	6.50[-15]
748.296	6.11[-15]	1.81[-14]	3.02[-14]	1.57[-14]	1.50[-15]	1.63[-15]	6.49[-15]	2.37[-15]	1.09[-15]	4.46[-15]
972.784	4.25[-15]	1.26[-14]	2.10[-14]	1.09[-14]	1.03[-15]	1.13[-15]	4.46[-15]	1.66[-15]	7.44[-16]	3.05[-15]
1264.620	2.93[-15]	8.69[-15]	1.45[-14]	7.49[-15]	7.13[-16]	7.82[-16]	3.06[-15]	1.16[-15]	5.07[-16]	2.09[-15]
1644.005	2.02[-15]	5.97[-15]	9.96[-15]	5.14[-15]	4.89[-16]	5.37[-16]	2.09[-15]	8.00[-16]	3.45[-16]	1.42[-15]
T_e eV	$3p4d$ 3D_1	$3p4d$ 1D_2	$3p4d$ 3D_2	$3p4d$ 3D_3	$3p4d$ 3F_2	$3p4d$ 3F_3	$3p4d$ 3F_4	$3p4d$ 1F_3	$3p4d$ 3P_2	$3p4d$ 3P_1
0.100	4.38[-16]	1.37[-15]	7.27[-16]	8.39[-16]	1.06[-16]	7.41[-17]	5.25[-24]	8.09[-18]	1.22[-16]	9.25[-17]
0.130	2.80[-15]	7.88[-15]	4.80[-15]	5.92[-15]	6.09[-16]	5.23[-16]	1.16[-21]	5.70[-17]	8.33[-16]	5.73[-16]
0.169	1.08[-14]	2.77[-14]	1.88[-14]	2.43[-14]	2.15[-15]	2.15[-15]	8.00[-20]	2.35[-16]	3.35[-15]	2.16[-15]
0.220	2.85[-14]	6.77[-14]	5.00[-14]	6.68[-14]	5.23[-15]	5.89[-15]	2.63[-18]	6.47[-16]	9.01[-15]	5.56[-15]
0.286	5.78[-14]	1.29[-13]	1.02[-13]	1.40[-13]	9.90[-15]	1.23[-14]	4.90[-17]	1.39[-15]	1.84[-14]	1.10[-14]
0.371	1.02[-13]	2.15[-13]	1.81[-13]	2.53[-13]	1.65[-14]	2.21[-14]	5.43[-16]	2.89[-15]	3.24[-14]	1.89[-14]
0.483	1.70[-13]	3.43[-13]	3.02[-13]	4.28[-13]	2.71[-14]	3.87[-14]	3.89[-15]	7.16[-15]	5.39[-14]	3.11[-14]
0.627	2.65[-13]	5.16[-13]	4.70[-13]	6.72[-13]	4.67[-14]	6.88[-14]	1.90[-14]	2.10[-14]	8.76[-14]	5.07[-14]
0.816	3.73[-13]	7.06[-13]	6.56[-13]	9.45[-13]	8.31[-14]	1.23[-13]	6.46[-14]	5.85[-14]	1.38[-13]	8.08[-14]
1.060	4.66[-13]	8.64[-13]	8.13[-13]	1.18[-12]	1.43[-13]	2.09[-13]	1.59[-13]	1.34[-13]	2.08[-13]	1.23[-13]
1.379	5.23[-13]	9.52[-13]	9.05[-13]	1.31[-12]	2.21[-13]	3.20[-13]	2.99[-13]	2.46[-13]	2.89[-13]	1.73[-13]
1.792	5.38[-13]	9.64[-13]	9.25[-13]	1.34[-12]	3.02[-13]	4.35[-13]	4.56[-13]	3.72[-13]	3.68[-13]	2.21[-13]
2.330	5.21[-13]	9.18[-13]	8.87[-13]	1.29[-12]	3.71[-13]	5.31[-13]	5.97[-13]	4.89[-13]	4.31[-13]	2.61[-13]
3.029	4.85[-13]	8.44[-13]	8.21[-13]	1.18[-12]	4.19[-13]	5.99[-13]	7.01[-13]	5.82[-13]	4.72[-13]	2.87[-13]
3.937	4.49[-13]	7.68[-13]	7.52[-13]	1.09[-12]	4.53[-13]	6.46[-13]	7.78[-13]	6.53[-13]	4.97[-13]	3.04[-13]
5.119	4.19[-13]	7.07[-13]	6.99[-13]	1.01[-12]	4.79[-13]	6.84[-13]	8.41[-13]	7.08[-13]	5.17[-13]	3.18[-13]
6.654	3.99[-13]	6.64[-13]	6.61[-13]	9.54[-13]	5.02[-13]	7.16[-13]	8.92[-13]	7.45[-13]	5.31[-13]	3.27[-13]
8.650	3.80[-13]	6.29[-13]	6.27[-13]	9.03[-13]	5.14[-13]	7.29[-13]	9.19[-13]	7.56[-13]	5.34[-13]	3.30[-13]
11.245	3.55[-13]	5.89[-13]	5.84[-13]	8.38[-13]	5.06[-13]	7.13[-13]	9.06[-13]	7.33[-13]	5.18[-13]	3.20[-13]
14.619	3.20[-13]	5.35[-13]	5.27[-13]	7.49[-13]	4.75[-13]	6.60[-13]	8.44[-13]	6.78[-13]	4.79[-13]	2.97[-13]
19.005	2.77[-13]	4.68[-13]	4.54[-13]	6.43[-13]	4.23[-13]	5.81[-13]	7.47[-13]	5.95[-13]	4.22[-13]	2.62[-13]
24.706	2.29[-13]	3.94[-13]	3.76[-13]	5.31[-13]	3.60[-13]	4.87[-13]	6.31[-13]	4.99[-13]	3.55[-13]	2.22[-13]
32.118	1.83[-13]	3.19[-13]	3.01[-13]	4.22[-13]	2.93[-13]	3.92[-13]	5.10[-13]	4.02[-13]	2.87[-13]	1.80[-13]
41.754	1.42[-13]	2.52[-13]	2.33[-13]	3.26[-13]	2.30[-13]	3.06[-13]	4.02[-13]	3.14[-13]	2.24[-13]	1.42[-13]
54.280	1.07[-13]	1.93[-13]	1.76[-13]	2.46[-13]	1.77[-13]	2.32[-13]	3.09[-13]	2.39[-13]	1.71[-13]	1.09[-13]
70.564	7.98[-14]	1.45[-13]	1.30[-13]	1.82[-13]	1.33[-13]	1.73[-13]	2.35[-13]	1.79[-13]	1.28[-13]	8.16[-14]
91.733	5.83[-14]	1.07[-13]	9.55[-14]	1.33[-13]	9.86[-14]	1.27[-13]	1.75[-13]	1.32[-13]	9.43[-14]	6.03[-14]
119.253	4.22[-14]	7.79[-14]	6.90[-14]	9.63[-14]	7.20[-14]	9.22[-14]	1.30[-13]	9.63[-14]	6.86[-14]	4.38[-14]
155.029	3.02[-14]	5.61[-14]	4.94[-14]	6.90[-14]	5.20[-14]	6.63[-14]	9.48[-14]	6.96[-14]	4.92[-14]	3.15[-14]
201.538	2.14[-14]	4.00[-14]	3.50[-14]	4.89[-14]	3.71[-14]	4.72[-14]	6.85[-14]	4.97[-14]	3.49[-14]	2.24[-14]
261.999	1.50[-14]	2.82[-14]	2.46[-14]	3.44[-14]	2.63[-14]	3.33[-14]	4.91[-14]	3.52[-14]	2.47[-14]	1.58[-14]
340.599	1.05[-14]	1.98[-14]	1.71[-14]	2.40[-14]	1.85[-14]	2.33[-14]	3.47[-14]	2.48[-14]	1.72[-14]	1.10[-14]
442.779	7.28[-15]	1.38[-14]	1.19[-14]	1.67[-14]	1.29[-14]	1.62[-14]	2.44[-14]	1.73[-14]	1.20[-14]	7.66[-15]
575.612	5.03[-15]	9.51[-15]	8.20[-15]	1.16[-14]	8.92[-15]	1.12[-14]	1.70[-14]	1.20[-14]	8.26[-15]	5.28[-15]
748.296	3.45[-15]	6.54[-15]	5.63[-15]	7.94[-15]	6.14[-15]	7.73[-15]	1.18[-14]	8.27[-15]	5.67[-15]	3.63[-15]
972.784	2.36[-15]	4.48[-15]	3.85[-15]	5.44[-15]	4.22[-15]	5.31[-15]	8.10[-15]	5.67[-15]	3.88[-15]	2.49[-15]
1264.620	1.61[-15]	3.06[-15]	2.63[-15]	3.71[-15]	2.88[-15]	3.63[-15]	5.55[-15]	3.88[-15]	2.65[-15]	1.69[-15]
1644.005	1.10[-15]	2.08[-15]	1.79[-15]	2.53[-15]	1.96[-15]	2.47[-15]	3.80[-15]	2.65[-15]	1.80[-15]	1.15[-15]
T_e eV	$3d4p$ 1D_2	$3d4p$ 3D_1	$3d4p$ 3D_2	$3d4p$ 3F_3	$3d4p$ 3F_2	$3d4p$ 3D_3	$3d4p$ 3F_4	$3d4p$ 3P_1	$3d4p$ 3P_0	$3d4p$ 3P_2
0.100	6.31[-18]	6.10[-18]	5.67[-18]	5.38[-18]	2.40[-18]	2.38[-19]	4.27[-25]	2.36[-17]	1.13[-17]	1.35[-18]
0.130	4.09[-17]	4.46[-17]	3.84[-17]	3.80[-17]	1.53[-17]	1.68[-18]	9.91[-23]	1.60[-16]	7.28[-17]	9.42[-18]
0.169	1.59[-16]	1.89[-16]	1.53[-16]	1.56[-16]	5.83[-17]	6.93[-18]	6.16[-21]	6.43[-16]	2.80[-16]	3.83[-17]
0.220	4.12[-16]	5.24[-16]	4.07[-16]	4.21[-16]	1.50[-16]	1.94[-17]	1.41[-19]	1.71[-15]	7.23[-16]	1.03[-16]

T_e eV	$3d4p$ 1D_2	$3d4p$ 3D_1	$3d4p$ 3D_2	$3d4p$ 3F_3	$3d4p$ 3F_2	$3d4p$ 3D_3	$3d4p$ 3F_4	$3d4p$ 3P_1	$3d4p$ 3P_0	$3d4p$ 3P_2
0.286	7.88[-16]	1.05[-15]	7.90[-16]	8.30[-16]	2.88[-16]	4.34[-17]	1.51[-18]	3.33[-15]	1.37[-15]	2.02[-16]
0.371	1.19[-15]	1.67[-15]	1.22[-15]	1.29[-15]	4.48[-16]	9.23[-17]	9.29[-18]	5.08[-15]	2.05[-15]	3.18[-16]
0.483	1.49[-15]	2.21[-15]	1.58[-15]	1.67[-15]	6.10[-16]	1.96[-16]	3.68[-17]	6.44[-15]	2.56[-15]	4.45[-16]
0.627	1.63[-15]	2.57[-15]	1.84[-15]	1.92[-15]	7.68[-16]	3.83[-16]	1.04[-16]	7.07[-15]	2.78[-15]	6.12[-16]
0.816	1.63[-15]	2.74[-15]	1.98[-15]	2.03[-15]	9.21[-16]	6.55[-16]	2.22[-16]	6.98[-15]	2.71[-15]	8.57[-16]
1.060	1.54[-15]	2.72[-15]	2.04[-15]	2.10[-15]	1.07[-15]	9.92[-16]	4.05[-16]	6.38[-15]	2.44[-15]	1.18[-15]
1.379	1.62[-15]	2.68[-15]	2.21[-15]	2.37[-15]	1.36[-15]	1.56[-15]	8.50[-16]	5.61[-15]	2.11[-15]	1.64[-15]
1.792	2.91[-15]	3.22[-15]	3.29[-15]	3.92[-15]	2.57[-15]	3.45[-15]	2.73[-15]	5.40[-15]	1.95[-15]	2.88[-15]
2.330	8.37[-15]	6.20[-15]	7.56[-15]	9.95[-15]	7.03[-15]	9.99[-15]	9.65[-15]	7.32[-15]	2.42[-15]	6.97[-15]
3.029	2.29[-14]	1.47[-14]	1.89[-14]	2.58[-14]	1.86[-14]	2.66[-14]	2.79[-14]	1.39[-14]	4.28[-15]	1.76[-14]
3.937	5.02[-14]	3.13[-14]	3.99[-14]	5.54[-14]	4.04[-14]	5.74[-14]	6.31[-14]	2.70[-14]	8.10[-15]	3.77[-14]
5.119	8.86[-14]	5.41[-14]	6.94[-14]	9.66[-14]	7.13[-14]	1.00[-13]	1.18[-13]	4.56[-14]	1.37[-14]	6.64[-14]
6.654	1.31[-13]	7.78[-14]	1.01[-13]	1.41[-13]	1.07[-13]	1.49[-13]	2.00[-13]	6.59[-14]	1.98[-14]	9.81[-14]
8.650	1.69[-13]	9.63[-14]	1.26[-13]	1.81[-13]	1.45[-13]	1.96[-13]	3.23[-13]	8.33[-14]	2.52[-14]	1.26[-13]
11.245	1.95[-13]	1.06[-13]	1.41[-13]	2.07[-13]	1.79[-13]	2.39[-13]	4.93[-13]	9.46[-14]	2.89[-14]	1.46[-13]
14.619	2.07[-13]	1.05[-13]	1.44[-13]	2.20[-13]	2.08[-13]	2.69[-13]	6.80[-13]	9.86[-14]	3.03[-14]	1.54[-13]
19.005	2.04[-13]	9.79[-14]	1.37[-13]	2.17[-13]	2.22[-13]	2.83[-13]	8.34[-13]	9.56[-14]	2.97[-14]	1.51[-13]
24.706	1.88[-13]	8.58[-14]	1.22[-13]	2.02[-13]	2.20[-13]	2.78[-13]	9.13[-13]	8.73[-14]	2.71[-14]	1.40[-13]
32.118	1.65[-13]	7.20[-14]	1.06[-13]	1.78[-13]	2.04[-13]	2.57[-13]	9.05[-13]	7.56[-14]	2.36[-14]	1.22[-13]
41.754	1.37[-13]	5.86[-14]	8.81[-14]	1.50[-13]	1.78[-13]	2.23[-13]	8.27[-13]	6.26[-14]	1.96[-14]	1.01[-13]
54.280	1.10[-13]	4.64[-14]	7.15[-14]	1.22[-13]	1.48[-13]	1.85[-13]	7.07[-13]	5.01[-14]	1.56[-14]	8.11[-14]
70.564	8.55[-14]	3.60[-14]	5.65[-14]	9.54[-14]	1.17[-13]	1.48[-13]	5.75[-13]	3.88[-14]	1.21[-14]	6.31[-14]
91.733	6.45[-14]	2.74[-14]	4.35[-14]	7.27[-14]	9.02[-14]	1.14[-13]	4.48[-13]	2.94[-14]	9.13[-15]	4.78[-14]
119.253	4.76[-14]	2.04[-14]	3.28[-14]	5.43[-14]	6.75[-14]	8.51[-14]	3.38[-13]	2.19[-14]	6.76[-15]	3.55[-14]
155.029	3.46[-14]	1.49[-14]	2.42[-14]	3.96[-14]	4.95[-14]	6.25[-14]	2.50[-13]	1.60[-14]	4.92[-15]	2.59[-14]
201.538	2.47[-14]	1.08[-14]	1.76[-14]	2.85[-14]	3.56[-14]	4.50[-14]	1.80[-13]	1.15[-14]	3.53[-15]	1.86[-14]
261.999	1.75[-14]	7.69[-15]	1.26[-14]	2.02[-14]	2.53[-14]	3.20[-14]	1.28[-13]	8.16[-15]	2.51[-15]	1.32[-14]
340.599	1.22[-14]	5.42[-15]	8.92[-15]	1.42[-14]	1.77[-14]	2.24[-14]	9.04[-14]	5.74[-15]	1.76[-15]	9.26[-15]
442.779	8.47[-15]	3.79[-15]	6.25[-15]	9.88[-15]	1.23[-14]	1.56[-14]	6.29[-14]	4.00[-15]	1.23[-15]	6.45[-15]
575.612	5.84[-15]	2.62[-15]	4.34[-15]	6.83[-15]	8.52[-15]	1.08[-14]	4.35[-14]	2.77[-15]	8.51[-16]	4.46[-15]
748.296	4.01[-15]	1.81[-15]	2.99[-15]	4.70[-15]	5.86[-15]	7.43[-15]	2.99[-14]	1.91[-15]	5.85[-16]	3.07[-15]
972.784	2.75[-15]	1.24[-15]	2.06[-15]	3.22[-15]	4.01[-15]	5.09[-15]	2.05[-14]	1.31[-15]	4.02[-16]	2.11[-15]
1264.620	1.87[-15]	8.49[-16]	1.41[-15]	2.19[-15]	2.74[-15]	3.47[-15]	1.40[-14]	8.95[-16]	2.74[-16]	1.44[-15]
1644.005	1.27[-15]	5.78[-16]	9.60[-16]	1.49[-15]	1.86[-15]	2.37[-15]	9.52[-15]	6.09[-16]	1.87[-16]	9.79[-16]
T_e eV	$3d4f$ 3H_4	$3d4f$ 1G_4	$3d4f$ 3H_5	$3d4f$ 3H_6	$3d4f$ 3F_2	$3d4f$ 3F_3	$3d4f$ 3F_4	$3d4f$ 1D_2	$3d4f$ 3P_0	$3d4f$ 1F_3
0.100	2.94[-23]	5.84[-24]	1.46[-23]	3.33[-26]	6.77[-19]	2.10[-19]	4.72[-24]	1.70[-18]	2.28[-17]	2.56[-19]
0.130	5.81[-21]	1.21[-21]	3.20[-21]	1.05[-23]	3.90[-18]	1.48[-18]	9.98[-22]	1.17[-17]	1.42[-16]	1.81[-18]
0.169	3.11[-19]	6.68[-20]	1.85[-19]	7.98[-22]	1.37[-17]	6.09[-18]	5.60[-20]	4.71[-17]	5.35[-16]	7.49[-18]
0.220	6.06[-18]	1.34[-18]	3.84[-18]	2.06[-20]	3.31[-17]	1.68[-17]	1.13[-18]	1.26[-16]	1.36[-15]	2.20[-17]
0.286	5.44[-17]	1.23[-17]	3.61[-17]	2.45[-19]	5.99[-17]	3.63[-17]	1.05[-17]	2.46[-16]	2.55[-15]	5.82[-17]
0.371	2.69[-16]	6.20[-17]	1.85[-16]	2.03[-18]	8.70[-17]	7.05[-17]	5.30[-17]	3.79[-16]	3.79[-15]	1.59[-16]
0.483	8.41[-16]	1.99[-16]	5.98[-16]	1.54[-17]	1.08[-16]	1.31[-16]	1.69[-16]	4.89[-16]	4.69[-15]	4.04[-16]
0.627	1.85[-15]	4.55[-16]	1.36[-15]	9.04[-17]	1.26[-16]	2.30[-16]	3.83[-16]	5.57[-16]	5.05[-15]	8.57[-16]
0.816	3.11[-15]	8.20[-16]	2.42[-15]	3.56[-16]	1.55[-16]	3.66[-16]	6.69[-16]	5.80[-16]	4.89[-15]	1.52[-15]
1.060	4.31[-15]	1.25[-15]	3.58[-15]	9.72[-16]	2.14[-16]	5.34[-16]	9.75[-16]	5.68[-16]	4.37[-15]	2.34[-15]
1.379	5.25[-15]	1.73[-15]	4.74[-15]	2.01[-15]	3.22[-16]	7.34[-16]	1.27[-15]	5.38[-16]	3.70[-15]	3.26[-15]
1.792	6.20[-15]	2.42[-15]	6.13[-15]	3.65[-15]	5.81[-16]	1.11[-15]	1.73[-15]	5.83[-16]	3.04[-15]	4.36[-15]
2.330	8.70[-15]	4.63[-15]	9.37[-15]	7.50[-15]	1.73[-15]	2.67[-15]	3.62[-15]	1.32[-15]	2.58[-15]	6.44[-15]
3.029	1.72[-14]	1.26[-14]	1.94[-14]	1.91[-14]	6.19[-15]	8.70[-15]	1.11[-14]	4.83[-15]	2.69[-15]	1.22[-14]
3.937	3.79[-14]	3.25[-14]	4.38[-14]	4.72[-14]	1.76[-14]	2.42[-14]	3.02[-14]	1.43[-14]	3.94[-15]	2.57[-14]
5.119	7.28[-14]	6.71[-14]	8.52[-14]	9.58[-14]	3.72[-14]	5.11[-14]	6.39[-14]	3.14[-14]	6.59[-15]	4.88[-14]
6.654	1.15[-13]	1.09[-13]	1.36[-13]	1.56[-13]	6.17[-14]	8.46[-14]	1.06[-13]	5.32[-14]	1.01[-14]	7.81[-14]
8.650	1.52[-13]	1.50[-13]	1.80[-13]	2.14[-13]	8.40[-14]	1.15[-13]	1.46[-13]	7.50[-14]	1.36[-14]	1.08[-13]
11.245	1.77[-13]	1.79[-13]	2.07[-13]	2.52[-13]	9.84[-14]	1.35[-13]	1.74[-13]	9.49[-14]	1.59[-14]	1.41[-13]

T_e eV	$3d4f$ 3H_4	$3d4f$ 1G_4	$3d4f$ 3H_5	$3d4f$ 3H_6	$3d4f$ 3F_2	$3d4f$ 3F_3	$3d4f$ 3F_4	$3d4f$ 1D_2	$3d4f$ 3P_0	$3d4f$ 1F_3
14.619	1.85[-13]	1.99[-13]	2.12[-13]	2.68[-13]	1.03[-13]	1.41[-13]	1.93[-13]	1.16[-13]	1.67[-14]	1.84[-13]
19.005	1.81[-13]	2.13[-13]	1.99[-13]	2.60[-13]	9.94[-14]	1.37[-13]	2.05[-13]	1.40[-13]	1.61[-14]	2.39[-13]
24.706	1.70[-13]	2.22[-13]	1.74[-13]	2.35[-13]	8.99[-14]	1.24[-13]	2.10[-13]	1.63[-13]	1.47[-14]	3.00[-13]
32.118	1.54[-13]	2.23[-13]	1.46[-13]	2.02[-13]	7.75[-14]	1.07[-13]	2.08[-13]	1.80[-13]	1.27[-14]	3.44[-13]
41.754	1.36[-13]	2.13[-13]	1.18[-13]	1.68[-13]	6.46[-14]	8.96[-14]	1.96[-13]	1.84[-13]	1.06[-14]	3.60[-13]
54.280	1.16[-13]	1.93[-13]	9.50[-14]	1.38[-13]	5.21[-14]	7.29[-14]	1.75[-13]	1.75[-13]	8.56[-15]	3.48[-13]
70.564	9.69[-14]	1.67[-13]	7.62[-14]	1.12[-13]	4.12[-14]	5.79[-14]	1.50[-13]	1.55[-13]	6.76[-15]	3.12[-13]
91.733	7.89[-14]	1.39[-13]	6.08[-14]	9.00[-14]	3.18[-14]	4.51[-14]	1.24[-13]	1.30[-13]	5.23[-15]	2.65[-13]
119.253	6.26[-14]	1.11[-13]	4.81[-14]	7.13[-14]	2.42[-14]	3.44[-14]	9.82[-14]	1.05[-13]	3.98[-15]	2.14[-13]
155.029	4.84[-14]	8.61[-14]	3.76[-14]	5.58[-14]	1.80[-14]	2.58[-14]	7.56[-14]	8.10[-14]	2.97[-15]	1.67[-13]
201.538	3.67[-14]	6.51[-14]	2.89[-14]	4.28[-14]	1.32[-14]	1.91[-14]	5.68[-14]	6.09[-14]	2.18[-15]	1.26[-13]
261.999	2.72[-14]	4.80[-14]	2.17[-14]	3.22[-14]	9.54[-15]	1.39[-14]	4.18[-14]	4.48[-14]	1.57[-15]	9.28[-14]
340.599	1.98[-14]	3.49[-14]	1.60[-14]	2.37[-14]	6.80[-15]	9.94[-15]	3.02[-14]	3.24[-14]	1.13[-15]	6.71[-14]
442.779	1.42[-14]	2.49[-14]	1.17[-14]	1.72[-14]	4.81[-15]	7.05[-15]	2.15[-14]	2.29[-14]	7.97[-16]	4.78[-14]
575.612	1.01[-14]	1.76[-14]	8.34[-15]	1.23[-14]	3.36[-15]	4.94[-15]	1.51[-14]	1.62[-14]	5.58[-16]	3.37[-14]
748.296	7.05[-15]	1.23[-14]	5.90[-15]	8.71[-15]	2.33[-15]	3.43[-15]	1.06[-14]	1.13[-14]	3.88[-16]	2.35[-14]
972.784	4.90[-15]	8.53[-15]	4.13[-15]	6.10[-15]	1.61[-15]	2.37[-15]	7.31[-15]	7.79[-15]	2.68[-16]	1.63[-14]
1264.620	3.40[-15]	5.88[-15]	2.87[-15]	4.24[-15]	1.10[-15]	1.63[-15]	5.04[-15]	5.35[-15]	1.84[-16]	1.12[-14]
1644.005	2.33[-15]	4.04[-15]	1.98[-15]	2.92[-15]	7.54[-16]	1.12[-15]	3.45[-15]	3.66[-15]	1.26[-16]	7.66[-15]
T_e eV	$3d4f$ 3G_3	$3d4f$ 3G_4	$3d4f$ 3G_5	$3d4f$ 3D_2	$3d4f$ 3D_1	$3d4f$ 3D_3	$3d4f$ 3P_2	$3d4f$ 3P_1	$3d4f$ 1H_5	$3d4f$ 1P_1
0.100	1.15[-20]	8.75[-24]	7.80[-24]	1.22[-18]	1.22[-17]	5.49[-19]	1.05[-18]	6.37[-17]	4.30[-23]	2.92[-18]
0.130	8.29[-20]	1.84[-21]	1.74[-21]	8.30[-18]	7.32[-17]	3.87[-18]	6.63[-18]	4.09[-16]	9.79[-21]	1.99[-17]
0.169	4.45[-19]	1.03[-19]	1.03[-19]	3.31[-17]	2.67[-16]	1.59[-17]	2.52[-17]	1.57[-15]	5.87[-19]	8.01[-17]
0.220	3.25[-18]	2.09[-18]	2.16[-18]	8.80[-17]	6.63[-16]	4.31[-17]	6.47[-17]	4.08[-15]	1.26[-17]	2.15[-16]
0.286	2.41[-17]	1.94[-17]	2.07[-17]	1.71[-16]	1.22[-15]	8.61[-17]	1.25[-16]	7.76[-15]	1.22[-16]	4.24[-16]
0.371	1.19[-16]	9.86[-17]	1.08[-16]	2.64[-16]	1.79[-15]	1.39[-16]	2.12[-16]	1.16[-14]	6.44[-16]	6.71[-16]
0.483	3.80[-16]	3.18[-16]	3.54[-16]	3.52[-16]	2.20[-15]	1.96[-16]	3.98[-16]	1.46[-14]	2.14[-15]	9.18[-16]
0.627	8.67[-16]	7.34[-16]	8.31[-16]	4.37[-16]	2.36[-15]	2.56[-16]	8.50[-16]	1.58[-14]	5.05[-15]	1.14[-15]
0.816	1.53[-15]	1.34[-15]	1.54[-15]	5.31[-16]	2.29[-15]	3.18[-16]	1.69[-15]	1.55[-14]	9.38[-15]	1.34[-15]
1.060	2.25[-15]	2.06[-15]	2.41[-15]	6.30[-16]	2.05[-15]	3.78[-16]	2.83[-15]	1.40[-14]	1.48[-14]	1.48[-15]
1.379	2.94[-15]	2.85[-15]	3.39[-15]	7.17[-16]	1.74[-15]	4.39[-16]	3.97[-15]	1.20[-14]	2.07[-14]	1.55[-15]
1.792	3.71[-15]	3.83[-15]	4.59[-15]	8.49[-16]	1.48[-15]	6.21[-16]	4.86[-15]	9.97[-15]	2.70[-14]	1.59[-15]
2.330	5.55[-15]	6.10[-15]	7.25[-15]	1.57[-15]	1.69[-15]	1.77[-15]	5.88[-15]	8.56[-15]	3.48[-14]	1.92[-15]
3.029	1.14[-14]	1.32[-14]	1.55[-14]	4.69[-15]	3.57[-15]	6.72[-15]	8.69[-15]	8.96[-15]	4.71[-14]	3.66[-15]
3.937	2.55[-14]	3.06[-14]	3.56[-14]	1.30[-14]	9.05[-15]	1.98[-14]	1.60[-14]	1.30[-14]	6.86[-14]	8.62[-15]
5.119	4.94[-14]	6.03[-14]	7.01[-14]	2.77[-14]	1.90[-14]	4.31[-14]	2.94[-14]	2.14[-14]	1.00[-13]	1.79[-14]
6.654	7.86[-14]	9.66[-14]	1.13[-13]	4.64[-14]	3.18[-14]	7.26[-14]	4.67[-14]	3.30[-14]	1.36[-13]	3.02[-14]
8.650	1.05[-13]	1.29[-13]	1.52[-13]	6.35[-14]	4.40[-14]	1.01[-13]	6.30[-14]	4.40[-14]	1.68[-13]	4.31[-14]
11.245	1.21[-13]	1.50[-13]	1.77[-13]	7.49[-14]	5.26[-14]	1.24[-13]	7.43[-14]	5.20[-14]	1.90[-13]	5.54[-14]
14.619	1.25[-13]	1.54[-13]	1.86[-13]	7.88[-14]	5.64[-14]	1.44[-13]	7.87[-14]	5.54[-14]	2.03[-13]	6.81[-14]
19.005	1.20[-13]	1.47[-13]	1.80[-13]	7.60[-14]	5.55[-14]	1.60[-13]	7.71[-14]	5.46[-14]	2.10[-13]	8.28[-14]
24.706	1.08[-13]	1.30[-13]	1.64[-13]	6.87[-14]	5.12[-14]	1.74[-13]	7.13[-14]	5.06[-14]	2.15[-13]	9.73[-14]
32.118	9.27[-14]	1.10[-13]	1.42[-13]	5.89[-14]	4.49[-14]	1.79[-13]	6.28[-14]	4.48[-14]	2.12[-13]	1.08[-13]
41.754	7.66[-14]	8.95[-14]	1.20[-13]	4.87[-14]	3.77[-14]	1.74[-13]	5.34[-14]	3.81[-14]	2.00[-13]	1.11[-13]
54.280	6.14[-14]	7.09[-14]	9.73[-14]	3.89[-14]	3.06[-14]	1.59[-13]	4.39[-14]	3.14[-14]	1.80[-13]	1.05[-13]
70.564	4.80[-14]	5.49[-14]	7.72[-14]	3.03[-14]	2.40[-14]	1.37[-13]	3.53[-14]	2.51[-14]	1.54[-13]	9.39[-14]
91.733	3.67[-14]	4.18[-14]	5.98[-14]	2.32[-14]	1.85[-14]	1.13[-13]	2.76[-14]	1.96[-14]	1.27[-13]	7.92[-14]
119.253	2.75[-14]	3.14[-14]	4.56[-14]	1.75[-14]	1.39[-14]	9.00[-14]	2.11[-14]	1.49[-14]	1.00[-13]	6.38[-14]
155.029	2.03[-14]	2.31[-14]	3.40[-14]	1.29[-14]	1.03[-14]	6.92[-14]	1.59[-14]	1.12[-14]	7.72[-14]	4.96[-14]
201.538	1.47[-14]	1.69[-14]	2.50[-14]	9.43[-15]	7.50[-15]	5.19[-14]	1.18[-14]	8.25[-15]	5.78[-14]	3.74[-14]
261.999	1.06[-14]	1.21[-14]	1.80[-14]	6.79[-15]	5.38[-15]	3.81[-14]	8.55[-15]	5.99[-15]	4.25[-14]	2.75[-14]
340.599	7.49[-15]	8.63[-15]	1.29[-14]	4.84[-15]	3.83[-15]	2.75[-14]	6.14[-15]	4.27[-15]	3.07[-14]	1.99[-14]
442.779	5.25[-15]	6.08[-15]	9.09[-15]	3.41[-15]	2.69[-15]	1.95[-14]	4.34[-15]	3.03[-15]	2.17[-14]	1.42[-14]
575.612	3.65[-15]	4.25[-15]	6.37[-15]	2.38[-15]	1.88[-15]	1.37[-14]	3.05[-15]	2.12[-15]	1.53[-14]	9.99[-15]

T_e eV	$3d4f$ 3G_3	$3d4f$ 3G_4	$3d4f$ 3G_5	$3d4f$ 3D_2	$3d4f$ 3D_1	$3d4f$ 3D_3	$3d4f$ 3P_2	$3d4f$ 3P_1	$3d4f$ 1H_5	$3d4f$ 1P_1
748.296	2.53[-15]	2.94[-15]	4.41[-15]	1.66[-15]	1.30[-15]	9.56[-15]	2.12[-15]	1.47[-15]	1.07[-14]	6.96[-15]
972.784	1.74[-15]	2.03[-15]	3.04[-15]	1.14[-15]	8.95[-16]	6.62[-15]	1.47[-15]	1.02[-15]	7.39[-15]	4.81[-15]
1264.620	1.19[-15]	1.39[-15]	2.09[-15]	7.82[-16]	6.13[-16]	4.55[-15]	1.01[-15]	6.98[-16]	5.09[-15]	3.31[-15]
1644.005	8.12[-16]	9.51[-16]	1.43[-15]	5.34[-16]	4.19[-16]	3.12[-15]	6.91[-16]	4.78[-16]	3.49[-15]	2.27[-15]

Table XIV: Total DR rate coefficients (α_d^{tot} in cm^3/s): $\alpha_d^{\text{tot}} = \alpha_d^{3a} + \alpha_d^{3b} + \alpha_d^{33} + \alpha_d^{4a} + \alpha_d^{4b}$. The contributions of α_d^{3a} and α_d^{3b} are sum from the $3l_1n_1l_1 - 3l'nl$ transitions with $n=10-12$ and $n=13-1000$, respectively. The α_d^{33} is the contribution from the high states $3snl - 3pnl$ transitions with $n=13-1000$. The contributions of α_d^{4a} and α_d^{4b} are sum from the $3l_1n_1l_1 - 4l'nl$ transitions with $n=4-7$ and $n=8-1000$, respectively. The $3l_1n_1l_1$ excited states include the $3sn_1l_1$ ($n_1 = 3 - 12$), $3pn_1l_1$ ($n_1 = 3 - 9$), and $3dn_1l_1$ ($n_1 = 3 - 6$) configurations.

T_e	α_d^{3a}	α_d^{3b}	α_d^{33}	α_d^{4a}	α_d^{4b}	α_d^{total}
0.100	6.00[-11]	3.24[-70]	7.22[-71]	1.72[-12]	0.00[00]	6.18[-11]
0.130	6.45[-11]	1.55[-56]	3.46[-57]	6.45[-12]	0.00[00]	7.10[-11]
0.169	6.32[-11]	4.90[-46]	1.09[-46]	1.73[-11]	0.00[00]	8.06[-11]
0.220	5.90[-11]	5.72[-38]	1.27[-38]	3.58[-11]	0.00[00]	9.48[-11]
0.286	5.45[-11]	9.38[-32]	2.07[-32]	6.02[-11]	0.00[00]	1.15[-10]
0.371	5.22[-11]	6.11[-27]	1.33[-27]	8.59[-11]	0.00[00]	1.38[-10]
0.483	5.43[-11]	3.42[-23]	7.40[-24]	1.07[-10]	0.00[00]	1.62[-10]
0.627	6.24[-11]	2.81[-20]	6.14[-21]	1.20[-10]	0.00[00]	1.82[-10]
0.816	7.56[-11]	5.13[-18]	1.14[-18]	1.21[-10]	0.00[00]	1.97[-10]
1.060	9.14[-11]	2.88[-16]	6.64[-17]	1.13[-10]	1.10[-82]	2.05[-10]
1.379	1.06[-10]	6.47[-15]	1.55[-15]	9.92[-11]	3.46[-66]	2.06[-10]
1.792	1.18[-10]	7.13[-14]	1.80[-14]	8.27[-11]	1.76[-53]	2.01[-10]
2.330	1.24[-10]	4.53[-13]	1.21[-13]	6.64[-11]	1.09[-43]	1.91[-10]
3.029	1.26[-10]	1.87[-12]	5.59[-13]	5.21[-11]	3.76[-36]	1.81[-10]
3.937	1.25[-10]	5.53[-12]	1.98[-12]	4.06[-11]	2.34[-30]	1.73[-10]
5.119	1.22[-10]	1.25[-11]	5.67[-12]	3.24[-11]	6.62[-26]	1.72[-10]
6.654	1.16[-10]	2.27[-11]	1.32[-11]	2.71[-11]	1.74[-22]	1.79[-10]
8.650	1.08[-10]	3.41[-11]	2.48[-11]	2.42[-11]	7.42[-20]	1.91[-10]
11.245	9.71[-11]	4.38[-11]	3.81[-11]	2.27[-11]	7.83[-18]	2.02[-10]
14.619	8.40[-11]	4.95[-11]	4.94[-11]	2.17[-11]	2.81[-16]	2.05[-10]
19.005	7.01[-11]	5.02[-11]	5.55[-11]	2.07[-11]	4.33[-15]	1.96[-10]
24.706	5.64[-11]	4.67[-11]	5.58[-11]	1.94[-11]	3.42[-14]	1.78[-10]
32.118	4.40[-11]	4.06[-11]	5.13[-11]	1.80[-11]	1.59[-13]	1.54[-10]
41.754	3.34[-11]	3.34[-11]	4.39[-11]	1.66[-11]	4.83[-13]	1.28[-10]
54.280	2.47[-11]	2.64[-11]	3.57[-11]	1.51[-11]	1.06[-12]	1.03[-10]
70.564	1.80[-11]	2.01[-11]	2.78[-11]	1.35[-11]	1.77[-12]	8.11[-11]
91.733	1.29[-11]	1.49[-11]	2.09[-11]	1.17[-11]	2.43[-12]	6.28[-11]
119.253	9.10[-12]	1.08[-11]	1.54[-11]	9.79[-12]	2.84[-12]	4.79[-11]
155.029	6.37[-12]	7.73[-12]	1.11[-11]	7.93[-12]	2.92[-12]	3.60[-11]
201.538	4.42[-12]	5.45[-12]	7.84[-12]	6.22[-12]	2.73[-12]	2.67[-11]
261.999	3.05[-12]	3.81[-12]	5.50[-12]	4.73[-12]	2.37[-12]	1.95[-11]
340.599	2.09[-12]	2.64[-12]	3.82[-12]	3.52[-12]	1.94[-12]	1.40[-11]
442.779	1.43[-12]	1.82[-12]	2.64[-12]	2.56[-12]	1.52[-12]	9.97[-12]
575.612	9.74[-13]	1.24[-12]	1.81[-12]	1.83[-12]	1.15[-12]	7.02[-12]
748.296	6.63[-13]	8.50[-13]	1.24[-12]	1.30[-12]	8.50[-13]	4.90[-12]
972.784	4.50[-13]	5.79[-13]	8.45[-13]	9.06[-13]	6.14[-13]	3.39[-12]
1264.620	3.05[-13]	3.93[-13]	5.74[-13]	6.29[-13]	4.37[-13]	2.34[-12]
1644.005	2.06[-13]	2.67[-13]	3.90[-13]	4.33[-13]	3.07[-13]	1.60[-12]